藥學博士 學位論文

Role of resolvin D1 in experimentally induced inflammation and colon carcinogenesis

Resolvin D1 에 의한 염증 해소 및 염증으로 유도된 대장암 억제 기전 연구

2013 年 **8** 月

서울大學校 大學院

藥學科 醫藥生命科學專攻

이 하 나

Role of resolvin D1 in experimentally induced inflammation and colon carcinogenesis

Resolvin D1에 의한 염증 해소 및

염증으로 유도된 대장암 억제 기전 연구

指導敎授　徐 榮 俊

이 論文을 藥學博士 學位論文으로 提出함
2013年 **8**月

서울大學校 大學院
藥學科 醫藥生命科學專攻
이 하 나

이 하 나 의 藥學博士 學位論文을 認准함
2013 年 **8** 月

委 員 長 _____ 印

副委員長 _____ 印

委　　員 _____ 印

委　　員 _____ 印

委　　員 _____ 印

Role of resolvin D1 in experimentally induced inflammation and colon carcinogenesis

by

Ha-Na Lee

A thesis submitted in parital fulfillment of the requirements
for the degree of

DOCTOR OF PHILOSOPHY

(Pharmacy: Pharmaceutical bioscience major)

under the supervision of Professor Young-Joon Surh

at the
College of Pharmacy,
Seoul National University

August 2013

ABSTRACT

Role of resolvin D1 in experimentally induced inflammation and colon carcinogenesis

HA-NA LEE

Under the supervision of Professor Young-Joon Surh
at the College of Pharmacy, Seoul National University

Acute inflammation, a physiologic response to protect cells from microbial infection and other noxious stimuli, can be successfully completed through effective resolution and tissue repair. Resolution of inflammation requires the elimination of key inflammatory cells and the concomitant downregulation of pro-inflammatory mediators in the inflamed sites. This process is actively regulated by coordinated biochemical mediators which possess anti-inflammatory and/or pro-resolving effects. Resolvins (Rvs), one of endogenous lipid mediators generated from omega-3 fatty acids, have emerged as a novel class of potent molecules that counteract excessive inflammatory responses and stimulate pro-resolving mechanisms; regulating the trafficking of leukocytes and stimulating non-phlogistic phagocytosis of apoptotic neutrophils by macrophages. The disruption of these anti-inflammatory and pro-resolving mechanisms can be related not only to the initiation of unnecessary inflammation, but also to the persistence of

inflammation which contributes to the pathogenesis and progression of chronic inflammatory diseases as well as cancer. Since inflammation has the beneficial effect on host defense, the complete resolution of inflammation is better to avoid chronic inflammatory situation, rather than merely blocking inflammation at the beginning. In this regards, understanding of the mechanism underlying resolution of inflammation will open new therapeutic approach to prevent and treat chronic inflammatory diseases and cancer.

Phagocytosis of apoptotic neutrophils, termed efferocytosis, is pre-requisite for complete resolution of inflammation as it prevents the exposure of surrounding tissues at the inflamed site to toxic contents of lytic cells. RvD1, endogenously generated from docosahexaenoic acid during resolution of inflammation, is known to stimulate efferocytosis. However, the molecular mechanism underlying RvD1-mediated enhancement of efferocytosis remains largely unresolved. In the present study, murine macrophage-like RAW264.7 cells treated with lipopolysaccharide (LPS) exhibited markedly reduced efferocytic activity, but this was restored by the co-incubation with RvD1. RvD1-induced restoration of the efferocytic activity appears to be mediated by down-regulating the LPS-induced TNF-α expression. The inhibitory effect of RvD1 on LPS-induced TNF-α expression was associated with enhanced nuclear localization of p50/p50 homodimer and concomitant reduction of p65/p50 heterodimer accumulation in the nucleus. RvD1 triggered phosphorylation and proteasomal degradation of nuclear factor κB1 (NF-κB1) p105 to generate p50, which was subsequently translocated to nucleus as p50/p50 homodimer. Knockdown of NF-κB p50 abolished the ability of

RvD1 to suppress TNF-α expression and also to restore efferocytosis, suggesting that the replacement of p65/p50 with p50/p50 homodimer in the nucleus is critical for RvD1-mediated stimulation of efferocytosis. These findings indicate that RvD1 expedites the resolution of inflammation through induction of efferocytosis through p50/p50 homodimer-mediated repression of TNF-α production.

Macrophage death during resolution of inflammation causes failure in resolution of inflammation, thereby leading to chronic inflammatory disorders such as atherosclerosis. During efferocytosis, engulfment of apopototic cells induces generation of reactive oxygen species (ROS) in abundance. Even though macrophages which possess apoptotic cells suffer from oxidative stress, they normally overcome oxidative stress-induced apoptosis and leave the inflamed site via lymphatics in physiological conditions. However, the mechanism underlying macrophage survival after efferocytosis has not been elucidated. In the present study, we found that RvD1 has the preventive effect on efferocytosis-induced apoptosis. The inhibitory effect of RvD1 on efferocytosis-induced oxidative burst appears to be mediated through the inactivation of NADPH oxidase (NOX), a key enzyme involved in intracellular ROS production. In RvD1-treated macrophages, efferocytosis-induced phosphorylation of $p47^{phox}$ and association between $p47^{phox}$ and $gp91^{phox}$ were downregulated, resulting in abrogation of generation of superoxide anion and hydrogen peroxide. Furthermore, RvD1-mediated suppression of NOX activation was found to be dependent on cAMP-activated protein kinase (PKA) signaling. Besides inhibiting NOX activation, RvD1 rescued macrophages from oxidative stress-induced apoptosis by upregulating the expression of Bcl-xL and Bcl-2.

However, knockdown of the RvD1 receptor, lipoxin A receptor/formyl-peptide receptor (ALX/FPR2), abolished the ability of RvD1 to activate cAMP-PKA signaling, to suppress NOX activation and to increase the expression of anti-apoptotic proteins, suggesting that ALX/FPR2 mediates the protective effect of RvD1 on effeocytosis-induced oxidative stress. Taken together, these data indicate that RvD1 protects macrophages against oxidative stress-induced apoptosis during efferocytosis through PKA-mediated repression of NOX activation and upregulation of anti-apoptotic protein expression, thereby promoting resolution of inflammation.

If timely resolution of inflammation is failed, inflammation persists and can progress to a chronic inflammation which has long been thought as a predisposing factor to carcinogenesis. Excessive and pathologic inflammation is considered to increase the risk of colorectal cancer, possibly by inducing chromosomal instability. However, the precise pathologic mechanisms underlying inflammation-induced chromosomal instability and subsequent tumorigenesis are not well understood. RvD1 is known to suppress excessive inflammatory responses and promote resolution of inflammation, and hence expected to protect against chronic inflammation-induced cancer. Using the azoxymethane (AOM) plus dextran sodium sulfate (DSS) colitis-associated colorectal cancer model, we revealed that RvD1 attenuated inflammation-induced tumorigenesis. Moreover, it reduced AOM/DSS-induced production of pro-inflammatory cytokine interleukin-6 (IL-6), which is considered to play a key role in chronic inflammation and cancer. IL-6 triggered malignant transformation and abnormalities of mitotic spindle and nucleus in intestinal epithelial CCD841CoN cells, and these effects were abolished by RvD1. The

inhibitory effect of RvD1 on chromosomal instability was associated with downregulation of IL-6-induced cyclin D1 expression which was mediated by inhibiting Janus kinase 2/signal transducer and activator of transcription 3 signaling. Knockdown of cyclin D1 abolished IL-6-induced mitotic spindle abnormality, but overexpression of cyclin D1 increased the number of cells showing multipolar spindles, leading further support to the notion that cyclin D1 contributes to mitotic spindle abnormality.

Taken together, these observations suggest that endogenous pro-resolving lipid mediator RvD1 facilitates resolution of inflammation by promoting efferocytosis and protecting macrophages from oxidative stress-induced apoptosis, thereby preventing chronic inflammation. Moreover, RvD1 exerts the chemopreventive effect on colitis-associated colon carcinogenesis.

Keywords

Resolvin D1, Resolution of inflammation, Efferocytosis, NF-κB, Oxidative stress-induced apoptosis, NADPH oxidase 2, ALX/FPR2, Inflammation-induced tumorigenesis, Spindle multipolarity, Cyclin D1, Signal transducer and activator of transcription 3

Student Number: 2008-31002

TABLE OF CONTENTS

LIST OF FIGURES

Chapter I

Chapter II

Chapter III

Chapter IV

LIST OF ABBREVIATIONS

AA, arachidonic acid

ALX/FRP2, a lipoxin A4 receptor/formyl-peptide receptor

AOM, azoxymethane

cAMP, cyclic adenosine monophosphate

CDK4, cyclin-dependent kinase 4

COX, cyclooxygenase

DHA, docosahexaenoic acid

DHE, dihydroethidium

DSS, dextran sodium sulfate

EPA, eicosapentaenoic acid

ERK, extracellular signal-regulated kinases

FITC, fluorescein isothiocyanate

GFP, green fluorescent protein

GPCR, G-protein-coupled receptor

IκB, inhibitor of kappa B

IKK, IκB kinase

IL, interleukin

JAK, Janus kinase

LOX, lipoxygenase

LPS, lipopolysaccharide

M1 macrophage, classical activated macropahge

M2 macrophage, alternatively activated macrophage

NAC, *N*-acetyl cysteine

NF-kB, nuclear factor-κB

NOX, nicotinamide adenine dinucleotide phosphate-oxidase

NSAID, non-steroidal anti-inflammatory drug

PKA, protein kinase A

PMN, polymorphonuclear leukocytes

PUFA, polyunsaturated fatty acid

RB, retinoblastoma protein

ROS, reactive oxygen species

RvD1, resolvin D1

STAT3, signal transducer and activator of transcription 3

TGF-β, transforming growth factor-β

TNF-α, tumor necrosis factor-α

Chapter I

Therapeutic potential of resolvins for the prevention and treatment of inflammatory disorders and cancer

1. Introduction

Inflammation has long been thought to cause and aggravate most prevalent disorders including cardiovascular disease, asthma, inflammatory bowel disease, neurodegenerative disease, rheumatoid arthritis, pulmonary disease, periodontal disease, diabetes and cancer (Serhan and Petasis, 2011). Nonetheless, acute inflammation is physiologically necessary to protect the host against microbial infection and tissue injury. It is characterized by activation of inflammatory cells, alterations in vascular permeability and production of pro-inflammatory mediators including cytokines, chemokines, lipid mediators, steroids and growth factors (Serhan et al., 2008). At the onset of inflammation, a lot of leukocytes, especially polymorphonuclear cells (PMNs), are recruited to the inflamed site and then activated to remove invading pathogens by phagocytosis. This response is triggered by the activation of tissue mast cells and resident macrophages and subsequent release of pro-inflammatory mediators, which stimulate the nearby microvasculature and attract leukocytes into the inflamed site (Serhan and Savill, 2005; Rajakariar et al., 2006; Medzhitov, 2008). Recruited PMNs release the toxic contents of their granules, including reactive oxygen species, reactive nitrogen species, proteinase and elastase, to eliminate or neutralize harmful stimuli (Nathan, 2006). However, these effectors of inflammation not only kill the invading microbes, but can also damage host tissues if persistently released (Bian et al., 2012). Thus, despite its critical function in host

protection, acute inflammation should not be prolonged to avoid chronic and systemic inflammation responsible for the pathogenesis of a wide variety of diseases (Serhan et al., 2007).

After degrading pathogens by phagocytosis, PMNs, which play a central role during the initial phase of inflammation, undergo apoptosis. Removal of apoptotic neutrophils is also an important step in preventing chronic inflammation which can occur by disgorgement of toxic contents from apoptotic cells into surrounding tissue (Fadok et al., 1998). Macrophages, which are recruited in the inflamed tissue following influx of PMNs, play a key role in engulfing apoptotic PMNs. Once phagocytosis is completed, macrophages exit the inflamed site by lymphatic drainage, allowing the tissue return to homeostasis (Serhan et al., 2007). Thus, the successful completion of inflammatory response in the early stage is followed by the return to non-inflammatory status, the process known as resolution of inflammation (Serhan and Savill, 2005; Spite and Serhan, 2010).

The cellular and molecular events involved in the acute inflammation have been unraveled, but much less is known about the mechanisms underlying resolution of inflammation. Resolution of inflammation had been considered as a passive process, which accompanies a decrease in diminishing pro-inflammatory mediators such as prostaglandins (PGs) and leukotrienes (LTs) (Serhan et al., 2002). However, in recent years, new lipid mediators have been suggested as an active modulator of resolution of

inflammation. Depending on the biological action of pro-resolving endogenous mediators, including lipoxins, resolvins and protectins, resolution of inflammation is accelerated (Serhan et al., 2000).

The typical therapeutic treatment of chronic inflammatory disease and inflammation-associated cancer primarily depends on the inhibition of pro-inflammatory signaling cascade, but in many cases such approaches are not effective (Lawrence et al., 2002). Understanding the role of anti-inflammatory and pro-resolving lipid mediators in the resolution of the inflammatory response leads to new approaches to establish potent therapeutic strategies for preventing and treating unresolved diseases.

2. Resolution of inflammation

2.1 What is resolution of inflammation?

Complete resolution is the ideal outcome of inflammation, limiting excessive tissue injury and preventing the development of chronic and immune-mediated inflammation. The switch from the initiation to the resolution of inflammation occurs both at the cellular (e.g. PMN infiltration, apoptosis and subsequent elimination by macrophages) and the molecular (from pro-inflammatory to anti-inflammatory/pro-resolving mediators) levels (**Fig. 1-1**) (Serhan and Savill, 2005). The resolution of inflammation is composed of three phases; downregulation of pro-inflammatory signaling, apoptosis

of PMNs and macrophage-mediated phagocytosis of apoptotic PMNs (efferocytosis) followed by migration to the draining lymph nodes. The initial phase of resolution involves the suppression of pro-inflammatory signaling and the release of endogenous anti-inflammatory mediators, including interleukin (IL)-10, transforming growth factor-β (TGF-β), proteolytic enzymes and lipid mediators. The changes to anti-inflammatory environment facilitate apoptosis of inflammatory PMNs, which is a prerequisite process for non-inflammatory removal of PMNs by macrophages. Upon phagocytosis, macrophages are stimulated to generate high levels of anti-inflammatory and pro-resolving mediators, which eventually promote tissue homeostasis through activating macrophages to leave the inflamed site via the nearest lymph nodes (Savill and Fadok, 2000; Bellingan et al., 2002; Vandivier et al., 2006; Schwab et al., 2007; Van Hove et al., 2008).

Accumulating evidence indicates that resolution of acute inflammation is a highly coordinated process tightly regulated by several endogenous anti-inflammatory and pro-resolving mediators including lipoxins and resolvins (Serhan, 2007). These factors further block PMN trafficking, attract monocytes, reverse vascular permeability, induce apoptosis of residual activated PMNs, promote non-inflammatory phagocytosis of apoptotic PMNs, induce efflux of macrophages engulfing apoptotic PMNs via lymphatics and activate the removal of exudate and fibrin from the inflamed tissue, thereby leading to homeostasis (Serhan and Chiang, 2008).

Although most endogenous lipid mediators, which are involved in resolution of inflammation, have dual anti-inflammatory and pro-resolving functions, anti-inflammation and pro-resolution are distinct mechanisms. Whereas a reduction in influx of PMNs to the inflamed site reflects an anti-inflammatory action, an increase in either influx of monocytes or efflux of macrophages is linked to a pro-resolving action. Paradoxically anti-inflammatory response can prolong the time to resolve and extend inflammation by disrupting formation of endogenous pro-resolving mediators. For example, cyclooxygenase (COX) inhibitors are powerful to block the production of pro-inflammatory eicosanoids, particularly classical PGs and LTs, but they can also disturb the biosynthesis of pro-resolving mediators including a group of resolvins and lipoxins (Gilroy et al., 1999; Simopoulos et al., 1999; Serhan et al., 2008).

2.2 The cellular process in resolution of inflammation: PMN apoptosis, efferocytosis and macrophage exfiltration

Extravasated PMNs are the major effector cells in acute inflammatory responses, so the clearance of PMNs from the inflamed site is a prerequisite for efficient resolution of inflammation. In the late phase of inflammation, PMNs spontaneously undergo apoptosis, thereby becoming readily recognized and engulfed by macrophages recruited into the inflammatory site. In this regard, macrophages can be thought as a key player in compromising resolution of inflammation. Besides eliminating apoptotic

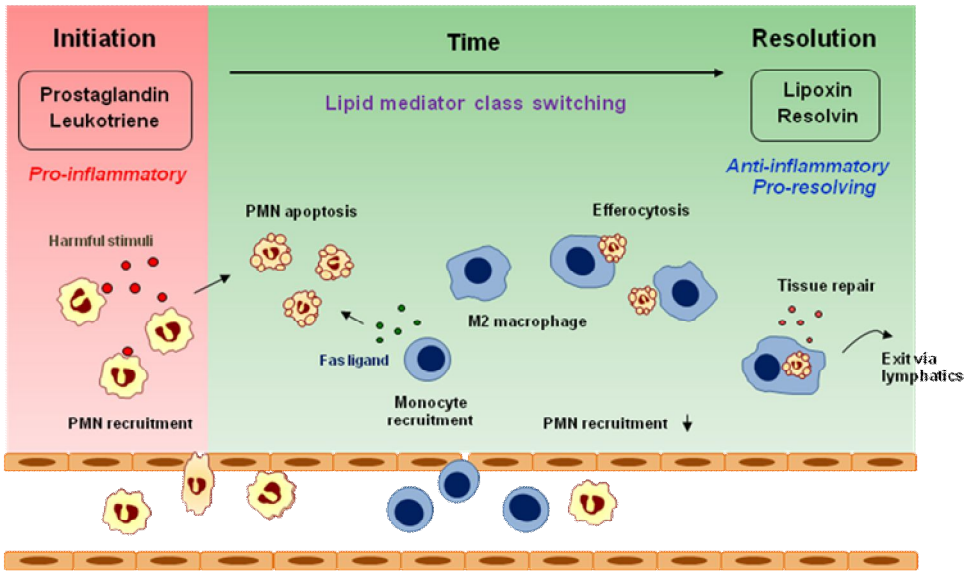

Fig. 1-1. The cellular and molecular changes during the onset and resolution of inflammation. During the initial phase of inflammation, PMNs are recruited into the inflamed site and release pro-inflammatory mediators to eliminate harmful stimuli. As the inflammatory response progresses, the switch from initiation to resolution occurs with generation of anti-inflammatory and pro-resolving lipid mediators such as lipoxins and resolvins. These mediators induce the termination of inflammation through several putative mechanisms: inhibiting further infiltration of PMNs; triggering apopotosis of PMNs; attracting more monocytes which differentiate into macrophages; stimulating efferocytosis, tissue repair and egression of macrophages to the lymphatics, etc.

cells and their secreted products, infiltrated macrophages actively trigger apoptosis in neighboring PMNs through releasing 'death cytokines' such as Fas ligand. The phagocytosis of apoptotic PMNs governed by macrophages are specially called 'efferocytosis'. Efferocytosis can stimulate macrophages to release anti-inflammatory mediators such as TGF-β1, which block Toll-like receptor-induced pro-inflammatory signaling. TGF-β1 has two essential roles in resolution of inflammation; one is suppression of inflammation, and the other is stimulation of tissue repair by inducing secretion of vascular endothelial growth factor and collagen (Voll et al., 1997; Golpon et al., 2004; Tabas, 2010). After efferocytosis, macrophages (which retain engulfed apoptotic PMNs) initiate the process of egress from the inflamed tissue to the nearest lymphatics, and tissue returns to normal status (Bellingan et al., 1996; Serhan and Savill, 2005). Consequently, macrophages are removed from the inflamed site through spontaneous exfiltration, rather than apoptosis as in the case of PMNs. If macrophages fail to migrate into lymph nodes, they will continuously accumulate in tissue, which is a hallmark of chronic inflammation (Bellingan et al., 1996).

2.3 The role of M2 polarized macrophages

Although macrophages can occasionally play a pro-inflammatory role, they importantly contribute to resolution of inflammation, wound healing, tissue repair and tissue remodeling in non-phlogistic manners (Serhan and Savill, 2005). Since the

concept of alternative activation of macrophages were introduced (Stein et al., 1992), macrophages have been classified into two main types: classically activated (M1) macrophages that promote inflammation and alternatively activated (M2) macrophages with anti-inflammatory and pro-resolving properties. Macrophages, observed during the resolution phase of acute inflammation, are mostly polarized to M2, and express scavenger, mannose and galactose receptors, arignase-1, Fizz1 and Ym1 (Martinez et al., 2009). These M2 macrophages participate in key processes of resolution; downregulation of inflammation, clearance of tissue debris and apoptotic cells and stimulation of angiogenesis (Lopez-Castejon et al., 2011). The switch of macrophage activation towards M2 is influenced by increases in T helper 2 (T_H2) cell-secreted molecules including IL-4 and IL-13, IL-10, glucocorticoid hormones, the bioactive lipid sphingosine 1-phosphate (S1P) or the transcription factor peroxisome proliferator-activated receptor-γ (PPARγ). The condition of atherosclerosis can be alleviated by stimulating T_H2 cell polarization, upregulating PPARγ transcriptional activity or activating S1P pathway, indicating that functional polarization of macrophages into M2 might be one of therapeutic strategies for the management of inflammatory diseases (Nofer et al., 2007; Odegaard et al., 2007; Martinez et al., 2009; Tabas, 2010; Lopez-Castejon et al., 2011).

2.4 Lipid mediator class switching toward pro-resolution

The initiation of inflammation is governed by lipid mediators generated from omega-6 polyunsaturated fatty acids (PUFAs), especially arachidonic acid (AA), but the termination of inflammation is regulated by omega-3 PUFA-derived lipid mediators. Conversion of omega-6 and omega-3 PUFAs to their derivates shares the same enzymes including COX and lipoxigenase (LOX). Although a competition exists between omega-6 and omega-3 PUFAs for metabolism, AA is predominantly used for eicosanoid biosynthesis since cellular membranes contain mainly AA compared to omega-3 PUFAs (Schmitz and Ecker, 2008).

During the initial phase of inflammation, peripheral blood neutrophils release eicosanoids formed as a consequence of the enzymatic oxygenation of AA by COX and LOX. These mediators including classical PGs and LTs are mostly pro-inflammatory, and can amplify inflammatory response by stimulating vasodilation that helps neutrophils to infiltrate into the inflamed site. Interestingly, the pro-inflammatory lipid mediators can also act as an inducer of anti-inflammatory responses. PGE_2, one of representative pro-inflammatory PGs modulating the initial phase of inflammation, increases the production of other pro-inflammatory cytokines through COX-2 induction. On the contrary, PGE_2 can also decrease the generation of pro-inflammatory leukotriene 4-series species through 5-LOX inhibition, and PGE_2-induced 15-LOX promotes the formation of anti-inflammatory and pro-resolving lipid mediators (Levy

et al., 2001; Bagga et al., 2003; Serhan et al., 2003). Thus, signaling pathways leading to PGE_2 production, in turn, activate the expression of enzymes, such as COX-2 required for the generation of another class of eicosanoids (i.e. lipoxins) as well as the novel family of lipid mediators (i.e. resolvins) generated from omega-3 PUFAs. Consistently, pro-inflammatory mediators are initially produced within seconds and minutes of acute challenge, while at a later time (hours up to days), the amount of anti-inflammatory and pro-resolving mediators is increasing. This subtle change in the class of lipid mediators from pro-inflammatory eicosanoids to resolvins and lipoxins, which possess anti-inflammatory and pro-resolving properties, is critical for transition from inflammation to resolution (Levy et al., 2001; Schwab and Serhan, 2006; Medzhitov, 2008).

3. The importance of resolution of inflammation for preventing and treating chronic inflammatory diseases and cancer

Inflammation usually resolves immediately to restore homeostasis, but it is occasionally prolonged because of inadequate production of pro-resolving mediators, persistent stimulation by overactivated pro-inflammatory signals, failed phenotypic switch of macrophage and T cell populations in the inflamed sites and uncontrolled infiltration of myeloid-derived suppressor cells (**Fig. 1-2**) (Nathan and Ding, 2010). Chronic inflammation is no more beneficial for the host, and leads to a loss of tissue or

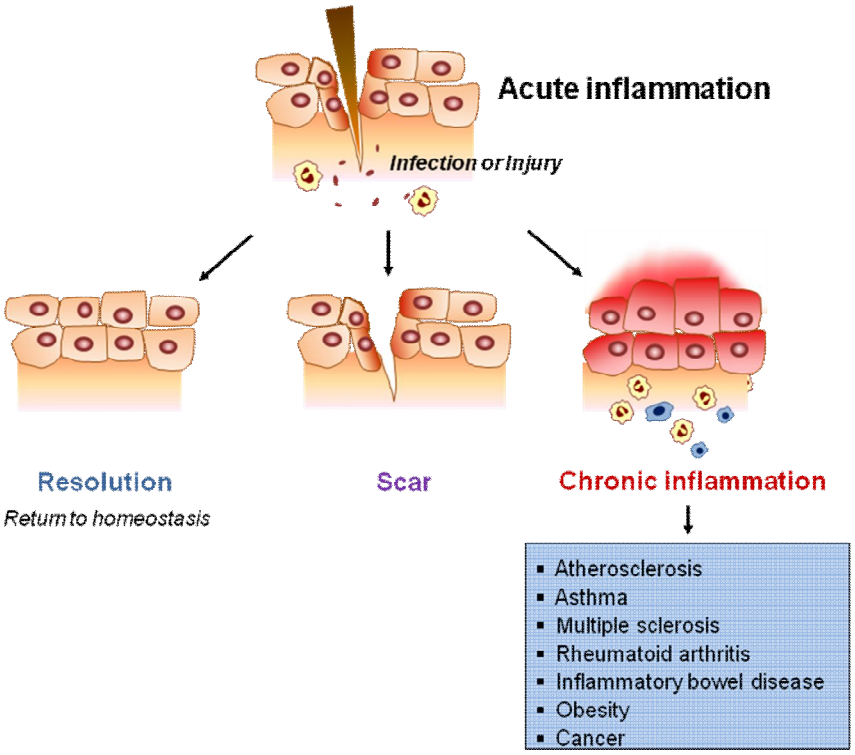

Fig. 1-2. Failure in resolution of inflammation drives chronic inflammatory diseases. Resolution of inflammation is the ideal outcome of acute inflammation, but it is sometimes failed and results in progression to chronic inflammation. Moreover, diverse diseases involve nonresolving inflammation, implying that resolution of inflammation might be important for prevention and treatment of chronic inflammatory diseases. Examples are found in atherosclerosis, asthma, multiple sclerosis, rheumatoid arthritis, IBD, obesity and cancer.

organ function. Whereas the frequent occurrence of inflammation is not necessarily linked to pathogenesis, the duration and severity of inflammation and the failure of resolution are considered as a high risk factor for several human diseases, such as rheumatoid arthritis, atherosclerosis, diabetes, asthma, inflammatory bowel disease and cancer (Nathan and Ding, 2010). Therefore, the current clinical approachs to prevention and treatment of chronic inflammatory disease and cancer move toward understanding of the mechanisms involved in resolution of inflammation and repair.

Traditionally, nonresolving inflammation was considered just as the phenomenon derived from chronic infections. However, it is now clear that continuous infection is not the sole factor for causing and exacerbating inflammatory diseases, because the clinical and pathological symptoms of inflammatory disease are different from those of chronic infection. Moreover, there are multiple lines of evidence supporting that the naturally occurring resolution systems dysfunction in most human prevalent diseases (Serhan et al., 2007). For example, macrophages isolated from wounds of diabetic mice are mostly impaired in effeocytosis, resulting in accumulation of apoptotic cells in damaged tissue. In addition, those macrophages express higher levels of pro-inflammatory and lower levels of anti-inflammatory cytokines, indicating that pro-resolving mechanisms is uncontrolled (Khanna et al., 2010).

Although nonresolving inflammation is not a primary cause of asthma, rheumatoid arthritis, inflammation bowel disease, psoriasis, astherosclerosis and cancer, it

contributes to the pathogenesis of those diseases (Nathan and Ding, 2010). Moreover, failure of resolution is highly related to tissue damage. In rheumatoid arthritis and asthma, continuous or repeated inflammatory response triggers tissue injury with fibrosis. Fibrosis is sufficient to disrupt organ functions, and hence considered as a major medical problem in inflammatory diseases (Gilroy et al., 2004).

Classical anti-inflammatory agents, including non-steroidal anti-inflammatory drugs (NSAIDs) and COX-2 inhibitors that antagonize pro-inflammatory signaling, only provide symptomatic relief but do not improve pathological conditions in most immune-mediated inflammatory disorders (Serhan et al., 2007). In addition, it is well known that the administration of a selective COX-2 inhibitor at the peak of inflammation may delay resolution of inflammation, possibly resulting in aggravation of inflammation-related diseases by disturbing endogenous pro-resolving mechanisms (Willoughby et al., 2000). Nonetheless, current therapeutic approaches to control chronic inflammatory diseases and cancer do not much consider pro-resolution and tissue repair which differ from anti-inflammation (Bannenberg et al., 2005). The focus on inflammation only, not resolution, may not be sufficient for successful prevention and treatment of chronic inflammatory diseases as well as cancer. Understanding the mechanisms involved in resolution of inflammation is expected to provide a new avenue for developing potent therapeutic agents for chronic inflammatory diseases and cancer.

4. Therapeutic potential of resolvins for chronic inflammatory diseases and cancer

4.1 Biosynthesis of resolvins

During resolution of inflammation, distinct series of anti-inflammatory and pro-resolving lipid mediators are generated, depending on the parent substrate. Novel bioactive lipid mediators, called resolvins (resolution-phase interaction products), have been identified in resolving exudates using liquid chromatography with tandem mass spectrometry detection (LC-MS-MS)-based approach (Arita et al., 2005b). Resolvins are endogenous lipid mediators derived from the omega-3 PUFA eicosapentaenoic acid (EPA) and docosahexaenoic acid (DHA). These include the E-series resolvins (RvE) derived from EPA, and the D-series resolvins (RvD), neuroprotectins/protectins (NPD1/PD1), maresins and aspirin-triggered epimers which are derived from DHA. Additional series of resolvin D generated in the presence of aspirin were also discovered, such as aspirin-triggered 17R-resolvin D series, all of which are converted by aspirin-acetylated COX-2 that acts as a modified dioxygenase inserting a molecule of oxygen with opposite stereochemistry (**Fig. 1-3**) (Serhan, 2007; Serhan, 2008; Serhan and Petasis, 2011).

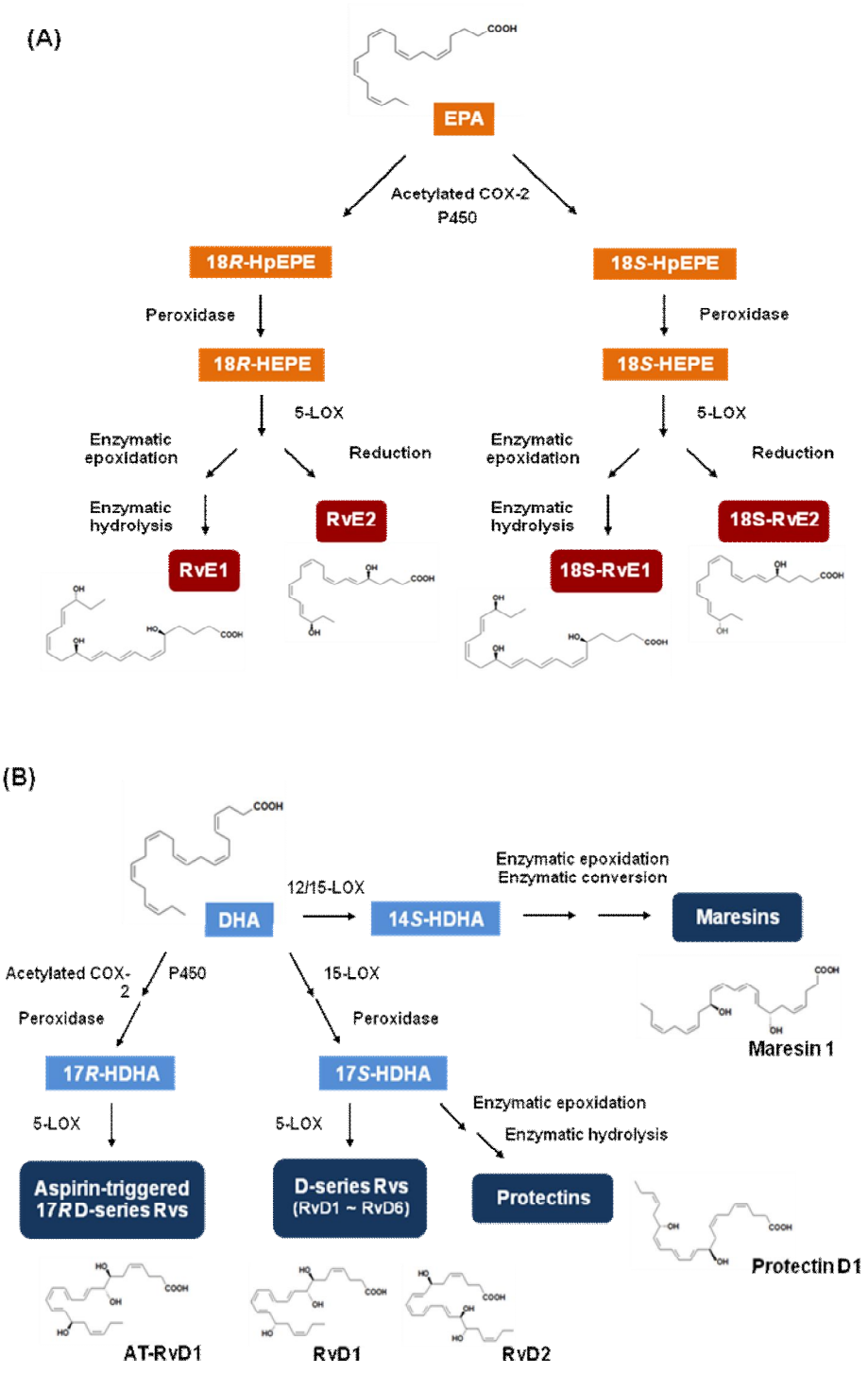
(A)
EPA
Acetylated COX-2
P450
18R-HpEPE
18S-HpEPE
Peroxidase
Peroxidase
18R-HEPE
18S-HEPE
5-LOX
5-LOX
Enzymatic epoxidation
Reduction
Enzymatic epoxidation
Reduction
Enzymatic hydrolysis
RvE2
Enzymatic hydrolysis
18S-RvE2
RvE1
18S-RvE1
(B)
DHA
12/15-LOX
14S-HDHA
Enzymatic epoxidation
Enzymatic conversion
Maresins
Maresin 1
Acetylated COX-2
P450
15-LOX
Peroxidase
Peroxidase
17R-HDHA
17S-HDHA
5-LOX
5-LOX
Enzymatic epoxidation
Enzymatic hydrolysis
Aspirin-triggered 17R D-series Rvs
D-series Rvs
(RvD1 ~ RvD6)
Protectins
Protectin D1
AT-RvD1
RvD1
RvD2

Fig. 1-3. Pathways and enzymes involved in biosynthesis of E- and D-series of resolvins, protectins and maresin 1. (A) EPA is converted to 18*R* and 18*S* E-series resolvins through acetylated COX-2 and 5-LOX mechanisms. (B) DHA gives rise to either 17*R* or 17*S* D-series resolvins, protectins or maresins. Aspirin-triggered acetylation of COX-2 mediates the generation of 17*R* D-series resolvins, thereby, termed aspirin-triggered D-series resolvins. Through LOX pathway, three distinct families of resolvins including 17*S* D-series resolvins, protectins and maresins are generated. Despite different structures, those metabolites from EPA or DHA share anti-inflammatory and pro-resolving properties.

4.1.1 E-series of resolvins

The E-series resolvins are categorized into two groups: 18*R* and 18*S* E-series resolvins. Both of them are generated from EPA during inflammation when endothelial cells interact with leukocytes. In the presence of aspirin, EPA can be enzymatically transformed to 18*R*- or 18*S*-hydroxyeicosapentaenoic acid (18*R*- or 18*S*-HEPE) by acetylated COX-2 in endothelial cells. Upon cell-cell interaction, 18*R*- and 18*S*-HEPEs are released to neighboring leukocytes for subsequent conversion by 5-LOX to RvE1 and 18*S*-RvE1, respectively. The structure of RvE1/18S-RvE1 was elucidated as 5*S*,12*R*,18(*R/S*)-trihydroxy-6*Z*,8*E*,10*E*,14*Z*,16*E*-EPA (Serhan et al., 2000; Arita et al., 2005b; Oh et al., 2011). The other RvE2/18*S*-RvE2 is structurally distinct from RvE1/18S-RvE1 as 5*S*,18(*R/S)*-dihydroxy-EPA (Tjonahen et al., 2006; Oh et al., 2011).

4.1.2 D-series of resolvins

DHA is the precursor for two groups of resolvins, which are referred to as 17*S* D-series resolvins and 17*R* D-series aspirin-triggered-resolvins (AT-Rvs). DHA can be converted by LOX to 17*S*-hydroxy-containing series of resolvins, known as RvD1 to RvD6. Especially, RvD1 biosynthesis involves sequential oxygenations by 15-LOX and 5-LOX. In the presence of aspirin, DHA is transformed to 17*R*-hydroxy-DHA (17*R*-HDHA) by aspirin-acetylated COX-2 and subsequently oxygenated by 5-LOX, resulting in the production of AT-RvD1. Recently, the complete stereochemistry of

RvD1 and AT-RvD1 was established as 7*S*,8*R*,17*S*-trihydroxy-4*Z*,9*E*,11*E*,13*Z*,15*E*,19*Z*-DHA and 7*S*,8*R*,17*R*-trihydroxy-4*Z*,9*E*,11*E*,13*Z*,15*E*,19*Z*-DHA, respectively (Hong et al., 2003; Serhan et al., 2006; Sun et al., 2007; Chiang et al., 2012).

4.1.3 Protectins

In addition to the D-series resolvins, DHA can be converted to protectins through enzymatic epoxidation and hydrolysis. The representative member of protectins, protectin D1 (known as neuroprotectin D1 when generated in neural tissues), is distinguished by the presence of its conjugated triene containing structure. Protectin D1 biosynthesis proceeds via 15-LOX-catalyzed epoxide intermediates, and its structure is also completely established as 10*R*,17*S*-dihyroxy-docosa-4*Z*,7*Z*,11*E*,13*E*,15*Z*,19*Z*-hexaenoic acid (Hong et al., 2003; Sun et al., 2007).

4.1.4 Maresins

Recently, a novel family of portent DHA-derived mediators has been identified, which are denoted as the maresins (macrophage mediators in resolving inflammation). This new molecule is produced by macrophages, and act directly on phagocytes. Initial 14-lipoxygenation of DHA produces the hydroperoxy-containing intermediate 14*S*-hydroperoxy-docosa-4*Z*,7*Z*,10*Z*,12*E*,16*Z*,19*Z*-hexaenoic acid that undergoes further conversion via 13(14)-epoxidation, which is an essential process in the biosynthesis of

potent mediators such as maresin 1 (7,14-dihydroxy-docosa-4*Z*,8*Z*,10,12,16*Z*,19*Z*-hexaenoic acid) (Serhan et al., 2009).

4.2 Anti-inflammatory and pro-resolving effects of resolvins

Accumulated evidence indicates that resolvins and protectins possess anti-inflammatory and pro-resolving actions. Among the E-series resolvins, the biological action of RvE1 was the first one whose biological actions were elucidated in detail. At low nanomolar concentrations, RvE1 suppresses inflammation by blocking transendothelial PMN migration, pro-inflammatory signaling (e.g. NF-κB activation) and pro-inflammatory cytokine release including TNF-α, IL-1 and IL-6 (Serhan et al., 2000; Gronert et al., 2004; Arita et al., 2007). It is also known as a potent counter-regulator of superoxide anion generation, thereby, preventing tissue destruction resulting from inflammation (Hasturk et al., 2006). In addition to these anti-inflammatory effects, RvE1 attracts nonphlogistic (i.e. non-inflammatory) monocytes and macrophages, and promotes PMN clearance from the inflamed site through macrophage-mediated phagocytosis (Schwab et al., 2007). More recently, the role of RvE1 as a chemokine scavenger has been discovered. RvE1-induced upregulation of C-C chemokine receptor type 5 (CCR5) expression on apoptotic PMNs and T cells increases the binding of CCR5 with chemokines such as CCL3 and CCL5, which are involved in inflammation and autoimmunity. Macrophages engulf those apoptotic cells

interacting with chemokines, and RvE1 facilitates chemokine clearance (Ariel et al., 2006). Like the E-series resolvins, the D-series resolvins and protectins also terminate PMN infiltration, suppress pro-inflammatory cytokine secretion and promote monocyte infiltration and phagocytosis. The pro-resolving effect of RvD1 is correlated to macrophage polarization toward the M2-like phenotype with overproduction of IL-10, CD206, arginase 1, resistin-like molecule α and chitinase-3 like protein (Titos et al., 2011). Moreover, RvD1 can not only abolish TNF-α-mediated disruption of tight junction and cytoskeleton, but also stimulate cell migration and polarity in salivary epithelial, thereby promoting tissue repair (Odusanwo et al., 2012). Protectin D1 proved to be more potent than its precursor DHA in regulating ion channels in isolated microglial cell (Hong et al., 2003). Protectin D1 protects brain and retina from oxidative stress-induced apoptosis by upregulating anti-apoptotic Bcl-2 and Bcl-$_{xL}$ proteins while downregulating pro-apoptotic Bad and Bax protein expression (Mukherjee et al., 2004). These stereoselective actions of resolvins were studied in a wide range of experimental inflammatory disease models including peritonitis, periodontitis, asthma, colitis, allergic airway inflammation, arthritis, dry eye, obesity-induced diabetes and inflammatory pain.

4.3 G protein-coupled receptor (GPCR) as a receptor for resolvins

Since resolvins and protectins are endogenously generated at very low concentrations,

the mechanism of their actions relies on specific receptors which amplify the signal. Using [^{3}H]-labeled resolvins, it was revealed that each resolvin signals through the distinct receptor. Similar to other potent lipid mediators (LTs, PGs and lipoxins), the biological actions of resolvins are mediated via G protein-coupled receptors (GPCR). The first identified receptor for RvE1 is a ChemR23 expressed in monocytes and dendritic cells. Moreover, RvE1 displays high binding affinity for leukotriene B_4 (LTB_4) receptor (BLT1) present in PMNs, and can block LTB_4 signaling as an antagonist (Arita et al., 2005b). Screening systems to identify receptors for RvD1 gave two GPCR candidates, one is ALX/FPR2 (a lipoxin A4 receptor/formyl peptide receptor 2) and the other is GPR32 (an orphan human receptor). By binding to ALX/FRP2, RvD1 activated the mitogen activated protein kinase (MAPK) pathway, especially extracellular-signal-regulated kinase 1/2 (ERK1/2). Moreover, RvD1 stimulated macrophages to engulf apoptotic PMNs or zymosan particles, and upregulated specific microRNAs (including miR-208, miR-146b and miR219) associated with resolution of inflammation through interaction with GPR32 and ALX. However, these pro-resolving effects of RvD1 were abolished by selective knockdown of these GPCRs (Krishnamoorthy et al., 2010; Norling et al., 2012; Krishnamoorthy et al., 2012). Not only RvD1, but RvD5 also enhanced the phagocytic ability of macrophages in a GPR32-dependent manner (Chiang et al., 2012). Recently, resolvins have been suggested as potent endogenous inhibitors for transient receptor potential

subtype vanilloid 1 (TRPV1) and TRP ankyryn 1 (TRPA1) which are involved in the genesis of inflammatory pain. In particular, distinct roles of RvE1, RvD1 and RvD2 in regulating TRP channel activity were demonstrated; RvE1 strongly interacts with TRPV1, RvD1 suppresses TRPA1 and RvD2 inhibits both TRPV1 and TRPA1 with superior potency (Park et al., 2011). Although a cognate GPCR for RvE2 has yet to be identified, RvE2 seems to interact with distinct receptors because the protective actions of RvE1 and RvE2 are additive when given together (Tjonahen et al., 2006).

4.4 NF-κB as a major target of resolvins

NF-κB signaling plays a key role in mediating inflammation and immune response through induction of pro-inflammatory cytokines, chemokines and other proteins. NF-κB, as a dimeric transcription factor composed of p65 (RelA), RelB, c-Rel, NF-κB1 (p50/p105) or NF-κB2 (p52/p100), exists in the cytoplasm as an inactive complex with the inhibitory protein, called the inhibitor of NF-κB (IκB). When cells are exposed to pro-inflammatory stimuli, such as lipopolysaccharide (LPS), phorbol ester and TNF-α, IκB is phosphorylated and ubiquitinated, thereby allowing NF-κB to translocate to the nucleus. Consequently, NF-κB binds to κB enhancer elements in the promoter region of pro-inflammatory genes (Tak and Firestein, 2001).

A number of studies have shown that resolvins and protectins exert anti-inflammatory actions by blocking NF-κB activation. RvE1 inhibited TNF-α-induced

nuclear translocation of NF-κB in ChemR23-dependent manners, leading to suppressing production of pro-inflammatory cytokines including TNF-α and IL-12p40 (Ishida et al., 2010a). Recently, it has been reported that the protective effect of RvD1 on LPS-induced lung injury in mice is also mediated by inhibition of nuclear translocation of NF-κB (Wang et al., 2011). According to the study by Krishnamoorthy et al., GPCR, especially ALX and GPR32, has been suggested to be involved in mediating the effect of RvD1 on suppression of NF-κB signaling (Krishnamoorthy et al., 2010).

In diverse inflammatory diseases, the activation of NF-κB is frequently observed, and this correlates with overproduction of pro-inflammatory cytokines, adhesion molecules, COX-2, inducible nitric oxide (iNOS) and matrix metalloproteinase (MMP). For instance, in rheumatoid arthritis, it is well known that overexpressed NF-κB promotes the recruitment of inflammatory cells and production of pro-inflammatory mediators including IL-1, IL-6 and TNF-α at the inflamed synovium (Han et al., 1998). Moreover, in *Helicobacter pylori*-associated gastritis, the number of cells with NF-κB activation correlates with the degree of pathogenesis, indicating that NF-κB-targeted therapy might be effective in inflammatory disorders (Hart et al., 1998). In this respect, it is expected that resolvins which possess the inhibitory effect on NF-κB activation can be potent therapeutic agents for inflammatory disorders.

4.5 The importance of omega-3 PUFAs as precursors of resolvins

Since beneficial effects of omega-3 PUFA-derived mediators were discovered, dietary supplementation with fish oil rich in EPA or DHA has emerged as a therapeutic recommendation for the prevention and treatment of many prevalent diseases associated with inflammation. Omega-3 fatty acids are well known to decrease the risk of coronary heart disease, hypertension, rheumatoid arthritis, asthma, type 1 diabetes mellitus, psoriasis, multiple sclerosis, inflammatory bowel disease and cancer, whereas the uptake of omega-6 PUFA rich in Western food is associated with the high risk of those diseases (Simopoulos, 2002; Simopoulos, 2008). Transgenic mice overexpressing the *Caenorhabditis elegans* (*C. elegans*) *fat-1* gene, which encodes desaturase, an enzyme catalyzing conversion of omega-6 PUFAs to omega-3, are protected from a number of inflammatory insults and have higher concentrations of resolvins and protectins. While wild-type mice lacking the *fat-1* are more susceptible to extensive vaso-obliteration and suffered from severe retinal neovascularization compared with *fat-1* mice, administration of RvD1, RvE1 or neuroprotectin D1 ameliorated such symptoms in wild-type mice. Also, in mice without omega-3 PUFA diet supplementation, intraperitoneal injection of resolvins conferred significant protection against pathological retinal angiogenesis. These results indicate that the protective effect of omega-3 PUFAs against retinal neovascularization is mediated, in part, by their potent bioactive metabolites (Connor et al., 2007).

It is estimated that the present Western diet contains more omega-6 than omega-3 PUFAs with a ratio of omega-6/omega-3 of 15-20. Because of the increased uptake of omega-6 PUFAs, AA-derived eicosanoids, especially pro-inflammatory PGs, thromboxanes and LTs, are generated in larger amounts than anti-inflammatory mediators derived from omega-3 PUFAs. Thus, the omega-6 and omega-3 ratio in the diet strongly affects production of lipid mediators; increased consumption of omega-3 PUFAs leads to both reduced synthesis of pro-inflammatory eicosanoids from omega-6 PUFAs and elevated production of anti-inflammatory autacoids from omega-3 PUFAs (Schmitz and Ecker, 2008). Moreover, the dietary supplement rich in omega-6 PUFAs shifts the physiological state to prothrombotic and proaggregatory conditions. Therefore, a high ratio of omega-6/omega-3 is a risk factor for cardiovascular disease. Unlike *C. elegans*, mammalian cells are unable to convert omega-6 to omega-3 PUFAs endogenously because they lack the converting enzyme, omega-3 desaturase (Simopoulos, 2008). In this regard, it is essential to increase the omega-3 but decrease the omega-6 PUFA intake in order to reduce the risk of many of the chronic inflammatory diseases.

4.6 Development of resolvins as new drug candidates for chronic inflammatory diseases

Anti-inflammatory drugs have traditionally been developed based on their capability to

interfere with the pro-inflammatory signaling cascade. Although the clinical result of these anti-inflammatory drugs, such as selective COX inhibitors, is promising, some delay resolution of inflammation and show serious side effects including heart attack and stroke. Therefore, the therapeutic approach to overcome these side effects is needed (Dogne et al., 2006). Given the biological effects of resolvins, the pathway involved in formation and activation of these molecules provides a new paradigm for investing fascinating anti-inflammatory drugs. Even though several pharmacological effects have been demonstrated in animal models, the potential of resolvins as therapeutic agents for human remains to be clarified. However, it is clear that resolvins have a number of benefits over classical anti-inflammatory drugs which block single immune mediators such as pro-inflammatory cytokines. Resolvins are anticipated as desirable therapeutics for inflammation treatment as they exert showing receptor-specific actions, possess both anti-inflammatory and pro-resolving effects and reduce inflammation without immunesuppression. In addition to dampening entire networks of multiple pro-inflammatory mediators, but resolvins can also activate endogenous resolution pathway. Moreover, they protect healthy tissue and promote tissue repair. Recently, Rexolvyx pharmaceuticals has developed resolvins as therapeutics for multiple inflammatory diseases such as dry eyes, retinal diseases, asthma, inflammatory bowel diseases, rheumatoid arthritis, cardiovascular diseases and lung inflammation. The clinical study of RX-10001 (RvE1), formulated for oral delivery,

showed the positive Phase I result in asthma, inflammatory bowel diseases, rheumatic arthritis and cardiovascular diseases. Especially, RX-10045 (a synthetic resolvin analogue) has been revealed to improve the signs and symptoms of dry eye effectively in Phase II study, thereby, now moving on to Phase III trials. Besides RX-10001 and RX-10045, RX-20001 (protectin D1) and other resolvin analogs have been developed and examined clinically (www.resolvyx.com) (Lee, 2012).

4.7 Resolvins as cancer chemopreventive agents

As mentioned, resolvins have the potential to prevent chronic inflammatory diseases, especially colitis, by regulating the action of immune cells, inhibiting the production of pro-inflammatory cytokines and promoting the generation of anti-inflammatory cytokines (Arita et al., 2005a; Ishida et al., 2010b). Moreover, the correlation between omega-3 PUFA and cancer prevention indirectly supports the cancer preventive potential of resolvins. The increase in endogenous levels of omega-3 PUFA was inversely associated with the reduced incidence of colorectal tumors induced by azoxymethane plus dextran sodium sulfate in the *fat-1* transgenic mouse model. In the colons of these *fat-1* transgenic mice, the levels of omega-3 PUFA-derived mediators including RvE1, RvD3 and NPD1/PD1 were significantly elevated, whereas the levels of pro-inflammatory cytokines were reduced (Nowak et al., 2007). In this context, resolvins are anticipated to have a potential in preventing colitis and colon cancer.

5. Conclusion and future perspectives

Acute inflammation is a protective mechanism, but excessive uncontrolled inflammatory responses lead to chronic inflammatory diseases which are linked to cancer. It is clear that inflammation is a tightly regulated process, controlled by several mediators and cell-mediated responses limiting the duration and magnitude of inflammation. For complete resolution of inflammation, multiple cellular responses are necessary; apoptosis of PMNs, efferocytosis and exfiltration of inflammatory cells, all of which are regulated by a decrease of proinflammatory mediators and a concomitant increase of anti-inflammatory and pro-resolving mediators. This lipid mediator class switching, from pro-inflammatory (derived from omega-6 PUFAs) to anti-inflammatory and pro-resolving mediators (mostly derived from omega-3 PUFAs), is a key event for driving pro-resolution state. Defects in endogenous pro-resolving and anti-inflammatory pathways will undoubtedly predispose to the development of chronic inflammatory diseases and cancer. Therefore, a further understanding and analysis of these pathways in the pathogenesis of chronic inflammation and tumorigenesis is required.

Existing drugs for chronic inflammatory diseases mostly rely on their anti-inflammatory effects. However, some of them are potentially resolution-toxic as they can prolong the time to resolve and repair tissues injured by inflammation, and increase the morbidity in inflammatory diseases. To more successfully prevent and treat chronic

inflammatory diseases and inflammation-associated cancer, it would be better to develop therapeutic drugs that can promote resolution of inflammation, thereby blocking the progression to the chronic inflammatory state. The recently uncovered families of omega-3 PUFA-derived mediators, resolvins and protectins, now open novel approaches to design ‘resolution-friendly’ replacement therapies. Furthermore, biological mimetics of naturally generated pro-resolving mediators are expected as good alternatives for the management of inflammatory diseases and inflammation-induced cancer.

6. References

Ariel, A., Fredman, G., Sun, Y. P., Kantarci, A., Van Dyke, T. E., Luster, A. D. and Serhan, C. N. (2006). Apoptotic neutrophils and T cells sequester chemokines during immune response resolution through modulation of CCR5 expression. *Nature immunology,* 7, 1209-1216.

Arita, M., Ohira, T., Sun, Y. P., Elangovan, S., Chiang, N. and Serhan, C. N. (2007). Resolvin E1 selectively interacts with leukotriene B4 receptor BLT1 and ChemR23 to regulate inflammation. *J Immunol,* 178, 3912-3917.

Arita, M., Yoshida, M., Hong, S., Tjonahen, E., Glickman, J. N., Petasis, N. A., Blumberg, R. S. and Serhan, C. N. (2005a). Resolvin E1, an endogenous lipid mediator derived from omega-3 eicosapentaenoic acid, protects against 2,4,6-trinitrobenzene sulfonic acid-induced colitis. *P Natl Acad Sci USA,* 102, 7671-7676.

Arita, M., Bianchini, F., Aliberti, J., Sher, A., Chiang, N., Hong, S., Yang, R., Petasis, N. A. and Serhan, C. N. (2005b). Stereochemical assignment, antiinflammatory properties, and receptor for the omega-3 lipid mediator resolvin E1. *The Journal of experimental medicine,* 201, 713-722.

Bagga, D., Wang, L., Farias-Eisner, R., Glaspy, J. A. and Reddy, S. T. (2003). Differential effects of prostaglandin derived from omega-6 and omega-3 polyunsaturated fatty acids on COX-2 expression and IL-6 secretion. *P Natl Acad Sci USA,* 100, 1751-1756.

Bannenberg, G. L., Chiang, N., Ariel, A., Arita, M., Tjonahen, E., Gotlinger, K. H., Hong, S. and Serhan, C. N. (2005). Molecular circuits of resolution: formation and actions of resolvins and protectins. *J Immunol,* 174, 4345-4355.

Bellingan, G. J., Caldwell, H., Howie, S. E., Dransfield, I. and Haslett, C. (1996). In vivo fate of the inflammatory macrophage during the resolution of inflammation: inflammatory macrophages do not die locally, but emigrate to the draining lymph nodes. *J Immunol*, 157, 2577-2585.

Bellingan, G. J., Xu, P., Cooksley, H., Cauldwell, H., Shock, A., Bottoms, S., Haslett, C., Mutsaers, S. E. and Laurent, G. J. (2002). Adhesion molecule-dependent mechanisms regulate the rate of macrophage clearance during the resolution of peritoneal inflammation. *The Journal of experimental medicine,* 196, 1515-1521.

Bian, Z., Guo, Y., Ha, B., Zen, K. and Liu, Y. (2012). Regulation of the inflammatory response: enhancing neutrophil infiltration under chronic inflammatory conditions. *J Immunol,* 188, 844-853.

Chiang, N., Fredman, G., Backhed, F., Oh, S. F., Vickery, T., Schmidt, B. A. and Serhan, C. N. (2012). Infection regulates pro-resolving mediators that lower antibiotic requirements. *Nature,* 484, 524-528.

Connor, K. M., SanGiovanni, J. P., Lofqvist, C., Aderman, C. M., Chen, J., Higuchi, A., Hong, S., Pravda, E. A., Majchrzak, S., Carper, D. et al. (2007). Increased dietary intake of omega-3-polyunsaturated fatty acids reduces pathological retinal angiogenesis. *Nature medicine,* 13, 868-873.

Dogne, J. M., Hanson, J., Supuran, C. and Pratico, D. (2006). Coxibs and

cardiovascular side-effects: from light to shadow. *Current pharmaceutical design,* 12, 971-975.

Fadok, V. A., Bratton, D. L., Konowal, A., Freed, P. W., Westcott, J. Y. and Henson, P. M. (1998). Macrophages that have ingested apoptotic cells in vitro inhibit proinflammatory cytokine production through autocrine/paracrine mechanisms involving TGF-beta, PGE2, and PAF. *The Journal of clinical investigation*,101, 890-898.

Gilroy, D. W., Lawrence, T., Perretti, M. and Rossi, A. G. (2004). Inflammatory resolution: new opportunities for drug discovery. *Nature reviews. Drug discovery,* 3, 401-416.

Gilroy, D. W., Colville-Nash, P. R., Willis, D., Chivers, J., Paul-Clark, M. J. and Willoughby, D. A. (1999). Inducible cyclooxygenase may have anti-inflammatory properties. *Nature medicine,* 5, 698-701.

Golpon, H. A., Fadok, V. A., Taraseviciene-Stewart, L., Scerbavicius, R., Sauer, C., Welte, T., Henson, P. M. and Voelkel, N. F. (2004). Life after corpse engulfment: phagocytosis of apoptotic cells leads to VEGF secretion and cell growth. *FASEB journal : official publication of the Federation of American Societies for Experimental Biology,* 18, 1716-1718.

Gronert, K., Kantarci, A., Levy, B. D., Clish, C. B., Odparlik, S., Hasturk, H., Badwey, J. A., Colgan, S. P., Van Dyke, T. E. and Serhan, C. N. (2004). A molecular defect in intracellular lipid signaling in human neutrophils in localized aggressive periodontal tissue damage. *J Immunol,* 172, 1856-1861.

Han, Z., Boyle, D. L., Manning, A. M. and Firestein, G. S. (1998). AP-1 and NF-kappaB regulation in rheumatoid arthritis and murine collagen-induced arthritis. *Autoimmunity,* 28, 197-208.

Hart, L. A., Krishnan, V. L., Adcock, I. M., Barnes, P. J. and Chung, K. F. (1998). Activation and localization of transcription factor, nuclear factor-kappaB, in asthma. *American journal of respiratory and critical care medicine,* 158, 1585-1592.

Hasturk, H., Kantarci, A., Ohira, T., Arita, M., Ebrahimi, N., Chiang, N., Petasis, N. A., Levy, B. D., Serhan, C. N. and Van Dyke, T. E. (2006). RvE1 protects from local inflammation and osteoclast- mediated bone destruction in periodontitis. *FASEB journal : official publication of the Federation of American Societies for Experimental Biology,* 20, 401-403.

Hong, S., Gronert, K., Devchand, P. R., Moussignac, R. L. and Serhan, C. N. (2003). Novel docosatrienes and 17S-resolvins generated from docosahexaenoic acid in murine brain, human blood, and glial cells. Autacoids in anti-inflammation. *The Journal of biological chemistry,* 278, 14677-14687.

Ishida, T., Yoshida, M., Arita, M., Nishitani, Y., Nishiumi, S., Masuda, A., Mizuno, S., Takagawa, T., Morita, Y., Kutsumi, H. et al. (2010a). Resolvin E1, an endogenous lipid mediator derived from eicosapentaenoic acid, prevents dextran sulfate sodium-induced colitis. *Inflammatory bowel diseases,* 16, 87-95.

Ishida, T., Yoshida, M., Arita, M., Nishitani, Y., Nishiumi, S., Masuda, A., Mizuno, S., Takagawa, T., Morita, Y., Kutsumi, H. et al. (2010b). Resolvin E1, an

Endogenous Lipid Mediator Derived from Eicosapentaenoic Acid, Prevents Dextran Sulfate Sodium-Induced Colitis. *Inflamm Bowel Dis,* 16, 87-95.
Khanna, S., Biswas, S., Shang, Y., Collard, E., Azad, A., Kauh, C., Bhasker, V., Gordillo, G. M., Sen, C. K. and Roy, S. (2010). Macrophage dysfunction impairs resolution of inflammation in the wounds of diabetic mice. *PloS one,* 5, e9539.
Krishnamoorthy, S., Recchiuti, A., Chiang, N., Yacoubian, S., Lee, C. H., Yang, R., Petasis, N. A. and Serhan, C. N. (2010). Resolvin D1 binds human phagocytes with evidence for proresolving receptors. *P Natl Acad Sci USA,* 107, 1660-1665.
Krishnamoorthy, S., Recchiuti, A., Chiang, N., Fredman, G. and Serhan, C. N. (2012). Resolvin D1 receptor stereoselectivity and regulation of inflammation and proresolving microRNAs. *Am J Pathol,* 180, 2018-2027.
Lawrence, T., Willoughby, D. A. and Gilroy, D. W. (2002). Anti-inflammatory lipid mediators and insights into the resolution of inflammation. *Nature reviews Immunology,* 2, 787-795.
Lee, C. H. (2012). Resolvins as new fascinating drug candidates for inflammatory diseases. *Archives of pharmacal research,* 35, 3-7.
Levy, B. D., Clish, C. B., Schmidt, B., Gronert, K. and Serhan, C. N. (2001). Lipid mediator class switching during acute inflammation: signals in resolution. *Nature immunology,* 2, 612-619.
Lopez-Castejon, G., Baroja-Mazo, A. and Pelegrin, P. (2011). Novel macrophage polarization model: from gene expression to identification of new anti-inflammatory molecules. *Cellular and molecular life sciences : CMLS,* 68, 3095-3107.
Martinez, F. O., Helming, L. and Gordon, S. (2009). Alternative activation of macrophages: an immunologic functional perspective. *Annual review of immunology,* 27, 451-483.
Medzhitov, R. (2008). Origin and physiological roles of inflammation. *Nature,* 454, 428-435.
Mukherjee, P. K., Marcheselli, V. L., Serhan, C. N. and Bazan, N. G. (2004). Neuroprotectin D1: a docosahexaenoic acid-derived docosatriene protects human retinal pigment epithelial cells from oxidative stress. *P Natl Acad Sci USA,* 101, 8491-8496.
Nathan, C. (2006). Neutrophils and immunity: challenges and opportunities. *Nature reviews. Immunology,* 6, 173-182.
Nathan, C. and Ding, A. (2010). Nonresolving inflammation. *Cell,* 140, 871-882.
Nofer, J. R., Bot, M., Brodde, M., Taylor, P. J., Salm, P., Brinkmann, V., van Berkel, T., Assmann, G. and Biessen, E. A. (2007). FTY720, a synthetic sphingosine 1 phosphate analogue, inhibits development of atherosclerosis in low-density lipoprotein receptor-deficient mice. *Circulation,* 115, 501-508.
Norling, L. V., Dalli, J., Flower, R. J., Serhan, C. N. and Perretti, M. (2012). Resolvin D1 Limits Polymorphonuclear Leukocytes Recruitment to Inflammatory Loci: Receptor-Dependent Actions. *Arteriosclerosis, thrombosis, and vascular biology.*
Nowak, J., Weylandt, K. H., Habbel, P., Wang, J., Dignass, A., Glickman, J. N. and Kang, J. X. (2007). Colitis-associated colon tumorigenesis is suppressed in

transgenic mice rich in endogenous n-3 fatty acids. *Carcinogenesis,* 28, 1991-1995.

Odegaard, J. I., Ricardo-Gonzalez, R. R., Goforth, M. H., Morel, C. R., Subramanian, V., Mukundan, L., Red Eagle, A., Vats, D., Brombacher, F., Ferrante, A. W. et al. (2007). Macrophage-specific PPARgamma controls alternative activation and improves insulin resistance. *Nature,* 447, 1116-1120.

Odusanwo, O., Chinthamani, S., McCall, A., Duffey, M. E. and Baker, O. J. (2012). Resolvin D1 prevents TNF-alpha-mediated disruption of salivary epithelial formation. *American journal of physiology. Cell physiology,* 302, C1331-1345.

Oh, S. F., Pillai, P. S., Recchiuti, A., Yang, R. and Serhan, C. N. (2011). Pro-resolving actions and stereoselective biosynthesis of 18S E-series resolvins in human leukocytes and murine inflammation. *The Journal of clinical investigation,* 121, 569-581.

Park, C. K., Xu, Z. Z., Liu, T., Lu, N., Serhan, C. N. and Ji, R. R. (2011). Resolvin D2 is a potent endogenous inhibitor for transient receptor potential subtype V1/A1, inflammatory pain, and spinal cord synaptic plasticity in mice: distinct roles of resolvin D1, D2, and E1. *The Journal of neuroscience : the official journal of the Society for Neuroscience,* 31, 18433-18438.

Rajakariar, R., Yaqoob, M. M. and Gilroy, D. W. (2006). COX-2 in inflammation and resolution. *Molecular interventions,* 6, 199-207.

Savill, J. and Fadok, V. (2000). Corpse clearance defines the meaning of cell death. *Nature,* 407, 784-788.

Schmitz, G. and Ecker, J. (2008). The opposing effects of n-3 and n-6 fatty acids. *Progress in lipid research*, 47, 147-155.

Schwab, J. M. and Serhan, C. N. (2006). Lipoxins and new lipid mediators in the resolution of inflammation. *Current opinion in pharmacology,* 6, 414-420.

Schwab, J. M., Chiang, N., Arita, M. and Serhan, C. N. (2007). Resolvin E1 and protectin D1 activate inflammation-resolution programmes. *Nature,* 447, 869-874.

Serhan, C. N. (2007). Resolution phase of inflammation: novel endogenous anti-inflammatory and proresolving lipid mediators and pathways. *Annual review of immunology,* 25, 101-137.

Serhan, C. N. (2008). Controlling the resolution of acute inflammation: a new genus of dual anti-inflammatory and proresolving mediators. *Journal of periodontology,* 79, 1520-1526.

Serhan, C. N. and Savill, J. (2005). Resolution of inflammation: the beginning programs the end. *Nature immunology,* 6, 1191-1197.

Serhan, C. N. and Chiang, N. (2008). Endogenous pro-resolving and anti-inflammatory lipid mediators: a new pharmacologic genus. *British journal of pharmacology,* 153 Suppl 1, S200-215.

Serhan, C. N. and Petasis, N. A. (2011). Resolvins and protectins in inflammation resolution. *Chemical reviews,* 111, 5922-5943.

Serhan, C. N., Hong, S. and Lu, Y. (2006). Lipid mediator informatics-lipidomics: novel pathways in mapping resolution. *The AAPS journal,* 8, E284-297.

Serhan, C. N., Chiang, N. and Van Dyke, T. E. (2008). Resolving inflammation: dual anti-inflammatory and pro-resolution lipid mediators. *Nature reviews. Immunology,* 8, 349-361.

Serhan, C. N., Clish, C. B., Brannon, J., Colgan, S. P., Chiang, N. and Gronert, K. (2000). Novel functional sets of lipid-derived mediators with antiinflammatory actions generated from omega-3 fatty acids via cyclooxygenase 2-nonsteroidal antiinflammatory drugs and transcellular processing. *The Journal of experimental medicine,* 192, 1197-1204.

Serhan, C. N., Hong, S., Gronert, K., Colgan, S. P., Devchand, P. R., Mirick, G. and Moussignac, R. L. (2002). Resolvins: a family of bioactive products of omega-3 fatty acid transformation circuits initiated by aspirin treatment that counter proinflammation signals. *The Journal of experimental medicine,* 196, 1025-1037.

Serhan, C. N., Yang, R., Martinod, K., Kasuga, K., Pillai, P. S., Porter, T. F., Oh, S. F. and Spite, M. (2009). Maresins: novel macrophage mediators with potent antiinflammatory and proresolving actions. *The Journal of experimental medicine,* 206, 15-23.

Serhan, C. N., Brain, S. D., Buckley, C. D., Gilroy, D. W., Haslett, C., O'Neill, L. A., Perretti, M., Rossi, A. G. and Wallace, J. L. (2007). Resolution of inflammation: state of the art, definitions and terms. *FASEB journal : official publication of the Federation of American Societies for Experimental Biology,* 21, 325-332.

Serhan, C. N., Jain, A., Marleau, S., Clish, C., Kantarci, A., Behbehani, B., Colgan, S. P., Stahl, G. L., Merched, A., Petasis, N. A. et al. (2003). Reduced inflammation and tissue damage in transgenic rabbits overexpressing 15-lipoxygenase and endogenous anti-inflammatory lipid mediators. *J Immunol,* 171, 6856-6865.

Simopoulos, A. P. (2002). Omega-3 fatty acids in inflammation and autoimmune diseases. *Journal of the American College of Nutrition,* 21, 495-505.

Simopoulos, A. P. (2008). The importance of the omega-6/omega-3 fatty acid ratio in cardiovascular disease and other chronic diseases. *Exp Biol Med (Maywood),* 233, 674-688.

Simopoulos, A. P., Leaf, A. and Salem, N., Jr. (1999). Workshop on the Essentiality of and Recommended Dietary Intakes for Omega-6 and Omega-3 Fatty Acids. *Journal of the American College of Nutrition,* 18, 487-489.

Spite, M. and Serhan, C. N. (2010). Novel lipid mediators promote resolution of acute inflammation: impact of aspirin and statins. *Circulation research,* 107, 1170-1184.

Stein, M., Keshav, S., Harris, N. and Gordon, S. (1992). Interleukin 4 potently enhances murine macrophage mannose receptor activity: a marker of alternative immunologic macrophage activation. *The Journal of experimental medicine,* 176, 287-292.

Sun, Y. P., Oh, S. F., Uddin, J., Yang, R., Gotlinger, K., Campbell, E., Colgan, S. P., Petasis, N. A. and Serhan, C. N. (2007). Resolvin D1 and its aspirin-triggered 17R epimer. Stereochemical assignments, anti-inflammatory properties, and enzymatic inactivation. *The Journal of biological chemistry,* 282, 9323-9334.

Tabas, I. (2010). Macrophage death and defective inflammation resolution in

atherosclerosis. *Nature reviews. Immunology,* 10, 36-46.
Tak, P. P. and Firestein, G. S. (2001). NF-kappaB: a key role in inflammatory diseases. *The Journal of clinical investigation,* 107, 7-11.
Titos, E., Rius, B., Gonzalez-Periz, A., Lopez-Vicario, C., Moran-Salvador, E., Martinez-Clemente, M., Arroyo, V. and Claria, J. (2011). Resolvin D1 and its precursor docosahexaenoic acid promote resolution of adipose tissue inflammation by eliciting macrophage polarization toward an M2-like phenotype. *J Immunol,* 187, 5408-5418.
Tjonahen, E., Oh, S. F., Siegelman, J., Elangovan, S., Percarpio, K. B., Hong, S., Arita, M. and Serhan, C. N. (2006). Resolvin E2: identification and anti-inflammatory actions: pivotal role of human 5-lipoxygenase in resolvin E series biosynthesis. *Chemistry & biology,* 13, 1193-1202.
Van Hove, C. L., Maes, T., Joos, G. F. and Tournoy, K. G. (2008). Chronic inflammation in asthma: a contest of persistence vs resolution. *Allergy,* 63, 1095-1109.
Vandivier, R. W., Henson, P. M. and Douglas, I. S. (2006). Burying the dead: the impact of failed apoptotic cell removal (efferocytosis) on chronic inflammatory lung disease. *Chest* 129, 1673-1682.
Voll, R. E., Herrmann, M., Roth, E. A., Stach, C., Kalden, J. R. and Girkontaite, I. (1997). Immunosuppressive effects of apoptotic cells. *Nature,* 390, 350-351.
Wang, B., Gong, X., Wan, J. Y., Zhang, L., Zhang, Z., Li, H. Z. and Min, S. (2011). Resolvin D1 protects mice from LPS-induced acute lung injury. *Pulmonary pharmacology & therapeutics,* 24, 434-441.
Willoughby, D. A., Moore, A. R., Colville-Nash, P. R. and Gilroy, D. (2000). Resolution of inflammation. *International journal of immunopharmacology,* 22, 1131-1135.

PURPOSE OF THE STUDY

Chronic inflammation has long been through to contribute to the development of several disorders including cancer. To prevent chronic inflammatory diseases and inflammation-associated cancer, resolution of inflammation is essential. Recently, it is uncovered that resolution of inflammation is controlled by pro-resolving lipid mediators such as RvD1. In the present study, the molecular mechanism underlying RvD1-mediated resolution of inflammation was investigated, especially focused on efferocytosis. Not only efferocytosis, but macrophage survival engulfing apoptotic PMNs is also an important factor for complete resolution of inflammation. In this regard, the preventive effect of RvD1 on efferocytosis-induced oxidative stress and apoptosis was examined. Finally, the present study aimed to elucidate whether pro-resolving lipid mediator RvD1 has the preventive effect on inflammation-induced tumorigenesis.

Chapter II

Resolvin D1 stimulates efferocytosis through p50/p50-mediated suppression of tumor necrosis factor-α expression

1. Abstract

Phagocytosis of apoptotic neutrophils, termed efferocytosis, is essential for the resolution of inflammation as it prevents the exposure of surrounding tissues at the inflamed site to toxic contents of lytic cells. Resolvin D1 (RvD1), endogenously generated from docosahexaenoic acid during resolution of inflammation, is known to stimulate efferocytosis. However, the molecular mechanism underlying RvD1-mediated enhancement of efferocytosis remains largely unresolved. In the present study, murine macrophage-like RAW264.7 cells treated with lipopolysaccharide (LPS) exhibited markedly reduced efferocytic activity, but this was restored by the co-incubation with RvD1. RvD1-induced restoration of the efferocytic activity appears to be mediated by down-regulating the LPS-induced TNF-α expression. The inhibitory effect of RvD1 on LPS-induced TNF-α expression was associated with enhanced nuclear localization of p50/p50 homodimer and concomitant reduction of p65/p50 heterodimer accumulation in the nucleus. RvD1 triggered phosphorylation and proteasomal degradation of nuclear factor κB1 (NF-κB1) p105 to generate p50, which was subsequently translocated to nucleus as p50/p50 homodimer. Knockdown of NF-κB p50 abolished the ability of RvD1 to suppress TNF-α expression and also to restore efferocytosis, suggesting that the replacement of p65/p50 with p50/p50 homodimer in the nucleus is critical for RvD1-mediated stimulation of efferocytosis. In a murine peritonitis model, intraperitoneal administration of RvD1 abrogated the zymosan A-

induced TNF-α production, thereby stimulating efferocytosis. Taken together, these findings indicate that RvD1 expedites the resolution of inflammation through induction of efferocytosis by p50/p50 homodimer-mediated repression of TNF-α production.

Key words

Resolvin D1, efferocytosis, TNF-α, NF-κB

2. Introduction

Acute inflammation is an essential process in defending the host against infection. During inflammation, circulating neutrophils infiltrate first into the inflamed site to eliminate the injurious stimuli, and subsequently undergo apoptosis. The removal of apoptotic neutrophils allows resolution of inflammation whereby tissue homeostasis can be restored. The clearance of apoptotic neutrophils by macrophages, the process termed 'efferocytosis', is an important step in preventing tissue necrosis and chronic inflammation which can be caused by disgorgement of toxic contents from apoptotic neutrophils (Serhan and Savill, 2005; Vandivier et al., 2006; Serhan et al., 2007). The process of efferocytosis has been reported to be controlled actively, in part, by the endogenously generated chemical mediators or local autacoids, which stimulate the pro-resolving ability of macrophages. Resolvin D1 is one of the pro-resolving lipid mediators formed from docosahexaenoic acid (DHA; C22:6), a representative omega-3 fatty acid in sequential reactions catalyzed by 15-lipoxygenase (15-LOX) and 5-LOX (Hong et al., 2003). It has been reported that RvD1 limits infiltration of polymorphonuclear leukocytes (PMN), but enhances the infiltration of monocytes to the inflammatory site. Furthermore, in a murine model of peritonitis, intraperitoneal administration of RvD1 has been shown to increase the efferocytic activity of macrophages (Sun et al., 2007). However, the molecular mechanisms responsible for the enhancement of efferocytic activity of macrophages by RvD1 have not been fully

clarified.

Tumor necrosis factor-α (TNF-α) is one of the major pro-inflammatory cytokines that stimulates the release of other mediators of inflammation, thereby inciting further inflammatory responses. Hence, prolonged or elevated production of TNF-α triggers chronic inflammation. Recent findings have demonstrated that TNF-α perturbs complete resolution of inflammation by inhibiting efferocytosis (McPhillips et al., 2007; Borges et al., 2009). The TNF-α expression is mainly under the regulation of nuclear factor-κB (NF-κB). The promoter region of *TNF-α* gene harbors four NF-κB binding sequences (κB_1, κB_2, κB_{2a} and κB_3) (Baer et al., 1998). The NF-κB family is composed of either hetero- or homodimers of five subunit members. These include p65 (RelA), p105/p50 (NF-κB1), p100/p52 (NF-κB2), c-Rel and RelB. Whereas NF-κB, present predominantly as a p65/p50 heterodimer, transactivates a battery of pro-inflammatory genes including *TNF-α*, an atypical NF-κB species (p50/p50 homodimer) induces transcriptional repression of target genes (Barchowsky et al., 2000; Wessells et al., 2004).

In resting cells, NF-κB1 (p105/p50) exists as an inactive complex in the cytoplasm, where the C-terminal domain of p105 (alternatively known as IκBγ) masks the nuclear localization signal domain of p50 and hampers its nuclear translocation (Moorthy and Ghosh, 2003)**.** During resolution of inflammation, proteasomal cleavage of the C-terminal portion of p105 generates p50, which then forms p50/p50 homodimer

(Salmeron et al., 2001). It has been reported that the p50/p50 homodimer forms a complex with Bcl3 and hastens the resolution of inflammation by inducing the transcription of anti-inflammatory genes (Singh and Jiang, 2004).

Since TNF-α acts as a mediator of inflammation partly by blocking efferocytosis, we investigated whether RvD1-induced efferocytosis and subsequent resolution of inflammation are mediated through the negative regulation of TNF-α. Here, we report that RvD1 potentiates efferocytic activity of macrophages through inhibition of TNF-α production by modulating the NF-κB signaling by two distinct mechanisms; 1) inhibition of the classical NF-κB (p65/p50) pathway and 2) activation of an atypical NF-κB (p50/p50) pathway. Our study reveals that RvD1 induces predominantly the formation of p50/p50 homodimer, while it inhibits lipopolysaccharide (LPS)-induced activation of p65/p50 heterodimer in RAW264.7 macrophages. Thus, the pro-resolving effect of RvD1 is preferentially mediated through modulation of the NF-κB-TNF-α axis.

3. Materials and Methods

Materials

RvD1 was purchased from Cayman Chemical Co. (Ann Arbor, MI, USA). LPS (*Escherichia coli* O111:B4) was obtained from Sigma-Aldrich (St Louis, MO, USA). Recombinant mouse TNF-α was produced from the R&D systems (Minneapolis, MN, USA). Dulbecco's Modified Eagle Medium (DMEM), RPMI 1640 and fetal bovine serum (FBS) were purchased from Gibco BRL (Grand Island, NY, USA). Primary antibodies against p105/p50, phospho-NF-κB p50, phospho-IKKα/β, IKKβ, IκB-α, ERK1/2, phospho-ERK (Tyr 204), phospho-JNK (Tyr 183/ Tyr 185), JNK, phospho-p38 (Tyr 182) and p38 were purchased from Santa Cruz Biotechnology (Santa Cruz, CA, USA), and antibodies against p65 and phospho-IκB-α was obtained from Cell Signaling (Beverly, MA, USA). The anti-rabbit and anti-mouse horseradish peroxidase-conjugated secondary antibodies, and anti-lamin B_1 were purchased from Zymed Laboratories (San Francisco, CA, USA).

Cell culture

RAW264.7 macrophages and Jurkat T cells were purchased from American Type Culture Collection (ATCC, Manassas, VA, USA). Cells were cultured in DMEM (for RAW264.7 cells) and RPMI 1640 (for peritoneal macrophages and Jurkat T cells) with 10% FBS, 100 μg/ml streptomycin and 100 U/ml penicillin in humidified 5% CO_2 at

37 °C.

Zymosan A-induced peritonitis

Institute of Cancer Research (ICR) mice (8 weeks of age) were purchased from Central Lab Animal Inc. (Seoul, South Korea). All the animals were maintained according to the Institutional Animal Care Guidelines. Animal experimental procedures were approved by the Institutional Animal Care and Use Committee at Seoul National University. Zymosan A (30 mg/kg, Sigma, St Louis, MO, USA) was administered intraperitonally 12 h before giving dimethyl sulfoxide (DMSO), RvD1 (300 ng/mouse, i.p.) or TNF-α **(**10 ng/mouse, i.p.**)** and mice were sacrificed 6 h later. Mice were sacrificed by exposure to carbon dioxide, and peritoneal leukocytes were harvested by washing with 3 ml of phosphate-buffered saline (PBS) containing 3 mM ehtylenediaminetetraacetate (EDTA).

Total and differential leukocyte counts

Total peritoneal leukocyte counts were carried out using Turk's solution (0.01% crystal violet in 3% acetic acid) in a hematocytometer. For the differential count, peritoneal exudate cells were spun in a cytocentrifuge at 400 x *g* for 5 min onto a slide and stained with Wright-Giemsa stain.

Efferocytosis assay

To assess the percentage of macrophages engulfing apoptotic PMNs in vivo, peritoneal exudate cells were exposed first to anti-mouse CD16/32 blocking antibody (eBioscience, San Diego, CA, USA) for 5 min and then labeled with the FluoroTag fluorescein isothiocyanate (FITC)-conjugated anti-mouse F4/80 antibody (eBioscience) for 20 min. The labeled cells were permeabilized for 10 min using 0.1% Triton X-100 and then labeled further for 20 min with PE-conjugated anti-mouse Gr-1 (Ly-6G) antibody (eBioscience). The proportion of macrophages containing neutrophils ($F4/80^{+}/Gr\text{-}1^{+}$) was determined by employing flow cytometry. For an *ex vivo* efferocytosis assay, mouse peritoneal macrophages were incubated in 6-well flat-bottom microtiter plates for 24 h. Non-adherent cells were collected and incubated for additional 24 h to induce apoptosis. After washed with medium, adherent monolayer cells were co-incubated for 1 h with apoptotic non-adherent cells which are mostly composed of neutrophils. Peritoneal macrophages engulfing apoptotic cells were evaluated as described above.

To determine the *in vitro* efferocytic activity of macrophages, RAW264.7 cells were co-incubated for 1 h with Jurkat T cells (stained with FITC-conjugated annexin V) undergoing apoptosis. To remove the non-engulfed apoptotic Jurkat T cells, RAW264.7 cells were washed three times with PBS and the proportion of RAW264.7 cells containing apoptotic Jurkat T cells (FITC-positive cells) were assessed by flow

cytometry and fluorescent microscopy. Apoptosis of Jurkat T cells was induced by serum withdrawal and UVB (180 mJ/cm^2) irradiation, followed by incubation for 8 h at 37 °C in 5 % CO_2 atmosphere.

Measurement of TNF-α

The concentrations of TNF-α in cell-free peritoneal lavage and in culture supernatant were determined by using Mouse TNF-α ELISA kits (KOMA BIOTECH Inc., Seoul, Korea) according to the manufacturer's instructions.

Flow cytometry

RAW264.7 cells were fixed with 10% buffered formalin solution (20 min), washed in PBS twice, and blocked with 2% BSA in PBS (30 min). FITC-conjuagated anti-CD36 antibodies (Abcam, Cambridge, England), diluted 1:50 in 2% bovine serum albumin (BSA) in PBS, were kept for 1 h on ice. Cells were analyzed using FACSCalibur Flow Cytometer (BD, Franklin Lakes, NJ, USA).

Reverse Transcription-Polymerase Chain Reaction (RT-PCR)

Total RNA was isolated from RAW264.7 cells using TRIzol® reagent (Invitrogen, Carlsbad, CA, USA) according to the manufacturer's protocol. One microgram of total RNA was reverse transcribed by using reverse transcriptase of murine leukemia virus

(Promega, Madison, WI, USA). PCR was carried out in a thermo-cycler using specific primers for *TNF-α, p50* and *actin*. The primers employed are as follows (forward and reverse, respectively): *TNF-α*; 5'-TGA ACT TCG GGG TGA TCG GTC-3' and 5'-AGC CTT GTC CCT TGA AGA GAA C-3', *p50*; 5'-ATG TTC ACA GCC TTC CTC CC-3' and 5'-GGT AAA TCT CCT CCC CTC CC-3', *actin*; 5'-AGA GCA TAG CCC TCG TAG AT-3' and 5'-CCC AGA GCA AGA GAG GTA TC-3'. PCR products were resolved by 2% agarose gel electrophoresis, stained with ethidium bromide, and photographed under ultraviolet light.

NF-κB reporter gene analysis

RAW264.7 cells were grown to 80% confluence in 6-well plates and transfected with 1 μg of the NF-κB reporter construct, along with 0.5 ug of pSVGal plasmid using LipofectAMINE 2000 (Invitrogen) in Opti-MEM medium (Gibco). After 24 h of transfection, cells were treated with LPS or RvD1 for additional 2 h, and then lysed using the reporter lysis buffer (Promega). Luciferase assays were performed using 20 μl of cell extract and 100 μl of luciferin substrate (Promega), and the luciferase activity was measured by using a luminometer (AntoLumat LB953, EG and G Berthold, Bad Widbad, Germany). The obtained luciferase activity was normalized by comparing with β-galactosidase activity, which was carried out according to the manufacturer's instructions (Promega β-Galactosidase Enzyme Assay System).

Protein extraction and Western blot analysis

Cytosolic extracts were obtained by suspending the cells in hypotonic buffer A [10 mM hydroxyethyl piperazineethanesulfonic acid (HEPES; pH7.9), 10 mM KCl, 2 mM $MgCl_2$, 1 mM dithiothreitol (DTT), 0.1 mM ethylenediaminetetraacetic acid (EDTA) and 0.1 mM phenylmethane-sulphonylfluoride (PMSF)] and Nondiet P-40 solution (0.1 %). The mixture was then centrifuged for 5 min at 12000 x *g* to obtain the cytosolic fraction, and the pellet was washed once with buffer A. To obtain the nuclear fraction, cell pellets were then suspended in hypertonic buffer C [50 mM HEPES (pH7.9), 50 mM KCl, 300 mM NaCl, 0.1 mM EDTA, 1 mM DTT, 0.1 mM PMSF and 10% glycerol]. Whole cells extracts were prepared by suspending the cells directly in the RIPA lysis buffer [20 mM Tris-HCl (pH 7.5), 150 mM NaCl, 1 mM Na_2EDTA, 1 mM ethylene glycol tetraacetic acid (EGTA), 1% Triton X-100, 2.5 mM sodium pyrophosphate, 1 mM β-glycerophosphate, 1 mM Na_3VO_4, 1 μg/ml leuptin, 1 mM PMSF] for 1 hr on ice and this was followed by centrifugation for 15 min at 12000 x *g*. Protein lysates (15 μg) were electrophoresed by sodium dodecyl sulphate (SDS)-polyacrylamide gel electrophoresis (PAGE) and the separated proteins were transferred to polyvinyl difluoride (PVDF) membrane (0.22 μm thickness; Gelman Laboratory, Ann Arbor, MI, USA). To block the non-specific binding of proteins with primary antibodies, the blots were incubated in a 5% non-fat dry milk-PBST buffer [PBS containing 0.1% Tween-20] for 1 hr at room temperature. The membranes were then

incubated with the primary antibody suspended in 3% non-fat milk PBST buffer overnight at 4 °C. This was followed by washing with 1X PBST and incubation using appropriate secondary antibody coupled to horseradish peroxidase. Proteins tagged with specific primary antibodies were visualized with an enhanced chemiluminescence detection kit (Amersham Pharmacia Biotech, Buckinghamshire, UK).

Electrophoretic mobility-gel shift assay (EMSA)

Customized double-stranded oligonucleotide containing the NF-κB binding domains was obtained from Promega, and 100 ng of the oligonucleotide was labeled with [γ-^{32}P]ATP by employing T4 polynucleotide kinase and was purified on a Nick column (Amersham Pharmacia Biotech, Buckinghamshire, UK). The nuclear protein (10 μg) was mixed with 4 μl of concentrated incubation buffer [10 mM Tris-HCl (pH7.5), 100 mM NaCl, 1 mM DTT, 1 mM EDTA, 4% glycerol and 0.1 mg/ml sonicated salmon sperm DNA] and the hypertonic buffer was added to make up the final volume 20 μl. After preincubation at room temperature for 15 min, the labeled oligonucleotide (400,000 cpm) was added to the nuclear fraction and incubation was continued for additional 50 min at room temperature. To ensure the specific binding of the labeled oligonucleotide to nuclear protein, a competition assay was carried out with the excess amounts of unlabeled oligonucleotide. After the incubation, 0.1% bromophenol blue (2 μl) was added, and NF-κB-DNA complexes were separated from the unbound free

probe by electrophoresis on 6% nondenaturing polyacrylamide gel in 1X TBE buffer [90 mM Tris base, 90 mM boric acid and 0.5 mM EDTA (pH 8.0)] at 140 V for 3 h. Gels were dried and exposed to X-ray film. For the antibody supershift assay, 1 μl of antibody specific either for NF-κB p50 or p65 was incubated with the nuclear protein extract for 30 min on ice prior to addition of the reaction mixture containing radiolabelled nucleotide.

In vitro IKK activity assay

Precleared cytosolic extracts (200 μg) were subjected to immunoprecipitation by using anti-IKKβ antibody for overnight. 20 μl of protein G-agarose beads (Santa Cruz Biotech) was then added to the mixture and rotated for 4 h at 4 °C. The immunoprecipitate thus obtained was suspended in 50 ul of reaction mix containing 47 μl 1 x kinase buffer [25 mM Tris-HCl (pH7.5), 5 mM glycerolphosphate, 2 mM DTT, 0.1 mM Na_3VO_4 and 10 mM $MgCl_2$], 1 μg GST-IκBα substrate protein and 10 μCi [γ-^{32}P]ATP and incubated at 30 °C for 45 min. The kinase reaction was stopped by the addition of 2 x SDS loading dye, boiled at 99 °C for 5 min. The supernatant was subjected to SDS-PAGE analysis, and the gel was stained with coomassie brilliant blue and destained with destaining solution (glacial acetic acid : methanol : distrilled water = 1 : 4 : 5, v/v). The destained gel was dried at 80 °C for 1 h and visualized by autoradiography.

Evaluation of DNA binding activity of p50

The DNA binding activity of p50 was measured in nuclear protein extracts (20 μg) by the TransAM^{TM} NF-kB p50 protein assay (Active Motif, Carlsbad, CA, USA), an ELISA-based method designed to detect and quantify NF-kB p50 subunit activation. The assay was performed according to the manufacturer's protocol.

Construction of p105

The cDNA of p105 was PCR amplified using the primers 5'-CCG CTC GAG ATG GCA GAC GAT GAT C-3' and 5'-CCG GAA TTC CTA AAT TTT GCC TTC AAT AGG-3'. The PCR product was sub-cloned into the pEGFP-C3 vector, and was validated by sequence analysis.

Immunocytochemistry

RAW264.7 macrophages were seeded at 3 x 10^4 cells per well in an 8 chamber plate and cultured in the serum-starved medium for 4 h. The cells were incubated for 30 min in the absence or presence of RvD1 and then fixed with 10% buffered formalin solution (20 min). The cells were then washed in PBS (twice for 5 min each), permeabilized with 0.2% triton X-100 (5 min), washed in PBS (twice for 5 min each), and blocked with 5% BSA in PBS (30 min). Polyclonal rabbit anti-p50 or -p65, diluted 1:100 in 1% BSA in PBS, were applied overnight at 4 °C. This was followed by

washing cells in PBS (twice for 5 min each) and then incubation for 1 h at room temperature with FITC-conjugated anti-rabbit IgG secondary antibody diluted at 1:1000 in 1% BSA-PBS. After washing (twice for 5 min each), cells were treated with propidium iodide. The p50 and p65 signals were detected using a confocal microscope (Nikon, Tokyo, Japan).

4. Results

RvD1 expedites the resolution of zymosan A-induced murine peritonitis by suppressing TNF-α production

In zymosan A-induced mouse acute peritonitis, the total leukocyte count in the peritoneal fluid normally reaches the maximum about at 12 h (Bannenberg et al., 2005). However, the number of inflammatory leukocytes (especially PMNs) in zymosan A-treated mouse peritoneal exudates sharply decreases during the resolution of peritonitis. In assessing its pro-resolving effect, RvD1 was given at the peak of peritoneal inflammation (12 h after zymosan A injection). RvD1 dramatically stimulated the resolution of peritonitis by decreasing the number of total leukocytes in the peritoneal exudates, as compared to that observed in mice challenged with zymosan A alone (**Fig. 2-1A**). The reduced PMNs count, but not that of mononuclear cells, reflected the loss of total leukocytes in peritoneal exudates (**Fig. 2-1B**). Therefore, administration of RvD1 altered the cellular composition in peritoneal exudates with an increase in the proportion of mononuclear cells and a concomitant decrease in the number of PMNs. Whereas PMNs are the principal inflammatory cells that appear in the initial phase of inflammation, mononuclear cells are predominant during the resolution phase of inflammation. Hence, it is ascertained that RvD1 accelerates resolution of zymosan A-induced murine peritonitis. In addition to reducing the proportion of peritoneal neutrophils, RvD1 suppressed the secretion of pro-inflammatory cytokine TNF-α in the

peritoneal exudates (**Fig. 2-1C**). Intraperitoneal administration of TNF-α to mice reversed the pro-resolving effect of RvD1. Moreover, TNF-α abrogated the RvD1-mediated decrease in accumulation of peritoneal leukocytes (especially PMNs) (**Fig. 2-1D**). Zymosan A-injected mice co-treated with RvD1 and TNF-α retained the cellular composition, in terms of the proportion of monocytes and PMNs of the peritoneal exudates similar to that observed in mice given zymosan A alone (**Fig. 2-1E**). RvD1 accelerated the resolution of peritonitis in the zymosan A-treated mice by increasing the proportion of mononuclear cells up to ~43% at the expense of lowering the proportion of PMNs by ~32%. However, when TNF-α was given, the ability of RvD1 to enhance the resolution of peritonitis was abolished (**Fig. 2-1F**).

Increased efferocytosis by RvD1 is mediated through suppression of TNF-α production

Compared to animals challenged with zymosan A alone, mice treated with RvD1 plus zymosan A showed the increased proportion of macrophages engulfing apoptotic PMNs ($F4/80^{+}Gr\text{-}1^{+}$). Thus, it is evident that RvD1 facilitates the clearance of apoptotic PMNs by macrophages. However, this RvD1-mediated enhancement of the efferocytic activity of macrophages was significantly diminished by treatment with TNF-α (**Fig. 2-2A**). We then examined the potential contribution of RvD1-mediated suppression of TNF-α production to macrophage efferocytosis *in vitro and ex vivo*. As

a measure of *in vitro* efferocytic activity, murine macrophage RAW264.7 cells were allowed to engulf the FITC-stained apoptotic Jurkat T cells for 60 min. When RAW264.7 cells were pretreated with LPS, the ability of macrophages to uptake apoptotic Jurkat T cells was suppressed, but the efferocytic ability was restored by RvD1 co-treatment. However, when TNF-α was added at 2 h following the RvD1 treatment (the time when RvD1 effectively inhibited LPS-induced TNF-α expression; **Fig. 2-3A**), the RvD1-induced efferocytic activity was abolished (**Fig. 2-2B**). These findings suggest that the increase of efferocytosis induced by RvD1 in macrophages challenged with LPS is mediated through down-regulation of TNF-α expression. RvD1-induced restoration of efferocytosis was also confirmed by *ex vivo* assay (**Fig. 2-2C**). To investigate whether TNF-α suppresses the efferocytic ability of macrophages by altering the expression of cell surface receptors, we examined the level of CD36, a scavenger receptor involved in efferocytosis. In RAW264.7 cells treated with LPS or TNF-α, CD36 expression was markedly decreased, but restored by RvD1 (**Fig. 2-2D**). These findings suggest that LPS-induced TNF-α upregulation can suppress efferocytosis by downregulating the expression of scavenger receptor on macrophage surface, and that RvD1 reverses it.

The inhibitory effect of RvD1 on LPS-induced TNF-α expression is mediated through inhibition of the classical NF-κB pathway

LPS-induced stimulation of *TNF-α* transcription in RAW264.7 cells was completely suppressed by co-treatment of 50 nM RvD1 (**Fig. 2-3A**). Likewise, the secretion of TNF-α from LPS-stimulated macrophages was dampened by RvD1 treatment (**Fig. 2-3B**). Since the LPS-induced TNF-α expression is dependent primarily on the activation of the NF-κB, we assessed whether RvD1 could modulate the NF-κB signaling. To confirm whether the LPS-induced overproduction of TNF-α was mediated by NF-κB, RAW264.7 cells were transfected with siRNA against p65, a functionally active subunit of NF-κB. As shown in **Fig. 2-3C**, LPS failed to upregulate TNF-α expression in p65 knockdown cells. We then examined whether the RvD1 could inhibit the LPS-derived NF-κB activation. The LPS-induced DNA binding (**Fig. 2-3D**) and transcriptional activity (**Fig. 2-3E**) of NF-κB was significantly inhibited by RvD1. Consistent with the inhibition of NF-κB transcriptional activity by RvD1, the nuclear translocation of p65 was markedly reduced by co-incubation with RvD1 in LPS-stimulated macrophages (**Fig. 2-3F**).

It is well established that IκBα is bound to p65 in physiological conditions and inhibits nuclear translocation of p65. In cells stimulated with LPS, IκBα is subjected to proteolytic degradation upon phosphorylation catalyzed by activated IKKβ. We noticed that RvD1 had the inhibitory effect on LPS-induced IKKβ phosphorylation and

activation (**Fig. 2-3G**). As a consequence, phosphorylation and subsequent degradation of IκBα were significantly blocked by RvD1 co-treatment in LPS-stimulated macrophages (**Fig. 2-3H**). Taken together, these results suggest that RvD1 might block the LPS-induced activation of the classical NF-κB signaling pathway by suppressing the IKKβ activation, and subsequently the phosphorylation and degradation of IκBα.

RvD1 blocked LPS-induced nuclear translocation of p65, but not p50

Although RvD1 significantly inhibited the classical LPS-induced NF-κB activation pathways by blocking IKK-mediated IκBα phosphorylation/degradation and subsequently nuclear translocation and DNA binding of p65 (**Fig. 2-3D-H**), it failed to alter DNA binding and nuclear localization of p50 and degradation of its precursor p105 (**Fig. 2-4A**,**B**) under the same experimental conditions. Taken together, these results imply that p50 protein can form a complex with either p65 or p50, but forms preferentially p50/p50 homodimer in RvD1-treated cells due to lack of p65 in the nucleus.

p50/p50 formation by RvD1 accounts for inhibition of LPS-induced TNF-α, resulting in restoration of efferocytosis

To further investigate the role of nuclear p50/p50 homodimer in suppression of LPS-induced TNF-α, we utilized siRNA against *nfκb1* (especially targeting p50 coding part)

to RAW264.7 cells. In p50 knockdown cells, *TNF-α* mRNA expression was not significantly induced despite LPS stimulation, because the DNA binding capacity of p65 is compromised in the absence of the p50 subunit (Schmitz and Baeuerle, 1991). In our present study, RvD1 was found to lose its ability to suppress LPS-induced *TNF-α* mRNA expression in p50 knockdown cells (**Fig. 2-4C**), suggesting that not only inhibition of p65/p50 nuclear translocation but also facilitation of p50/p50 formation is essential for inhibition by RvD1 of LPS-induced transcriptional activation of TNF-α. Based on these findings, we speculate that the facilitated formation of p50/p50 homodimer and the repression of LPS-induced TNF-α expression by RvD1 are critical for its induction of efferocytosis. In support of this assumption, the decline in the efferocytic activity of RAW264.7 cells caused by LPS stimulation was partially restored upon co-treatment with RvD1, but this pro-resolving effect of RvD1 was abolished in p50 knockdown cells (**Fig. 2-4D**). Due to weak induction of TNF-α in p50 knockdown cells, efferocytic activity of macrophages lacking p50 was not significantly attenuated upon stimulation with LPS alone. Thus, it is likely that predominant formation of p50/p50 homodimer facilitated by RvD1 accounts for its restoration of efferocytosis in LPS-treated macrophages.

RvD1 increases production of the p50 subunit of NF-κB through p105 phosphorylation and degradation, thereby increasing nuclear translocation of p50/p50 homodimer

Notably, RvD1 alone exhibited increased transient nuclear translocation of p50, as determined by immunoblot (**Fig. 2-5A**) and immunocytochemical (**Fig. 2-5B**) analyses in RAW264.7 cells. This was accompanied by a concomitant reduction in the cytoplasmic levels of p50 and its precursor p105. In contrast, RvD1 treatment did not cause any substantial translocation of p65 into nucleus (**Fig. 2-5A,B**). Next, we determined whether RvD1-induced nuclear translocation of p50 occurred as a consequence of degradation of p105. Phosphorylation of NF-κB1 p105 on Serine 927 is known to facilitate its proteolysis to produce p50 (Salmeron et al., 2001). RvD1 treatment time-dependently increased the phosphorylation of p105 at Ser 927 with concomitant reduction in the total p105 levels (**Fig. 2-5C**). This was accompanied by accumulation of p50. The expression plasmid containing full-length p105, fused with the NH_2-terminus of green fluorescent protein (GFP), was used to ascertain that p50 accumulated upon RvD1 treatment was derived from p105. With RvD1 stimulation, the level of ectopically expressed GFP-tagged p105 was decreased, while GFP-tagged p50 was markedly accumulated (**Fig. 2-5D**). These data clearly support that the p50 NF-κB subunit forming a homodimer upon RvD1 treatment is mainly derived from p105 degradation. To identify kinase responsible for p105 phosphorylation and degradation,

we measured the activation of some candidate mitogen activated protein kinases (MAPK) after RvD1 treatment. Whereas RvD1 induced the phosphorylation of extracellular-signal related kinase 1/2 (ERK1/2) within 15 min, it did not change the phosphorylation of c-Jun-N-terminal kinase (JNK) and p38 MAPK (**Fig. 2-5E)**. Treatment with U0126, a pharmacological inhibitor of ERK1/2, abrogated RvD1-induced phosphorylation and degradation of p105, resulting in reduced accumulation of p50 (**Fig. 2-5F**). Moreover, treatment of RAW264.7 cells with the proteasome inhibitor MG132 prior to RvD1 stimulation completely blocked p105 degradation and consequently p50 generation, which co-related with diminished nuclear translocation of p50 (**Fig. 2-5G**). Taken together, these findings suggest that RvD1 triggers proteasomal degradation of p105 through activation of ERK1/2 signaling.

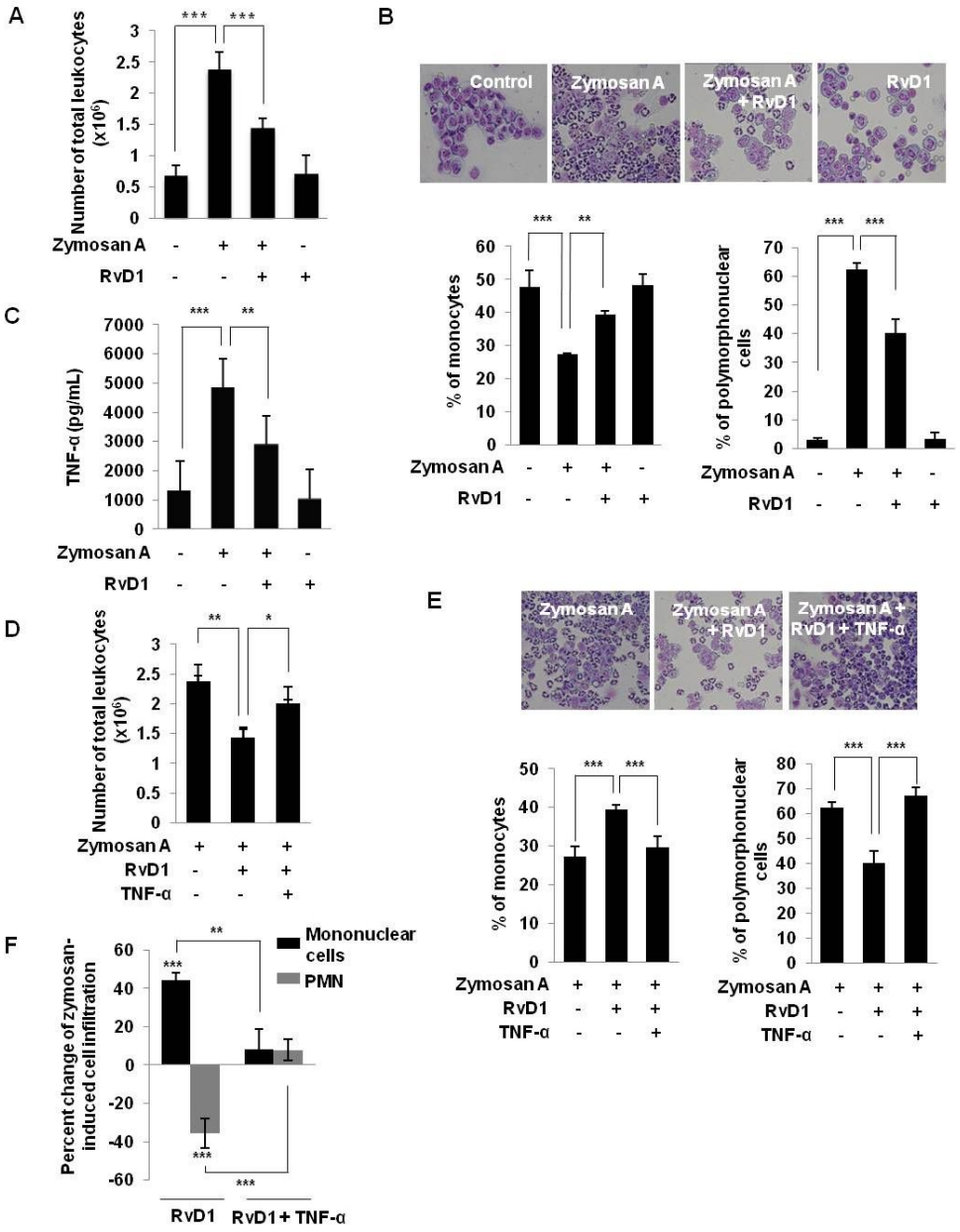
A
Number of total leukocytes (x10^6)
Zymosan A
RvD1
B
Control
Zymosan A
Zymosan A + RvD1
RvD1
% of monocytes
% of polymorphonuclear cells
C
TNF-α (pg/mL)
D
TNF-α
E
Zymosan A + RvD1 + TNF-α
F
Percent change of zymosan-induced cell infiltration
Mononuclear cells
PMN
RvD1
RvD1 + TNF-α

Fig. 2-1. RvD1 facilitates resolution of inflammation by inhibiting TNF-α production in zymosan A-induced peritonitis. Mice were administered intraperitonally with zymosan A (30 mg/kg) for 12 h followed by treatment with vehicle or RvD1 (300 ng). Some mice also received with TNF-α (10 ng) intraperitoneally together with RvD1. Six hours later, peritoneal exudates were collected. (A, D) The number of total leukocytes in peritoneal exudates was enumerated. (C) The concentrations of TNF-α in the cell free peritoneal lavage were measured by ELISA. (B,E,F) The proportions of mononuclear cells and PMNs in collected peritoneal exudates were determined by differential cell counting. Results are the means ± S.D. (n=4), $^{*}p<0.05$, $^{**}p<0.01$, $^{***}p<0.001$

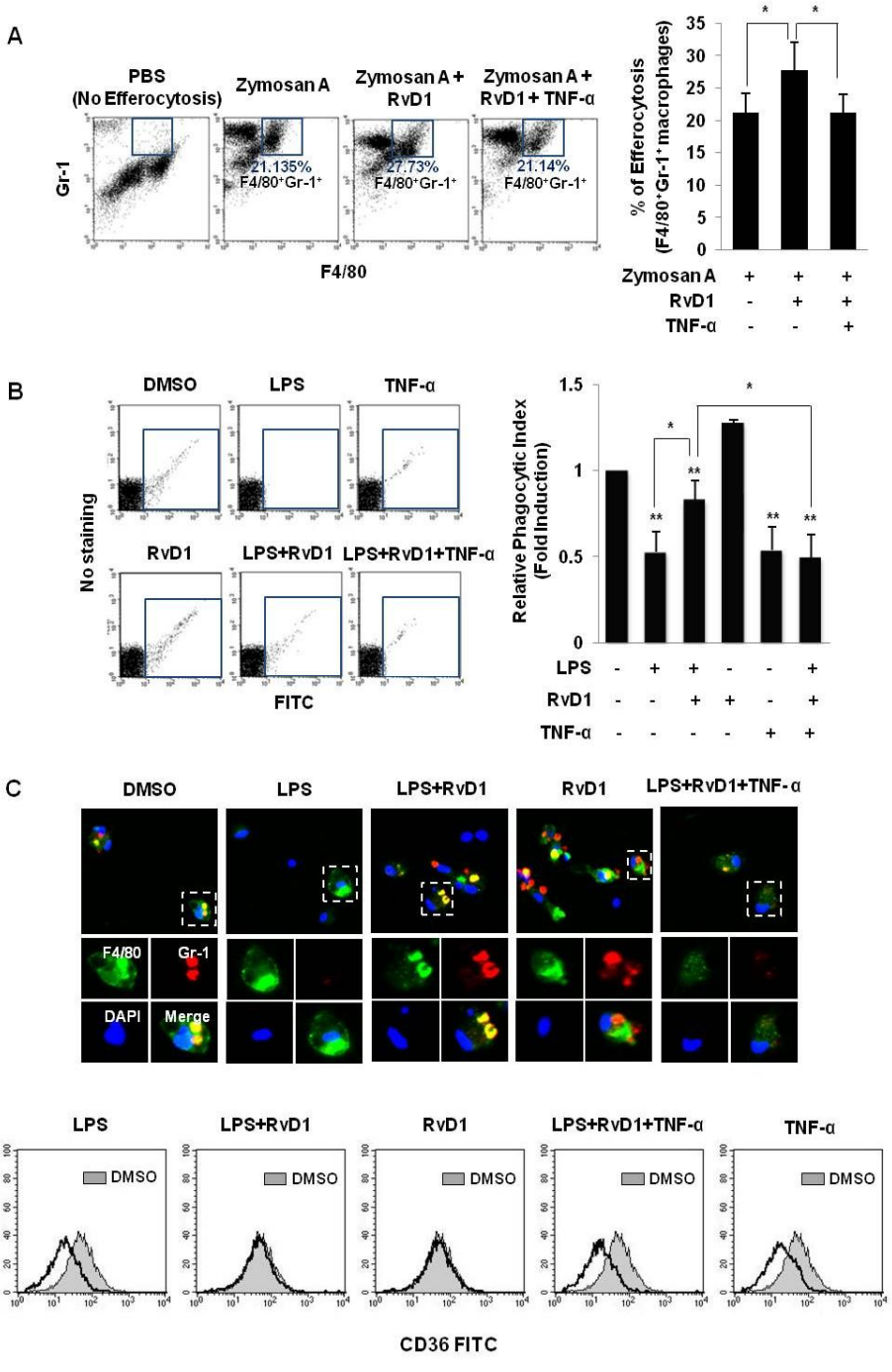
A
PBS (No Efferocytosis)
Zymosan A
Zymosan A + RvD1
Zymosan A + RvD1 + TNF-α
Gr-1
F4/80
21.135% F4/80+Gr-1+
27.73% F4/80+Gr-1+
21.14% F4/80+Gr-1+
% of Efferocytosis (F4/80+Gr-1+ macrophages)
Zymosan A + + +
RvD1 - + +
TNF-α - - +
B
DMSO
LPS
TNF-α
No staining
RvD1
LPS+RvD1
LPS+RvD1+TNF-α
FITC
Relative Phagocytic Index (Fold Induction)
LPS - + + - - +
RvD1 - - + + - +
TNF-α - - - - + +
C
DMSO
LPS
LPS+RvD1
RvD1
LPS+RvD1+TNF-α
F4/80
Gr-1
DAPI
Merge
D
LPS
LPS+RvD1
RvD1
LPS+RvD1+TNF-α
TNF-α
DMSO
Cell counts
CD36 FITC

Fig. 2-2. RvD1-mediated repression of TNF-α production increases the efferocytic activity of macrophages in vivo and in vitro. (A) In the zymosan A-induced peritonitis model, the proportion of macrophages with ingested PMN ($F4/80^+/Gr\text{-}1^+$) was determined by flow cytometry. Results are the means ± SD (n=4) and expressed as a percent increase of $F4/80^+/Gr\text{-}1^+$ macrophages. (B) Apoptosis of Jurkat T cells was induced by UVB (180 mJ/cm^2) irradiation, followed by incubation for 8 h. RAW264.7 cells treated with LPS (200 ng/mL), RvD1 (50 nM) or TNF-α (10 ng/mL) were co-incubated with FITC-annexin V stained-apoptotic Jurkat T cells for 1 h. The number of macrophages engulfing apoptotic Jurkat T cells was determined by flow cytometry. Histograms represent the relative phagocytic index over control. Means ± S.D. (n=3), $^{*}p<0.05$, $^{**}p<0.01$. (C) For an ex vivo efferocytosis assay, peritoneal macrophages were treated with LPS, RvD1 or TNF-α for 4 h, and co-incubated with apoptotic neutrophils for 1 h. The engulfment of apoptotic neutrophils by macrophages was determined by immunostaining using anti-F4/80 (green; macrophage marker) and anti-Gr-1 (red; neutrophil marker) antibodies. Representative fluorescent micrograph shows macrophages (green) engulfing apoptotic neutrophils (red). (D) The cell surface expression of CD36 was analyzed by flow cytometry using FITC-conjugated anti-CD36 antibodies after treatment of RAW264.7 cells with LPS, RvD1 or TNF-α for 4 h.

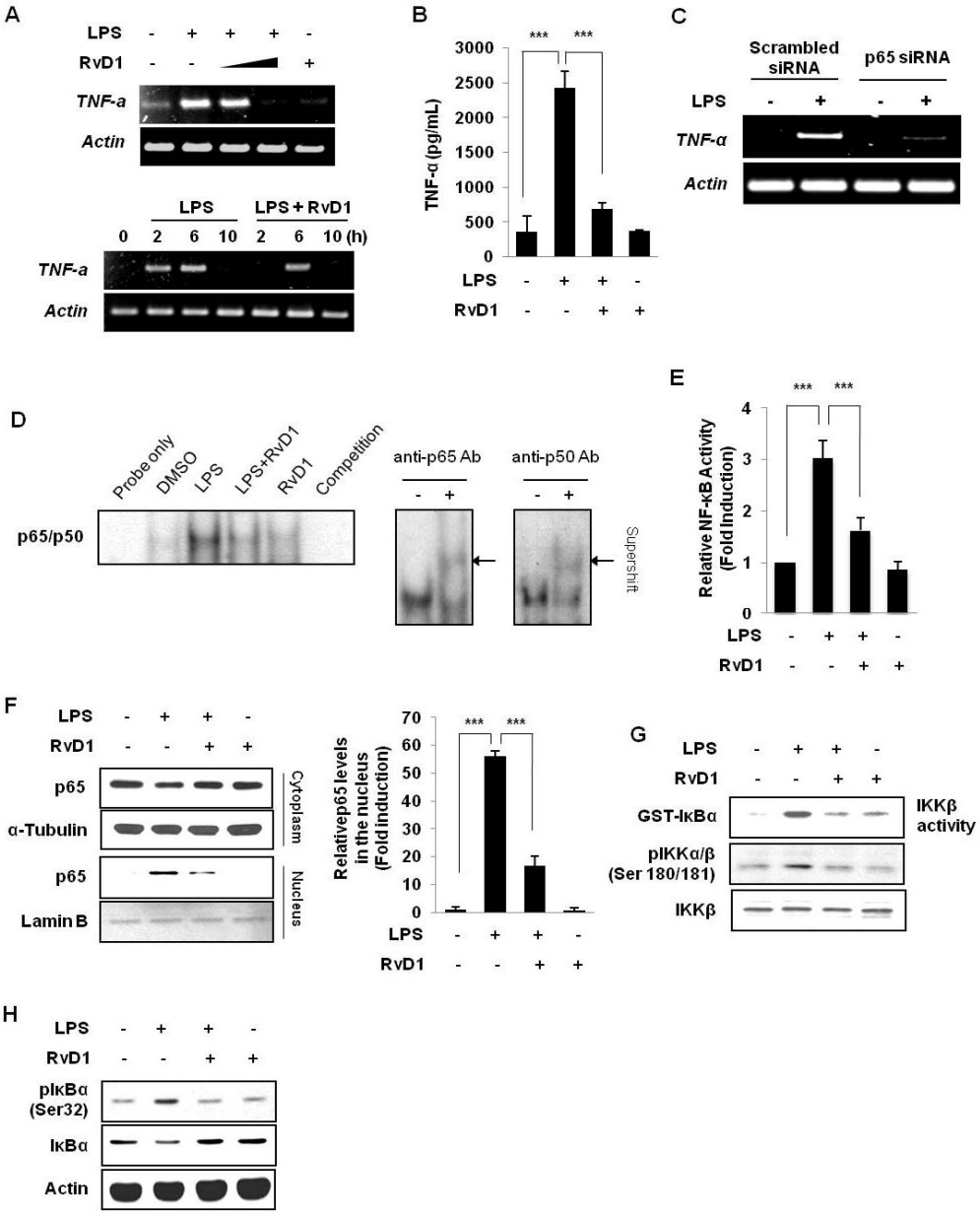
A
LPS
RvD1
TNF-a
Actin
LPS
LPS + RvD1
0 2 6 10 2 6 10 (h)
TNF-a
Actin
B
TNF-α (pg/mL)
3000
2500
2000
1500
1000
500
0
***
***
LPS
RvD1
C
Scrambled siRNA
p65 siRNA
LPS
TNF-α
Actin
D
Probe only
DMSO
LPS
LPS+RvD1
RvD1
Competition
p65/p50
anti-p65 Ab
anti-p50 Ab
Supershift
E
Relative NF-κB Activity (Fold Induction)
4
3
2
1
0
***
***
LPS
RvD1
F
LPS
RvD1
p65
α-Tubulin
Cytoplasm
p65
Lamin B
Nucleus
Relativep65 levels in the nucleus (Fold induction)
70
60
50
40
30
20
10
0
***
***
LPS
RvD1
G
LPS
RvD1
GST-IκBα
IKKβ activity
pIKKα/β (Ser 180/181)
IKKβ
H
LPS
RvD1
pIκBα (Ser32)
IκBα
Actin

Fig. 2-3. RvD1 suppresses LPS-induced TNF-α production by blocking the classical NF-κB pathway. (A) RAW264.7 cells were treated with LPS (200 ng/mL) in the absence or presence of RvD1 (10 or 50 nM) and harvested at 2 h or at indicated time intervals. Semi-quantitative RT-PCR was conducted to measure *TNF-α* mRNA levels. (B) Culture supernatants were collected at 4 h after LPS or RvD1 treatment (50 nM), and TNF-α concentrations were measured by ELISA. (C) Cells were transfected with scrambled or p65 siRNA for 16 h, and then LPS was treated for additional 2 h. The mRNA levels of *TNF-α* and *actin* were determined by RT-PCR. (D) Nuclear protein was prepared and incubated with the [γ-^{32}P]-labeled oligonucleotides containing the NF-κB consensus motif. Protein-DNA complexes were separated from free probe by electrophoresis. (E) The RvD1-mediated suppression of the transcriptional activation of NF-κB was measured by the luciferase reporter gene assay. (F) RAW264.7 cells were stimulated with LPS or RvD1 for 30 min. Localization of p65 in cytoplasm and nucleus was determined by Western blot analysis. α-Tubulin and lamin B were used as cytoplasmic and nuclear markers, respectively. Histogram represents the relative level of nuclear translocated p65. Means ± S.D. (n=3), $^{***}p<0.001$. (G, H) RAW264.7 cells were treated with RvD1 for 15 min in the presence or absence of LPS. The IKKβ kinase activity was measured by an immune complex kinase assay using GST-IκBα and [γ-^{32}P]ATP. Immunoblot analysis was carried out to measure the level of total IKKβ, phosphorylated IκBα and total IκBα.

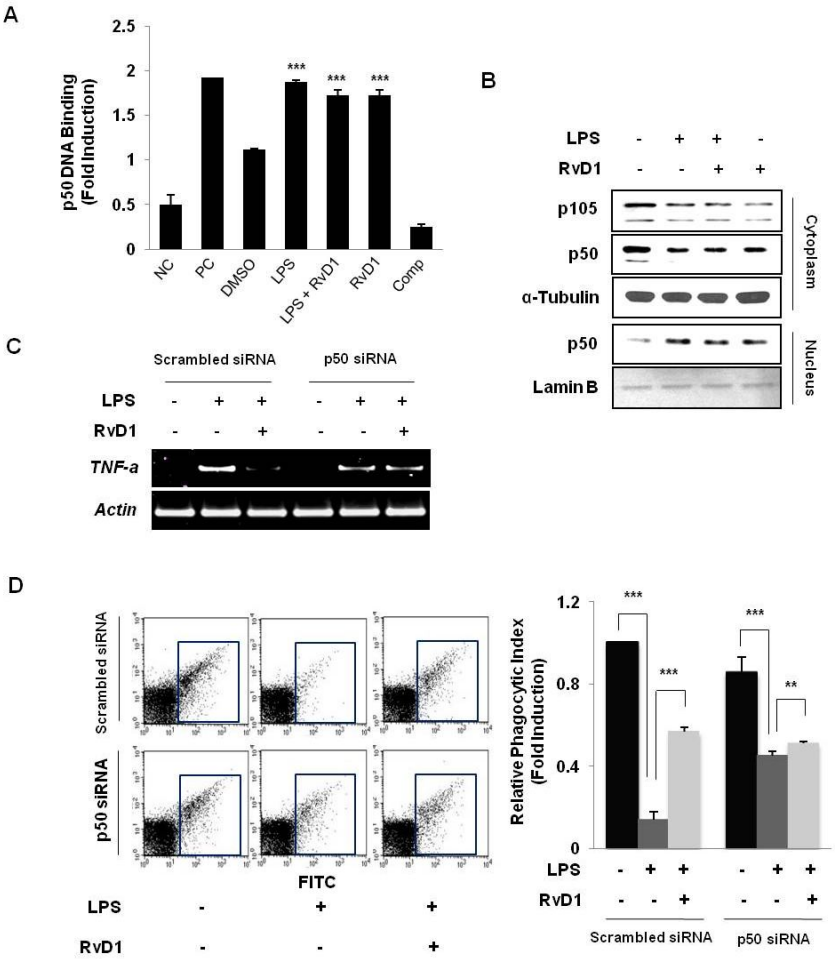

Fig. 2-4. Signaling through p50/p50 homodimer is critical for the inhibitory effects of RvD1 on LPS-induced TNF-α expression and restoration of efferocytosis. RAW264.7 cells treated with LPS in the absence or presence of RvD1 (50 nM) were harvested at 30 min. (A) p50 oligonucleotide binding in nuclear extracts was determined by the NF-κB TransAM assay. Means ± S.D. (n=3), ***p<0.001 when

compared with DMSO-treated group. NC, negative control; PC, positive control; Comp, competition (B) Levels of p105 and p50 in cytoplasm and nucleus were assayed by Western blot analysis. (C) Cells were transfected with scrambled or *nfκb1* (N-terminal) siRNA for 16 h, and then LPS was treated in the absence or presence of RvD1 for additional 2 h. The mRNA levels of *TNF-α* and *actin* were determined by RT-PCR. (D) RAW264.7 cells were transfected with scrambled or *nfκb1* siRNA for 16 h and the assay for efferocytosis was performed by incubating cells with FITC-annexin V stained-apoptotic Jurkat T cells for 1 h after preincubation with LPS in the absence or presence of RvD1 for 4 h. Representative flow cytometric dot plots demonstrating changes in the proportion of macrophages engulfing FITC-annexin V stained-apoptotic Jurkat T cells are shown. Graphs are expressed as fold increases in the phagocytic index over the control. Means ± S.D. (n=3), $^{**}P<0.01$, $^{***}p<0.001$.

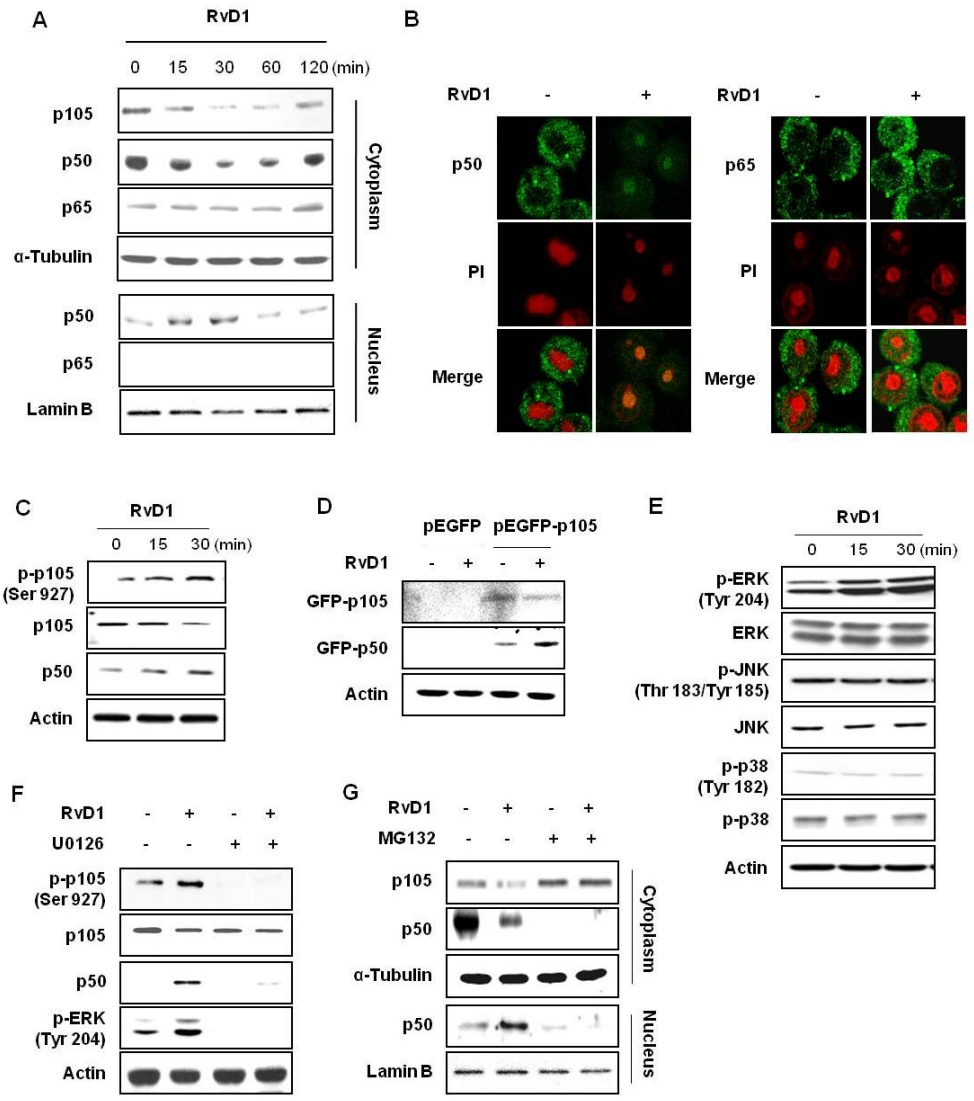

Fig. 2-5. RvD1-induced p105 degradation and concurrent p50 formation are dependent on proteasomal activity. (A) RAW264.7 cells were treated with RvD1 (50 nM) or vehicle for indicated time periods, and both cytosolic and nuclear extracts were prepared. Levels of p105, p50 and p65 in cytoplasm and nucleus were assayed by

Western blot analysis. (B) Nuclear translocation of p50 and p65 was determined by immunocytochemical analysis. (C) Total proteins isolated from RvD1-treated cells were subjected to immunoblot analysis for the measurement of phosphorylated p105 and total p105 as well as p50. Actin was used as an equal loading control for normalization. Histograms represent the relative levels of phosphorylated p105, total p105 and p50. Means ± S.D. (n=3), $^{*}P<0.05$, $^{**}P<0.01$, $^{***}p<0.001$. (D) RAW264.7 cells were transfected with NH_2-terminal GFP-tagged p105 vector, followed by incubation with RvD1 or vehicle for 30 min. Total protein isolated from cell lysates was subjected to immunoblot analysis for the measurement of p105 and p50 levels. (E) Lysates from RvD1-treated cells were subjected to Western blot analysis. RvD1-induced activation of ERK, JNK and p38 was assessed by using phospho-specific antibodies. (F) Cells were pre-incubated with the ERK inhibitor U0126 (10 μM) or DMSO for 2 h and then treated with RvD1 for additional 30 min. Levels of phosphorylated p105, total p105 and p50 were measured by Western blot analysis. (G) Cells were pre-incubated with or without the proteasome inhibitor MG132 (10 μM) for 2 h and then treated with RvD1 for 30 min. Levels of p105 and p50 in cytoplasm and nucleus were measured by Western blot analysis. Data represent at least three independent experiments.

5. Discussion

Efferocytosis is critical for the successful resolution of acute inflammatory response. Prolonged pro-inflammatory insults suppress macrophage efferocytosis, leading to chronic inflammation (Vandivier et al., 2006). Several recent studies have demonstrated that LPS significantly inhibits the ability of mouse peritoneal macrophages to uptake apoptotic neutrophils through overproduction of TNF-α (Michlewska et al., 2009; Feng et al., 2011). In agreement with these reports, our present study revealed that pro-inflammatory stimuli, such as zymosan A and LPS, suppressed efferocytosis through induction of TNF-α expression, and that the blockade of TNF-α production nullified LPS-mediated suppression of efferocytosis. In addition, we notably uncovered that TNF-α downregulates the expression of CD36, one of the principal scavenger receptors involved in efferocytosis, thereby suppressing the ability of macrophages to recognize and uptake apoptotic neutrophils. TNF-α is recognized as one of major cytokines responsible for chronic inflammation (Clark, 2007). We consider that TNF-α mediates the development of chronic inflammation is attributable, at least in part, to repression of efferocytosis.

Resolution of inflammation is an active and tightly regulated process controlled by anti-inflammatory and pro-resolving endogenous mediators, such as lipoxins and resolvins (Lawrence et al., 2002; Serhan, 2007). It has been reported that RvD1 inhibits Toll-like receptor-mediated activation of macrophages, limits infiltration of PMNs,

enhances the recruitment of nonphlogistic monocytes and promotes the engulfment of apoptotic leukocytes by macrophages (Serhan and Chiang, 2008; Schif-Zuck et al., 2011). Although the role of RvD1 in the resolution of inflammation has been extensively investigated, the molecular events associated with RvD1-induced activation of efferocytosis are not clearly defined. Few studies demonstrated that RvD1 stimulates phagocytosis via its receptor (e.g. ALX and GPR32) activation and M2 macrophage polarization (Krishnamoorthy et al., 2010; Titos et al., 2011). One of the salient features of our findings is that RvD1 regulates the efferocytic activity of macrophages by suppressing TNF-α production upon pro-inflammatory stimulation. In RvD1-treated macrophages, the LPS-induced TNF-α production was impaired, resulting in restoration of efferocytosis. These findings suggest that the restoration of efferocytosis by RvD1 is likely to be related to suppression of pro-inflammatory TNF-α expression.

The present study demonstrates that the inhibition of LPS-induced transcriptional activation of TNF-α by RvD1 involves modulation of at least two different NF-κB pathways; one being the suppression of nuclear translocation of p65/50 and the other being the preferential binding of p50/p50 homodimer (Gomez et al., 2005; Dai et al., 2007) to the κB consensus sequence present in the TNF-α gene promoter. p65/p50 heterodimer is known to be the predominant form of functionally active NF-κB with pro-inflammatory activity, while p50/p50 homodimer exerts the anti-inflammatory and

pro-resolving effects. p50/p50 homodimer is considered to compete with p65/50 heterodimer for DNA binding (Bohuslav et al., 1998; Ma et al., 2003). Unlike p65/p50 heterodimer, p50/p50 homodimer lacks the transactivation domain, and the binding of p50/p50 homodimer to DNA hence causes repression of target gene expression. In the present study, RvD1 enhanced localization of p50 in the nucleus, while it suppressed dissociation from IκB and concurrent nuclear translocation of p65. This led to an increased net nuclear accumulation of p50 and predominant formation of p50/p50 homodimer. Rather than simply stimulating the physical dissociation of p50 from the p65/p50 complex, RvD1 caused the nuclear accumulation of p50 by enhancing the degradation of p105. The proteolytic degradation of p105 is regulated by two pathways, a limited (processing to p50) and a complete degradation (releasing bound p50) (Moorthy and Ghosh, 2003). We note that p50 accumulated in the nucleus following RvD1 treatment is generated as a consequence of degradation of C-terminal of p105 encoding IκBγ, indicating the limited processing of p105. The possibility of RvD1 to release a p50/p50 homodimer from an inactive p105/p50 heterodimer (a complete degradation of p105) was excluded based on the observation from the experiment utilizing GFP-tagged-*nfkb1*. We found that GFP-p105 was mainly produced from GFP-tagged *nfkb1* in normal conditions, but the processing of GFP-p105 to yield GFP-p50 was increased after RvD1 treatment. Signal-induced processing of p105 to p50 was found to be dependent on phosphorylation and proteasome-mediated degradation of

IκBγ in RvD1-stimulated cells (Lawrence et al., 2001). We noted that RvD1 induced p105 phosphorylation on Ser 927, facilitating recruitment of the $SCF^{\beta\text{-}TrCP}$ (β-transducinrepeat-containing protein) ubiquitin ligase complex (Cohen et al., 2001). Pretreatment of the proteasome inhibitor MG132 blocked RvD1-induced proteolysis of p105, indicative of the involvement of 26S proteasomes in RvD1-induced degradation of IκBγ (C-terminal of p105). Besides stimulating conversion of p105 to p50, RvD1 exerted the inhibitory effect on LPS-induced IKKβ activity which is responsible for degradation of IκB .

Efferocytosis during resolution of inflammation is influenced by the surrounding environment in the inflamed site. At the onset of inflammation, pro-inflammatory cytokines, chemokines and lipid mediators are produced, and these molecules suppress nonphlogistic phagocytosis of apoptotic neutrophils by macrophages. Not only TNF-α, but prostaglandin E_2, a representative pro-inflammatory mediator, is also known to inhibit phagocytosis by macrophages (Aronoff et al., 2004). However, at the late phase of inflammation, the balance of cytokines, chemokines and lipid mediators shifts toward anti-inflammatory and pro-resolving mediators, facilitating the termination of inflammation. For example, previously published data demonstrate that the anti-inflammatory cytokine IL-10 augments efferocytosis and stimulates resolution of inflammation (Michlewska et al., 2009). Therefore, lipid mediator class switching and the balance between pro-inflammatory and anti-inflammatory cytokines are key factors

for regulating macrophages to undergo efferocytosis.

In summary, RvD1-derived suppression of TNF-α expression is responsible for complete resolution of inflammation. As proposed in **Fig. 2-6**, RvD1 suppresses TNF-α expression and restores efferocytosis during resolution of inflammation through two distinct mechanisms. Even though TNF-α exerts the beneficial function by triggering the immune response to bacterial infection or other harmful stimuli, sustained production of TNF-α is implicated in the pathogenesis of a variety of human diseases, such as rheumatoid arthritis (Cavazzana et al., 2007), inflammatory bowel disease (El Mourabet et al., 2010), Alzheimer's disease (Swardfager et al., 2010) and cancer (van Horssen et al., 2006). These disorders are linked to imperfect resolution of inflammation, caused by disturbance of efferocytosis which often results from overproduction of TNF-α. Therefore, timely blockade of TNF-α overproduction should be essential for resolution of inflammation and prevention of chronic inflammatory diseases. It is evident that endogenously produced RvD1, generated during resolution of inflammation, is one of the key molecules in the first line of cellular defense against persistent inflammatory responses. As exogenous administration of RvD1 stimulates efferocytosis by suppressing TNF-α overproduction, this molecule may have therapeutic potential in the management of chronic inflammatory diseases associated with impaired efferocytosis.

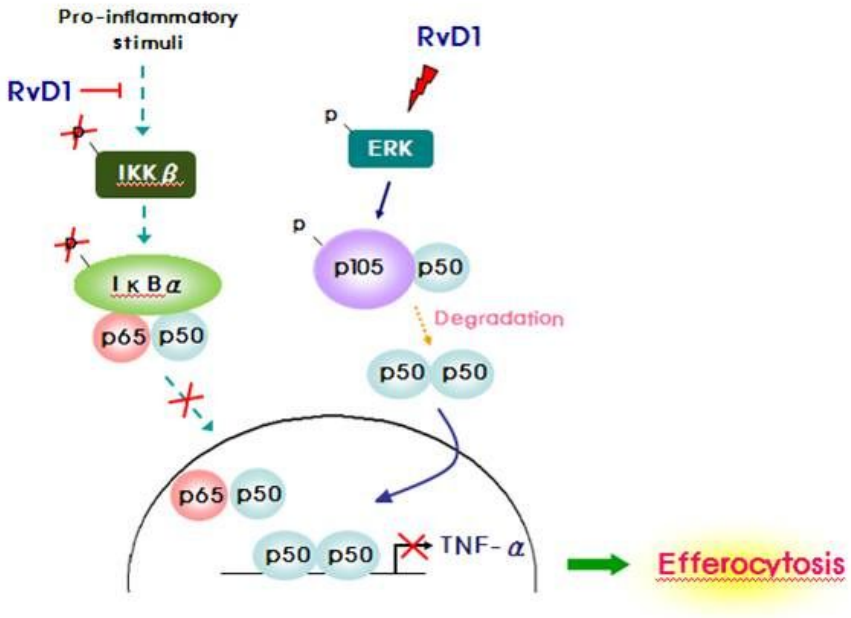

Fig. 2-6. The proposed mechanisms underlying RvD1-mediated suppression of TNF-α expression and restroration of efferocytosis during resolution of inflammation. Sustained production of TNF-α at inflamed sites and subsequent inhibition of efferocytosis of apoptotic neutrophils may cause noxious consequences such as chronic inflammation leading to cancer. In our study, it was demonstrated that RvD1 stimulates macrophages to engulf apoptotic neutrophils during resolution of inflammation by inhibiting TNF-α expression via two different NF-κB pathways: 1) suppression of nuclear translocation of p65/p50 by down-regulating IKKβ activity and 2) promotion of nuclear translocation of p50/p50 through p105 degradation.

6. References

Aronoff, D. M., Canetti, C. and Peters-Golden, M. (2004). Prostaglandin E2 inhibits alveolar macrophage phagocytosis through an E-prostanoid 2 receptor-mediated increase in intracellular cyclic AMP. *J. Immunol.* 173, 559-565.

Baer, M., Dillner, A., Schwartz, R. C., Sedon, C., Nedospasov, S. and Johnson, P. F. (1998). Tumor necrosis factor alpha transcription in macrophages is attenuated by an autocrine factor that preferentially induces NF-kappaB p50. *Mol. Cell Biol.* 18, 5678-5689.

Bannenberg, G. L., Chiang, N., Ariel, A., Arita, M., Tjonahen, E., Gotlinger, K. H., Hong, S. and Serhan, C. N. (2005). Molecular circuits of resolution: formation and actions of resolvins and protectins. *J. Immunol.* 174, 4345-4355.

Barchowsky, A., Frleta, D. and Vincenti, M. P. (2000). Integration of the NF-kappaB and mitogen-activated protein kinase/AP-1 pathways at the collagenase-1 promoter: divergence of IL-1 and TNF-dependent signal transduction in rabbit primary synovial fibroblasts. *Cytokine* 12, 1469-1479.

Bohuslav, J., Kravchenko, V. V., Parry, G. C., Erlich, J. H., Gerondakis, S., Mackman, N. and Ulevitch, R. J. (1998). Regulation of an essential innate immune response by the p50 subunit of NF-kappaB. *J. Clin. Invest.* 102, 1645-1652.

Borges, V. M., Vandivier, R. W., McPhillips, K. A., Kench, J. A., Morimoto, K., Groshong, S. D., Richens, T. R., Graham, B. B., Muldrow, A. M., Van Heule, L. et al. (2009). TNFalpha inhibits apoptotic cell clearance in the lung, exacerbating acute inflammation. *Am. J. Physiol. Lung Cell Mol. Physiol.* 297, L586-595.

Cavazzana, I., Bobbio-Pallavicini, F., Franceschini, F., Bazzani, C., Ceribelli, A., Bravi, E., Zingarelli, S., Caporali, R., Cattaneo, R. and Montecucco, C. M. (2007). Anti-TNF-alpha treatment in rheumatoid arthritis with anti-Ro/SSA antibodies. Analysis of 17 cases among a cohort of 322 treated patients. *Clin. Exp. Rheumatol.* 25, 676-683.

Clark, I. A. (2007). How TNF was recognized as a key mechanism of disease. *Cytokine Growth Factor Rev.* 18, 335-343.

Cohen, S., Orian, A. and Ciechanover, A. (2001). Processing of p105 is inhibited by docking of p50 active subunits to the ankyrin repeat domain, and inhibition is alleviated by signaling via the carboxyl-terminal phosphorylation/ ubiquitin-ligase binding domain. *J. Biol. Chem.* 276, 26769-26776.

Dai, R., Phillips, R. A. and Ahmed, S. A. (2007). Despite inhibition of nuclear localization of NF-kappa B p65, c-Rel, and RelB, 17-beta estradiol up-regulates NF-kappa B signaling in mouse splenocytes: the potential role of Bcl-3. *J. Immunol.* 179, 1776-1783.

El Mourabet, M., El-Hachem, S., Harrison, J. R. and Binion, D. G. (2010). Anti-TNF antibody therapy for inflammatory bowel disease during pregnancy: a clinical review. *Curr. Drug Targets* 11, 234-241.

Feng, X., Deng, T., Zhang, Y., Su, S., Wei, C. and Han, D. (2011). Lipopolysaccharide inhibits macrophage phagocytosis of apoptotic neutrophils by regulating the

production of tumour necrosis factor alpha and growth arrest-specific gene 6. *Immunology* 132, 287-295.

Gomez, P. F., Pillinger, M. H., Attur, M., Marjanovic, N., Dave, M., Park, J., Bingham, C. O., 3rd, Al-Mussawir, H. and Abramson, S. B. (2005). Resolution of inflammation: prostaglandin E2 dissociates nuclear trafficking of individual NF-kappaB subunits (p65, p50) in stimulated rheumatoid synovial fibroblasts. *J. Immunol.* 175, 6924-6930.

Hong, S., Gronert, K., Devchand, P. R., Moussignac, R. L. and Serhan, C. N. (2003). Novel docosatrienes and 17S-resolvins generated from docosahexaenoic acid in murine brain, human blood, and glial cells. Autacoids in anti-inflammation. *J Biol Chem* 278, 14677-14687.

Krishnamoorthy, S., Recchiuti, A., Chiang, N., Yacoubian, S., Lee, C. H., Yang, R., Petasis, N. A. and Serhan, C. N. (2010). Resolvin D1 binds human phagocytes with evidence for proresolving receptors. *Proc. Natl. Acad. Sci. U. S. A.* 107, 1660-1665.

Lawrence, T., Willoughby, D. A. and Gilroy, D. W. (2002). Anti-inflammatory lipid mediators and insights into the resolution of inflammation. *Nat. Rev. Immunol.* 2, 787-795.

Lawrence, T., Gilroy, D. W., Colville-Nash, P. R. and Willoughby, D. A. (2001). Possible new role for NF-kappaB in the resolution of inflammation. *Nat. Med.* 7, 1291-1297.

Ma, X. Y., Wang, H., Ding, B., Zhong, H., Ghosh, S. and Lengyel, P. (2003). The interferon-inducible p202a protein modulates NF-kappaB activity by inhibiting the binding to DNA of p50/p65 heterodimers and p65 homodimers while enhancing the binding of p50 homodimers. *J. Biol. Chem.* 278, 23008-23019.

McPhillips, K., Janssen, W. J., Ghosh, M., Byrne, A., Gardai, S., Remigio, L., Bratton, D. L., Kang, J. L. and Henson, P. (2007). TNF-alpha inhibits macrophage clearance of apoptotic cells via cytosolic phospholipase A2 and oxidant-dependent mechanisms. *J. Immunol.* 178, 8117-8126.

Michlewska, S., Dransfield, I., Megson, I. L. and Rossi, A. G. (2009). Macrophage phagocytosis of apoptotic neutrophils is critically regulated by the opposing actions of pro-inflammatory and anti-inflammatory agents: key role for TNF-alpha. *FASEB J.* 23, 844-854.

Moorthy, A. K. and Ghosh, G. (2003). p105.Ikappa Bgamma and prototypical Ikappa Bs use a similar mechanism to bind but a different mechanism to regulate the subcellular localization of NF-kappa B. *J. Biol. Chem.* 278, 556-566.

Salmeron, A., Janzen, J., Soneji, Y., Bump, N., Kamens, J., Allen, H. and Ley, S. C. (2001). Direct phosphorylation of NF-kappaB1 p105 by the IkappaB kinase complex on serine 927 is essential for signal-induced p105 proteolysis. *J. Biol. Chem.* 276, 22215-22222.

Schif-Zuck, S., Gross, N., Assi, S., Rostoker, R., Serhan, C. N. and Ariel, A. (2011). Saturated-efferocytosis generates pro-resolving CD11b low macrophages: modulation by resolvins and glucocorticoids. *European journal of immunology* 41, 366-379.

Schmitz, M. L. and Baeuerle, P. A. (1991). The p65 subunit is responsible for the strong transcription activating potential of NF-kappa B. *EMBO J.*10, 3805-3817.
Serhan, C. N. (2007). Resolution phase of inflammation: novel endogenous anti-inflammatory and proresolving lipid mediators and pathways. *Annu. Rev. Immunol.* 25, 101-137.
Serhan, C. N. and Savill, J. (2005). Resolution of inflammation: the beginning programs the end. *Nat. Immunol*. 6, 1191-1197.
Serhan, C. N. and Chiang, N. (2008). Endogenous pro-resolving and anti-inflammatory lipid mediators: a new pharmacologic genus. *Br. J. Pharmacol.* 153 Suppl 1, S200-215.
Serhan, C. N., Brain, S. D., Buckley, C. D., Gilroy, D. W., Haslett, C., O'Neill, L. A., Perretti, M., Rossi, A. G. and Wallace, J. L. (2007). Resolution of inflammation: state of the art, definitions and terms. *FASEB J.* 21, 325-332.
Singh, A. K. and Jiang, Y. (2004). Differential activation of NF kappa B/RelA-p50 and NF kappa B/p50-p50 in control and alcohol-drinking rats subjected to carrageenin-induced pleurisy. *Mediators Inflamm.* 13, 255-262.
Sun, Y. P., Oh, S. F., Uddin, J., Yang, R., Gotlinger, K., Campbell, E., Colgan, S. P., Petasis, N. A. and Serhan, C. N. (2007). Resolvin D1 and its aspirin-triggered 17R epimer. Stereochemical assignments, anti-inflammatory properties, and enzymatic inactivation. *J. Biol. Chem.* 282, 9323-9334.
Swardfager, W., Lanctot, K., Rothenburg, L., Wong, A., Cappell, J. and Herrmann, N. (2010). A meta-analysis of cytokines in Alzheimer's disease. *Biol. Psychiatry* 68, 930-941.
Titos, E., Rius, B., Gonzalez-Periz, A., Lopez-Vicario, C., Moran-Salvador, E., Martinez-Clemente, M., Arroyo, V. and Claria, J. (2011). Resolvin D1 and its precursor docosahexaenoic acid promote resolution of adipose tissue inflammation by eliciting macrophage polarization toward an M2-like phenotype. *J. Immunol.* 187, 5408-5418.
van Horssen, R., Ten Hagen, T. L. and Eggermont, A. M. (2006). TNF-alpha in cancer treatment: molecular insights, antitumor effects, and clinical utility. *Oncologist* 11, 397-408.
Vandivier, R. W., Henson, P. M. and Douglas, I. S. (2006). Burying the dead: the impact of failed apoptotic cell removal (efferocytosis) on chronic inflammatory lung disease. *Chest* 129, 1673-1682.
Wessells, J., Baer, M., Young, H. A., Brown, K., Siebenlist, U. and Johnson, P. F. (2004). BCL-3 and NF-kappaB p50 attenuate lipopolysaccharide-induced inflammatory responses in macrophages. *J. Biol. Chem.* 279, 49995-50003.

Chapter III

Resolvin D1-mediated NOX2 inactivation rescues macrophages undertaking efferocytosis from oxidative stress-induced apoptosis

1. Abstract

Effective clearance of apoptotic cells by macrophages, termed efferocytosis, is pre-requisite for successful resolution of inflammation, and drives macrophage emigration to the draining lymph node, thereby promoting restoration of tissue homeostasis. During efferocytosis, engulfment of apopototic cells induces generation of reactive oxygen species (ROS) in abundance. Macrophage apoptosis is an important feature of chronic inflammatory diseases including atherosclerosis. In the present study, we found that resolvin D1 (RvD1), one of endogenous pro-resolving lipid mediators derived from docosahexaenoic acid, prevented apoptosis of murine macrophage-like RAW264.7 cells engulfing apoptotic cells. The inhibitory effect of RvD1 on efferocytosis-induced oxidative burst appears to be mediated by the inactivation of NADPH oxidase (NOX), a key enzyme involved in intracellular ROS production. In RvD1-treated macrophages, efferocytosis-induced phosphorylation of $p47^{phox}$ and association between $p47^{phox}$ and $gp91^{phox}$ were downregulated, resulting in abrogation of generation of superoxide anion and hydrogen peroxide. Furthermore, RvD1-mediated suppression of NOX activation was found to be dependent on cAMP-activated protein kinase (PKA) signaling. Besides inhibiting NOX activation, RvD1 rescued macrophages from oxidative stress-induced apoptosis by upregulating the expression of Bcl-xL and Bcl-2. However, knockdown of the RvD1 receptor, lipoxin A receptor/formyl-peptide receptor (ALX/FPR2), abolished the ability of RvD1 to

activate cAMP-PKA signaling, to suppress NOX activation and to increase the expression of anti-apoptotic proteins, suggesting that ALX/FPR2 mediates the protective effect of RvD1 on effeocytosis-induced oxidative stress. Taken together, these findings indicate that RvD1 rescues macrophages from oxidative stress-induced apoptosis during efferocytosis through PKA-mediated repression of NOX activation and upregulation of anti-apoptotic protein expression.

Keywords

Resolvin D1, efferocytosis, oxidative stress-induced apoptosis, NADPH oxidase, ALX/FPR2

2. Introduction

The successful resolution of inflammation requires a series of processes, including inhibition of inflammatory cell infiltration, stimulation of clearance of apoptotic neutrophils by mononuclear phagocytes and promotion of macrophage egress (Tabas, 2010). At the initial phase of inflammation, a lot of neutrophils are recruited to the inflamed site to remove harmful invaders via phagocytosis, and subsequently undergo apoptosis. Clearance of apoptotic neutrophils from the inflamed site is important for the resolution of inflammation as it prevents disgorgement of toxic contents from apoptotic cells. Macrophages, which are recruited in the inflamed tissue following influx of neutrophils, play a key role in engulfing apoptotic polymorphonuclear leukocytes (PMNs) (Serhan et al, 2007; Serhan & Savill, 2005). Unlike neutrophils which have a short-life, macrophages do not undergo apoptosis in the inflamed site, but rather emigrate through local lymphatic vessels and accumulate in draining lymph nodes. Engulfment of apoptotic neutrophils, the process termed efferocytosis, drives macrophages to exit the inflamed site via lymphatics (Randolph, 2008). It has been recently reported that efferocytosis induces the oxidative burst in macrophages, thereby resulting in oxidative stress-induced apoptosis (Yvan-Charvet et al, 2010). However, during and after efferocytosis, macrophages normally overcome the oxidative stress-induced apoptosis, and leave the inflamed site together with engulfed apoptotic neutrophils. In several chronic inflammatory disorders such as atherosclerosis, the

accumulation of dead macrophages is frequently observed, indicating that macrophage death impairs resolution of inflammation (Randolph, 2008). However, the mechanism responsible for macrophage survival after efferocytosis remains largely unresolved.

During efferocytosis, a large amount of reactive oxygen species (ROS) is generated through the activation of the phagocyte NADPH oxidase (NOX2) complex (Russell, 2007). This enzyme is composed of a membrane bound flavocytochrome b558 (comprising $p22^{phox}$ and $gp91^{phox}$) and four cytosolic subunits ($p47^{phox}$, $p40^{phox}$, $p67^{phox}$ and the small GTPase Rac1/2). The activation of NOX2 occurs through phosphorylation of $p47^{phox}$ which is considered as the organizer subunit of NOX2 and also activation of Rac1/2, followed by assembly of all membrane-bound and cytosolic components on the membrane of intracellular vesicles (Bedard & Krause, 2007; Belambri et al, 2012; Groemping & Rittinger, 2005). Once activated by efferocytosis, NOX2-containing granules are fused with the phagosomal membrane and NOX transfers electrons from NADPH to phagosomal oxygen to produce superoxide, which is rapidly converted to hydrogen peroxide by superoxide dismutase (Brennan et al, 2009). Overactivated NOX2 generates excessive amounts of ROS, thereby triggering oxidative stress-induced damage and cell apoptosis. It has been reported that patients with Alzheimer's disease and Parkinson's disease show NOX overactivation (Miller et al, 2009; Shimohama et al, 2000). Under physiological conditions after efferocytosis, however, NOX2-mediated ROS generation is controlled in a manner that the resulting

oxidative stress is not intense enough to induce apoptosis (Bedard & Krause, 2007). However, the mechanism involved in regulation of NOX2 activity is largely unraveled.

Resolution of inflammation is an active process tightly regulated by several endogenous lipid mediators which possess anti-inflammatory and pro-resolving effects. Resolvin D1 (RvD1), one of the endogenous lipid mediators derived from docosahexaenoic acid (DHA), has been shown to promote non-phologistic phagocytosis of apoptotic neutrophils as well as to stimulate exfiltration of macrophages which complete efferocytosis (Serhan & Chiang, 2008). It is well known that RvD1 exerts its pro-resolving effects via specific G protein-coupled receptors such as lipoxin A receptor/formyl-peptide receptor (ALX/FPR2) (Fredman & Serhan, 2011). Although the role of RvD1 in promoting resolution of inflammation has been extensively investigated, little is known about whether RvD1 could affect macrophage survival after efferocytosis. It has been reported that neutroprotectin D1 can protect human retinal pigment epithelial cells from oxidative stress-induced apoptosis by inactivating pro-apoptotic signaling while stimulating anti-apoptotic signaling (Mukherjee et al, 2004). This prompted us to speculate that RvD1 helps macrophages overcome oxidative stress-induced apoptosis during and after efferocytosis. In the present study, we hypothesized that RvD1 downregulates efferocytosis-induced NOX2 activation, thereby protecting macrophages against oxidative stress.

3. Materials and methods

Materials

RvD1 was purchased from Cayman Chemical Co. (Ann Arbor, MI, USA). Dulbecco's Modified Eagle Medium (DMEM), RPMI 1640 and fetal bovine serum (FBS) were obtained from Gibco BRL (Grand Island, NY, USA). Primary antibodies against $p47^{phox}$, $gp91^{phox}$, ALX, Bcl-xL, Bcl-2 and actin were purchased from Santa Cruz Biotechnology (Santa Cruz, CA, USA), and antibodies against cleaved caspase-3 and cleaved PARP were obtained from Cell Signaling (Beverly, MA, USA). Phosphoserine antibody was the product of Abcam (Cambridge, UK). The anti-rabbit and anti-mouse horseradish peroxidase-conjugated secondary antibodies were purchased from Zymed Laboratories (San Francisco, CA, USA).

Cell culture

Murine macrophage-like RAW264.7 cells and Jurkat T cells were purchased from American Type Culture Collection (ATCC, Manassas, VA, USA). Cells were cultured in DMEM (for RAW264.7 cells) and RPMI 1640 (for Jurkat T cells) with 10% FBS, 100 μg/ml streptomycin and 100 U/ml penicillin in humidified 5% CO_2 at 37 °C.

Efferocytosis

Apoptosis of Jurkat T cells was induced by UVB (180 mJ/cm^2) irradiation, followed by

incubation for 8 h at 37 °C in 5% CO_2 atmosphere. The apoptotic Jurkat T cells were stained with fluorescein isothiocyanate (FITC)-conjugated annexin V (Invitrogen, Carlsbad, CA, USA), followed by co-incubation with RAW264.7 cells. To remove the non-engulfed apoptotic Jurkat T cells, RAW264.7 cells were washed three times with PBS.

Flow cytometry analysis

Apoptotic cell death was measured by Annexin-V-FITC staining according to the manufacturer's instructions. After efferocytosis, RAW264.7 cells were treated with RvD1, N-acetyl-cysteine (NAC; Sigma-Aldrich, St Louis, MO, USA) or apocynin (Calbiochem, San Diego, CA, USA) for 8 h and collected with suspended cells. Washed cell pellets were resuspended in 100 μl of annexin V binding buffer and incubated with 5 μl of FITC-conjugated annexin V and 1 μl of propidium iodide (Invitrogen) for 15 min in the dark. Annexin V binding buffer (400 μl) was then added, and cells were analyzed by flow cytometry.

Protein extraction and Western blot analysis

Cell extracts were prepared by suspending the cells directly in the radioimmunoprecipitation assay (RIPA) buffer [20 mM Tris-HCl (pH 7.5), 150 mM NaCl, 1 mM Na_2EDTA, 1 mM EGTA, 1% Triton X-100, 2.5 mM sodium

pyrophosphate, 1 mM β-glycerophosphate, 1 mM Na_3VO_4, 1 μg/ml leuptin, 1 mM phenylmethanesulphonylfluoride (PMSF)] for 1 hr on ice, followed by centrifugation for 15 min at 12000 x *g*. Protein lysates (15 μg) were electrophoresed by sodium dodecyl sulphate (SDS)-polyacrylamide gel electrophoresis (PAGE) and the separated proteins were transferred to polyvinyl difluoride (PVDF) membrane (0.22 μm thickness; Gelman Laboratory, Ann Arbor, MI, USA). To block the non-specific binding of proteins with primary antibodies, the blots were incubated in a 5% non-fat dry milk-PBST buffer [PBS containing 0.1% Tween-20] for 1 hr at room temperature. The membranes were then incubated with the primary antibody suspended in 3% non-fat milk PBST buffer overnight at 4 °C. This was followed by washing with 1X PBST and incubation using appropriate secondary antibody coupled to horseradish peroxidase. Proteins tagged with specific primary antibodies were visualized with an enhanced chemiluminescence detection kit (Amersham Pharmacia Biotech, Buckinghamshire, UK).

Measurement of intracellular accumulation of reactive oxygen species (ROS)

The intracellular accumulation of hydrogen peroxide and superoxide was assessed by fluorescence microscopy using the fluorescent probe 2',7'-dichlorofluorescein diacetate (DCF-DA) (Molecular Probe, Carlsbad, CA, USA) and dihydroethidium (DHE) (Santa Cruz). Cells were washed twice with Hanks balanced salt solution

(HBSS; Cellgro, Herndon, VA, USA) and incubated with 10 μM of DCF-DA or DHE in humidified 5% CO_2 at 37 °C. After 30 min, cells were washed twice with HBSS solution, suspended in the complete media and they were examined under a microscope.

NOX activity assay

NOX activity was measured based on lucigenin-enhanced chemiluminescence. Briefly, after efferocytosis, RAW264.7 cells were treated with RvD1 or apocynin for 1 h, then washed three times with cold PBS and suspended in Krebs buffer of pH 7.4 (130 mM NaCl, 5 mM KCl, 2 mM $MgCl_2$, 1.5 mM $CaCl_2$, 5 mM glucose, 35 mM phosphoric acid, and 20 mM HEPES) containing protease inhibitor cocktail (Roche). Cells were sonicated (3 s, four times on ice) and centrifuged at 3000 rpm at 4°C for 4 min. Lysates were incubated with 5 μM lucigenin (Sigma) and 100 μM NADPH, then the emitted luminescence was detected by luminometer (AntoLumat LB953, EG and G Berthold, Bad Widbad, Germany).

Transfection

siRNA oligonucleotide targeting for *p47^{phox}* and *ALX/FPR2* was purchased from Genolution Pharmaceuticals (Seoul, Korea). The sense and antisense strands of *p47^{phox}* and *ALX/FPR2* siRNA were as follows (forward and reverse, respectively): *p47^{phox}*; 5'-

GCACUCUCACUGAAUACUU-3'and 5'-AAGUA-UUCAGUGAGAGUGC-3', *ALX*/*FPR2*; 5'-GCUGGUUCCUGUGUAAAUU-3' and 5'-AATTTACACAGGAACCAGC-3'. RAW264.7 cells (6 x 10^5/60-mm dish) were transfected with 25 nM of specific or scrambled siRNA oligonucleotides using Lipofectamine RNAiMAX according to manufacturer's instruction (Invitrogen).

Immunoprecipitation

Cells were washed with ice-cold PBS and lysed in RIPA buffer for 1 h on ice, followed by centrifugation for 15 min at 12000 x *g*. 300 μg of pre-cleared lystates were incubated with 10 μl of anti-$p47^{phox}$ antibodies for overnight. 20 μl of protein G-agarose beads (Santa Cruz Biotech) was then added to the mixture and rotated for 4 h at 4 °C. The beads were washed with ice-cold PBS prior to western blot analysis.

Immunocytochemistry

After co-incubation for 1 h with apoptotic Jurkat T cells (stained with FITC-conjugated annexin V), RAW264.7 macrophages (3 x 10^4 cells per well in an 8 chamber plate) were washed three times with PBS to remove the non-engulfed apoptotic Jurkat T cells. Cells were incubated for 1 h in the absence or presence of RvD1 and then fixed with 10% buffered formalin solution (20 min). After a rinse with PBS, cells were permeabilized with 0.2% triton X-100 (5 min) and blocked with 5% BSA in PBST (30

min). Anti-p47^{phox} antibodies, diluted 1:50 in 1% bovine serum albumin (BSA) in PBST, were applied overnight at 4 °C. This was followed by washing cells in PBS (twice for 5 min each) and incubation for 1 h at room temperature with PE-conjugated anti-mouse IgG secondary antibody (Invitrogen) diluted at 1:1000 in 1% BSA-PBST. After washing (twice for 5 min each), cells were treated with DAPI. The signals were detected using an inverted microscope Eclipse Ti-U (Nikon, Tokyo, Japan).

Quantitation of intracellular cAMP

To measure intracellular cAMP concentrations, cells were lysed in 0.1 M HCl (1 x 10^6 cells/ml), followed by a cAMP-specific enzyme-linked immunosorbent assay (ELISA) (Direct cAMP EIA kit; Enzo life sciences, Farmingdale, NY) according to the manufacturer's instructions. cAMP levels were assayed in at least three independent experiments in duplicate.

Measurement of PKA activity

Cells were treated with lysis buffer [20 mM MOPS, 50 mM β-glycerolphosphate, 50 mM sodium fluoride, 1 mM sodium vanadate, 5 mM EGTA, 2 mM EDTA, 1 % NP-40, 1 mM dithiothreitol, 1 mM benzamidine, 1 mM PMSF and 10 μg/ml leupeptin and aprotinin] for 10 min on ice, followed by centrifugation for 15 min at 12000 x *g*. The PKA activity in cell lysate (2 μg) was determined by use of PKA kinase activity kit

(Enzo) according to the manufacturer's instructions. PKA activity was assayed in at least three independent experiments in duplicate.

Hydrogen peroxide scavenging assay

The concentration of hydrogen peroxide solution (40 mM), prepared in phosphate buffer (50 mM, pH 7.4), was determined by absorption at 230 nm using spectrophotometer. RvD1 was added to the solution of hydrogen peroxide and absorbance was measured after 10 min. The percentage of hydrogen peroxide scavenged is calculated using the following equation:

$[A_0 - A_1] / A_0 \times 100$, where A_0 is absorbance of hydrogen peroxide solution and A_1 is absorbance of hydrogen peroxide solution treated with RvD1

4. Results

RvD1 protects macrophages against apoptosis after efferocytosis

To examine the cytoprotective effect of RvD1 on efferocytosis-induced apoptosis, murine macrophage RAW264.7 cells were allowed to engulf apoptotic Jurkat T cells for 1 h and then incubated in the absence or presence of RvD1 (50 nM) for additional 10 h. Earlier studies have shown that RvD1 stimulates phagocytosis of apoptotic cells by macrophages (Fredman & Serhan, 2011; Krishnamoorthy et al, 2010). Therefore, to exclude the effect of RvD1-induced enhancement of efferocytosis, macrophages were exposed to RvD1 after efferocytosis. Following uptake of apoptotic Jurkat T cells, RAW264.7 cells underwent apoptosis whereas RvD1-exposed macrophages were more resistant to apoptosis (**Fig. 3-1A**). We then examined the cleavage of caspase-3 and PARP, hallmarks of apoptosis. Efferocytosis increased the levels of cleaved caspase-3 and PARP in macrophages, but RvD1 suppressed the cleavage of both proteins (**Fig. 3-1B**).

RvD1 attenuates efferocytosis-induced oxidative burst, thereby rescuing macrophages from apoptosis

It has been reported that efferocytosis increases ROS generation in macrophages (Yvan-Charvet et al, 2010). To determine whether RvD1 can reduce oxidative stress induced by efferocytosis, intracellular ROS accumulation was measured by use of the

fluorescent redox-sensitive dye carboxy-H_2DCFDA. Ingestion of apoptotic Jurkat T cells resulted in an increase of intracellular hydrogen peroxide generation in RAW264.7 cells. This ROS generation was continuously increased till 1 h after efferocytosis, but RvD1 or NAC (the ROS scavenger) markedly diminished the generation of ROS in macrophages (**Fig. 3-2A**). To check whether RvD1 has an ability to scavenge ROS directly, a hydrogen peroxide scavenging assay was performed. Following RvD1 addition, the level of H_2O_2 was not decreased, indicating that RvD1 seems to block ROS formation rather than directly eliminating preexisting ROS (**Fig 3-2B**). We next examined the possible involvement of oxidative stress in efferocytosis-induced apoptosis by use of NAC. As shown in **Fig. 3-2C**, efferocytosis-induced apoptosis was suppressed by NAC treatment. Consistent with this observation, the cleavage of caspase-3 and PARP after efferocytosis was inhibited by NAC treatment (**Fig. 3-2D**). These results clearly show that efferocytosis-induced oxidative stress leads to macrophage apoptosis, and that RvD1 can effectively inhibit efferocytosis-induced ROS generation.

RvD1 reduces efferocytosis-induced oxidative stress and apoptosis by inhibiting NOX activation

It has been reported that efferocytosis-induced ROS generation is mediated through activation of NOX, a superoxide generating enzyme (Yvan-Charvet et al, 2010). To

determine whether RvD1 inhibits efferocytosis-induced ROS generation through NOX inactivation, NOX activity was measured. In the presence of RvD1, efferocytosis-induced NOX activation was suppressed (**Fig. 3-3A**). The initial product generated by NOX is superoxide, which is rapidly converted to hydrogen peroxide as a consequence of spontaneous and enzymatic dismutation (Bedard & Krause, 2007). To verify that efferocytosis-induced generation of hydrogen peroxide is derived from superoxide, the intracellular level of superoxide was measured by DHE staining. Ingestion of apoptotic Jurkat T cells increased the number of DHE positive cells, and this was abolished by RvD1 treatment (**Fig. 3-3B**), indicating that RvD1 blocks efferocytosis-induced ROS generation through NOX inactivation. To confirm that NOX activation is critical for efferocytosis-induced oxidative stress and apoptosis, apocynin, a well-known NOX inhibitor, was utilized. As shown in **Fig. 3-3C**, efferocytosis-induced accumulation of hydrogen peroxide in RAW264.7 cells was markedly blocked by apocynin treatment. Apocynin-mediated NOX inactivation was confirmed by the lucigenin assay. Moreover, the blockade of NOX activity by apocynin inhibited efferocytosis-induced apoptosis (**Fig. 3-3D**). The cleavage of caspase-3 and PARP after efferocytosis was also attenuated by apocynin treatment (**Fig. 3-3E**). These findings indicate that the activation of NOX by uptaking apoptotic Jurkat T cells generates oxidative burst in macrophages, leading to apoptosis, but RvD1 protects macrophages from efferocytosis-induced apoptosis via NOX inactivation.

RvD1 suppresses efferocytosis-induced NOX assembly

Among several NOX family members, gp91^{phox}/NOX2 is regarded as the major catalytic component in macrophages. Activation of gp91^{phox}/NOX2, which is a plasma membrane-bound factor, requires association with cytosolic factors (p47^{phox}, p67^{phox} and Rac1/Rac2) (Bedard & Krause, 2007; Rotrosen et al, 1992). After efferocytosis, the interaction between gp91^{phox} and p47^{phox} was enhanced whereas RvD1 blocked their interaction (**Fig. 3-4A**). However, there were no changes in the expression of gp91^{phox} and p47^{phox} by efferocytosis and RvD1 treatment (**Fig. 3-4B**). These data suggest that efferocytosis activates NOX by promoting association of p47 with membrane *NOX subunit* gp91^{phox}, rather than upregulating NOX expression. Immunostaining for p47^{phox} (red staining) revealed that efferocytosis induces p47^{phox} clustering in phagolysosomal membranes surrounding engulfed apoptotic Jurkat T cells (green staining). However, the amount of p47^{phox} staining near phagosome was significantly reduced by RvD1 treatment, indicating that RvD1 suppresses p47^{phox} assembly on phagosomal membranes by blocking the association between gp91^{phox} and p47^{phox} (**Fig. 3-4C**). Moreover, using p47^{phox} siRNA, the importance of p47^{phox} on efferocytosis-induced ROS generation and apoptosis was confirmed (**Fig. 3-4D,E**).

The activation of cAMP/PKA signaling is important for RvD1-mediated suppression of NOX assembly

Above findings prompted us to investigate the mechanism underlying RvD1-mediated inhibition of the NOX2 complex assembly. It has been reported that phosphorylation of $p47^{phox}$ on serine residues leads to conformational changes, facilitating its interaction with other NOX2 components and subsequent formation of the active NOX2 enzyme complex (Bedard & Krause, 2007). To determine whether RvD1-mediated dissociation between $gp91^{phox}$ and $p47^{phox}$ is caused through inhibition of $p47^{phox}$ phosphorylation, the level of serine-phosphorylated $p47^{phox}$ was examined by immunoprecipitation. As expected, efferocytosis induced $p47^{phox}$ phosphorylation in macrophages. However, RvD1 treatment after efferocytosis markedly reduced the level of $p47^{phox}$ phosphorylation (**Fig. 3-5A**), suggesting that RvD1 stimulates dephosphorylation of $p47^{phox}$ on serine residues. We next investigated how RvD1 downregulates the phosphorylation of $p47^{phox}$. As PKA was reported to inhibit phosphorylation of $p47^{phox}$ (Bengis-Garber & Gruener, 1996), the possible involvement of PKA activation in RvD1-mediated dephosphorylation of $p47^{phox}$ in macrophages was determined. RvD1 reduced the phosphorylation of $p47^{phox}$ induced by efferocytosis, but this attenuation was reversed in the presence of H89, a selective inhibitor of PKA (**Fig. 3-5B**). Treatment of RAW264.7 cells with RvD1 resulted in an increase of PKA activity in a time-dependent manner (**Fig. 3-5C**). As PKA is a cyclic AMP (cAMP)-dependent

protein kinase, the effect of RvD1 on cAMP production was examined. Consistent with PKA activation, the concentration of intracellular cAMP was elevated following RvD1 treatment (**Fig. 3-5D**), indicating that RvD1 stimulates cAMP-PKA signaling, thereby downregulating the phosphorylation of $p47^{phox}$.

RvD1-induced activation of cAMP/PKA signaling is mediated by interaction with ALX/FPR2

RvD1 is well recognized to exert its action via cell surface G-protein coupled receptor, such as ALX/FPR2 (Krishnamoorthy et al, 2010). To investigate whether RvD1 activates cAMP-PKA signaling by binding to the membrane receptor ALX/FPR2, we utilized siRNA against ALX/FPR2. In ALX/FPR2 knockdown cells, the RvD1-mediated increase in the intracellular cAMP concentration was completely abrogated (**Fig. 3-6A**). In addition, PKA activity was not significantly induced in ALX/FPR2 knockdown cells upon RvD1 stimulation (**Fig. 3-6B**), indicating that RvD1-induced activation of cAMP-PKA signaling is mediated by ALX/FPR2.

RvD1 shifts the expression of pro- and anti-apoptotic Bcl-2 family proteins toward that overcoming oxidative stress-induced apoptosis

Since resistance to oxidative stress-induced apoptosis is normally accompanied by overexpression of anti-apoptotic proteins (Adams & Cory, 1998), we investigated

whether RvD1 could upregulate the expression of anti-apoptotic proteins including Bcl-xL and Bcl-2. RvD1 treatment time-dependently increased the expression of Bcl-xL and Bcl-2 in RAW264.7 cells (**Fig. 3-7A**). However, in ALX/FPR2 knockdown cells, the expression of these anti-apoptotic proteins was not increased upon RvD1 treatment (**Fig. 3-7B**), indicating that RvD1-mediated ALX activation is also involved in upregulation of Bcl-xL and Bcl-2 expression. Not only increasing the expression of anti-apoptotic Bcl-2 family proteins, but RvD1 downregulated oxidative stress-induced Bad expression, one of pro-apoptotic Bcl-2 family proteins (**Fig. 3-7C,D**). These results suggest that RvD1 protects macrophages against oxidative stress-induced apoptosis by modulating the expression of apoptosis-related proteins.

Nuclear Factor-κB p50 homodimer/Bcl-3 complexes are important for RvD1-induced expression of anti-apoptotic Bcl-2 proteins.

It has been reported that p50 homodimer is capable of transcriptional activation of Bcl-2 protein through association with Bcl-3, the NF-κB co-transactivator. Since p50 lacks a transactivation domain, p50 homodimer needs co-transactivators for inducing the expression of target genes (Kurland et al, 2001). Previously, we have shown that RvD1 facilitates formation of p50 homodimers. To determine whether RvD1-induced p50/p50 formation is involved in upregulation of anti-apoptotic Bcl-2 protein expression, we utilized siRNA against *nfκb1* (especially targeting p50 coding part) to

RAW264.7 cells. In p50 knockdown cells, the RvD1-induced upregulation of Bcl-xL and Bcl-2 expression was abrogated (**Fig. 3-8A**). Moreover, RvD1 increased the nuclear accumulation of p50 and Bcl3 (**Fig. 3-8B**) and the interaction between p50 and Bcl3 (**Fig. 3-8C**). These results suggest that RvD1-induced Bcl-xL and Bcl-2 expression is mediated by p50 homodimer/Bcl-3 complex.

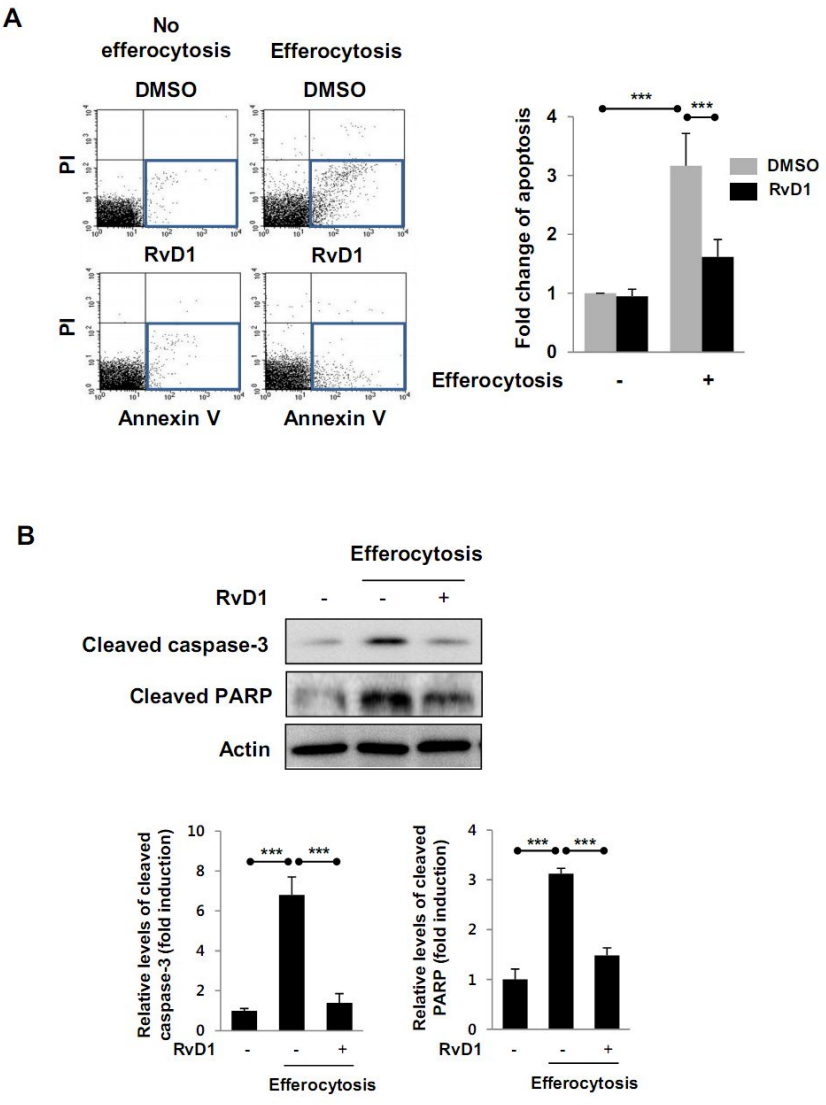
A
No efferocytosis
Efferocytosis
DMSO
DMSO
RvD1
RvD1
PI
PI
Annexin V
Annexin V
***
***
Fold change of apoptosis
DMSO
RvD1
Efferocytosis
-
+
B
Efferocytosis
RvD1
- - +
Cleaved caspase-3
Cleaved PARP
Actin
Relative levels of cleaved caspase-3 (fold induction)
Relative levels of cleaved PARP (fold induction)
RvD1
Efferocytosis

Fig. 3-1. RvD1 protects macrophages against apoptosis after efferocytosis. Jurkat T cells were irradiated with UVB (180 mJ/cm^2) followed by incubation for up to 8 h. RAW264.7 cells were co-incubated with apoptotic Jurkat T cells for 1 h, extensively washed and incubated for additional 10 h with or without RvD1 (50 nM). (A) Apoptosis of RAW264.7 cells was quantified by flow cytometry. Means ± S.D. (n=3), $^{***}p<0.001$. (B) The protein levels of cleaved caspase-3, cleaved PARP and actin were determined by Western blot analysis.

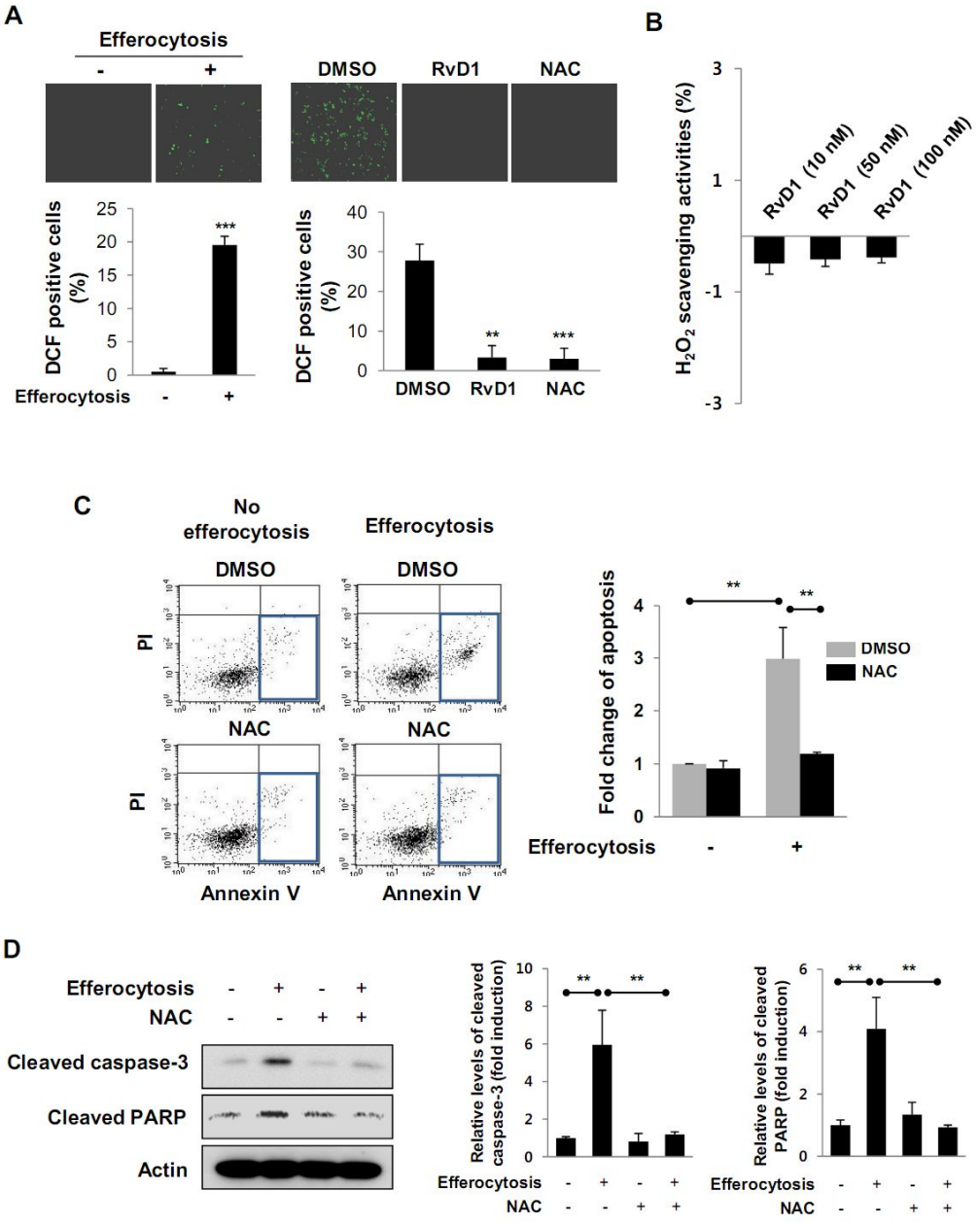
A
Efferocytosis
-
+
DMSO
RvD1
NAC
DCF positive cells (%)
25
20
15
10
5
0
***
Efferocytosis - +
40
30
20
10
0
**
***
DMSO RvD1 NAC
B
H_2O_2 scavenging activities (%)
3
1
-1
-3
RvD1 (10 nM)
RvD1 (50 nM)
RvD1 (100 nM)
C
No efferocytosis
Efferocytosis
DMSO
NAC
PI
Annexin V
Fold change of apoptosis
4
3
2
1
0
**
**
DMSO
NAC
Efferocytosis - +
D
Efferocytosis - + - +
NAC - - + +
Cleaved caspase-3
Cleaved PARP
Actin
Relative levels of cleaved caspase-3 (fold induction)
10
8
6
4
2
0
**
**
Relative levels of cleaved PARP (fold induction)
6
4
2
0
**
**

Fig. 3-2. RvD1 attenuates oxidative stress-induced apoptosis after efferocytosis. (A) RAW264.7 cells were co-incubated with UVB-irradiated apoptotic Jurkat T cells for 1 h, washed and incubated with RvD1 (50 nM) or NAC (10 mM) for additional 1 h. The intracellular ROS level was measured by DCF-DA staining. DCF-DA-stained cells were counted under a microscope with the aid of Image-Pro Plus Software. (B) Hydrogen peroxide scavenging activity of RvD1 was measured at the indicated concentrations. (C, D) After efferocytosis for 1 h, RAW264.7 cells were exposed to NAC for additional 10 h. Quantification of apoptosis was determined by flow cytometry. Means ± S.D. (n=3), $^{**}p<0.01$, $^{***}p<0.001$ (C). The protein levels of cleaved caspase-3, cleaved PARP and actin were determined by Western blot analysis. Histograms represent the relative levels of cleaved caspase-3 and PARP. Means ± S.D. (n=3), $^{**}P<0.01$ (D).

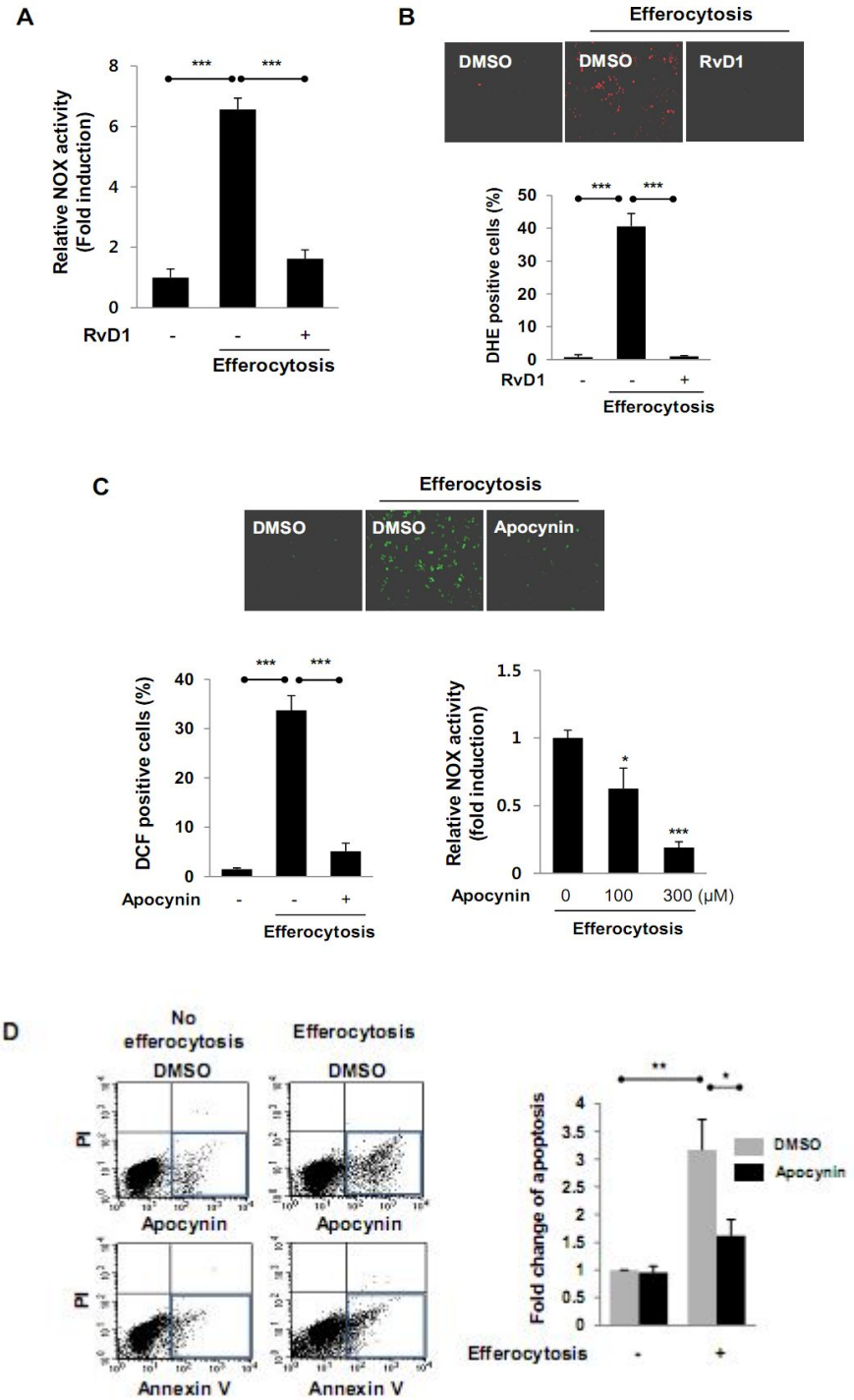
A
Relative NOX activity (Fold induction)
RvD1
Efferocytosis
B
Efferocytosis
DMSO
DMSO
RvD1
DHE positive cells (%)
RvD1
Efferocytosis
C
Efferocytosis
DMSO
DMSO
Apocynin
DCF positive cells (%)
Apocynin
Efferocytosis
Relative NOX activity (fold induction)
Apocynin
0
100
300 (μM)
Efferocytosis
D
No efferocytosis
Efferocytosis
DMSO
DMSO
PI
Apocynin
Apocynin
PI
Annexin V
Annexin V
Fold change of apoptosis
DMSO
Apocynin
Efferocytosis

Fig. 3-3. RvD1 suppresses efferocytosis-induced apoptosis by blocking NOX-mediated ROS production. (A, B) RAW264.7 cells were co-incubated with UVB-irradiated apoptotic Jurkat T cells for 1 h, extensively washed, and incubated in the absence or presence of 50 nM RvD1 for additional 1 h. NOX activity was measured by the lucigenin chemiluminescence assay. Means ± S.D. (n=3), $^{***}p<0.001$ (A). The intracellular superoxide anion level was measured by DHE staining. DHE-stained cells were counted under a microscope with the aid of Image-Pro Plus Software (B). (C) After efferocytosis, RAW264.7 cells were exposed to apocynin (300 μM) for additional 1 h. The intracellular ROS level was measured by DCF-DA staining. NOX inactivation by apocynin was confirmed using lucigenin. (D, E) After efferocytosis for 1 h, RAW264.7 cells were exposed to apocynin for additional 10 h. Quantification of apoptosis was determined by flow cytometry. Means ± S.D. (n=3), $^{*}p<0.05$, $^{**}p<0.01$ (D). The protein levels of cleaved caspase-3, cleaved PARP and actin were determined by Western blot analysis. Histograms represent the relative levels of cleaved caspase-3 and PARP. Means ± S.D. (n=3), $^{*}p<0.05$, $^{**}p<0.01$ (E).

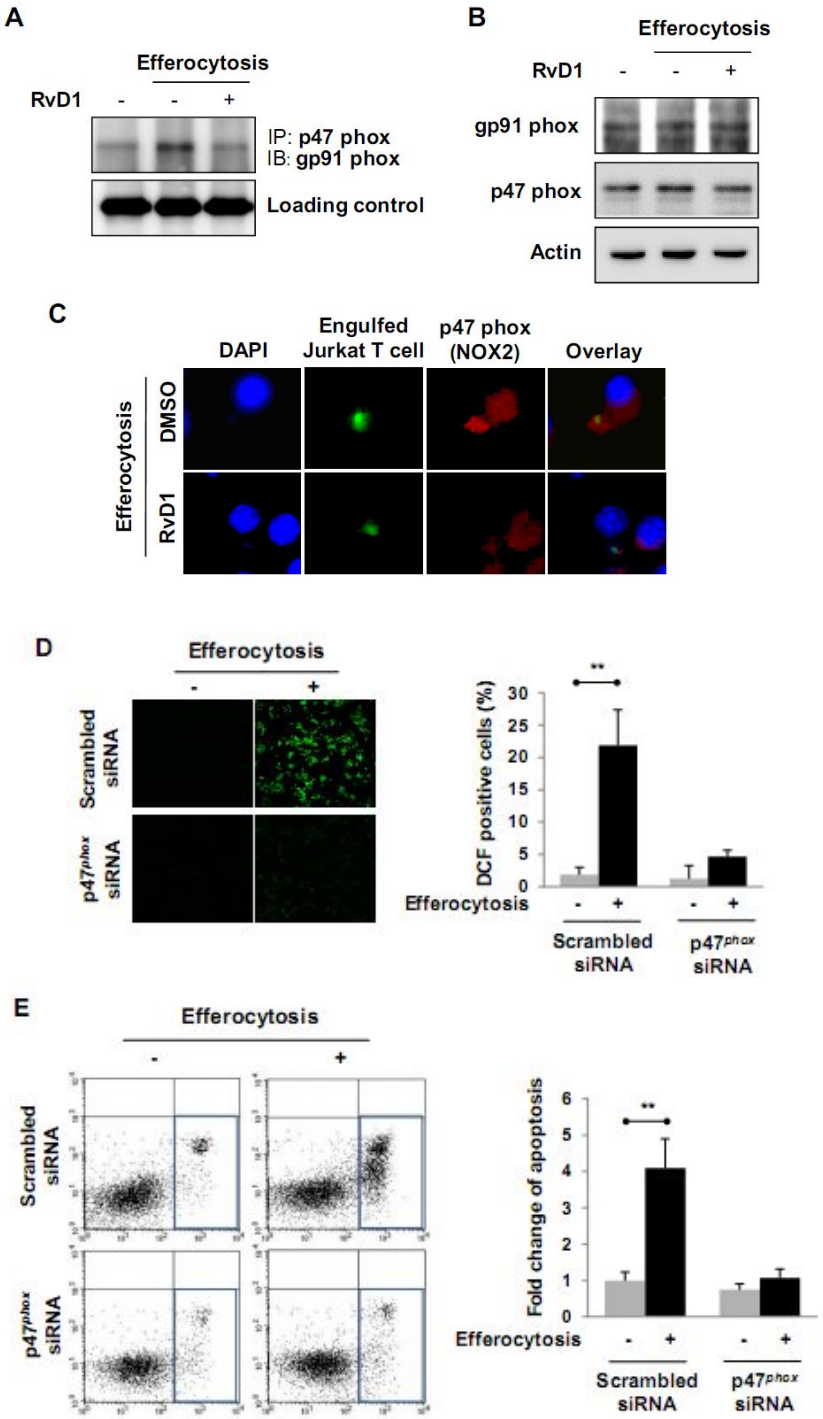
A
Efferocytosis
RvD1 - - +
IP: p47 phox
IB: gp91 phox
Loading control
B
Efferocytosis
RvD1 - - +
gp91 phox
p47 phox
Actin
C
DAPI
Engulfed Jurkat T cell
p47 phox (NOX2)
Overlay
Efferocytosis
DMSO
RvD1
D
Efferocytosis
- +
Scrambled siRNA
p47phox siRNA
DCF positive cells (%)
30
25
20
15
10
5
0
**
Efferocytosis
- + - +
Scrambled siRNA
p47phox siRNA
E
Efferocytosis
- +
Scrambled siRNA
p47phox siRNA
Fold change of apoptosis
6
5
4
3
2
1
0
**
Efferocytosis
- + - +
Scrambled siRNA
p47phox siRNA

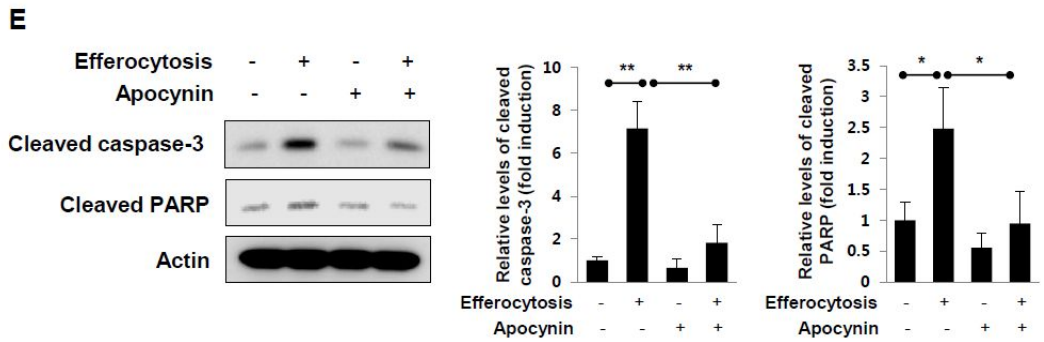

Fig. 3-4. RvD1 inhibits efferocytosis-induced NOX activation by disrupting the assembly of NOX complex. (A-C) After efferocytosis, RAW264.7 cells were incubated treated with RvD1 or vehicle for additional 1 h. $p47^{phox}$ was immunoprecipitated from cell lysates, followed by Western blot analysis for detecting $gp91^{phox}$ (A). The protein levels of $gp91^{phox}$, $p47^{phox}$ and actin were determined by Western blot analysis (B). The assembly of $p47^{phox}$ on phagosomes was determined by immunocytochemistry analysis (C). (D, E) Cells were transfected with scrambled or *$p47^{phox}$* siRNA for 16 h, and then co-incubated with apoptotic Jurkat T cells for additional 1 h. The intracellular ROS level was measured by DCF-DA staining. DCF-DA-stained cells were counted under a microscope with the aid of Image-Pro Plus Software. The levels of $p47^{phox}$ and actin were determined by Western blot analysis (D). Apoptosis of RAW264.7 cells was quantified by flow cytometry (E). Means ± S.D. (n=3), $^{**}p<0.01$

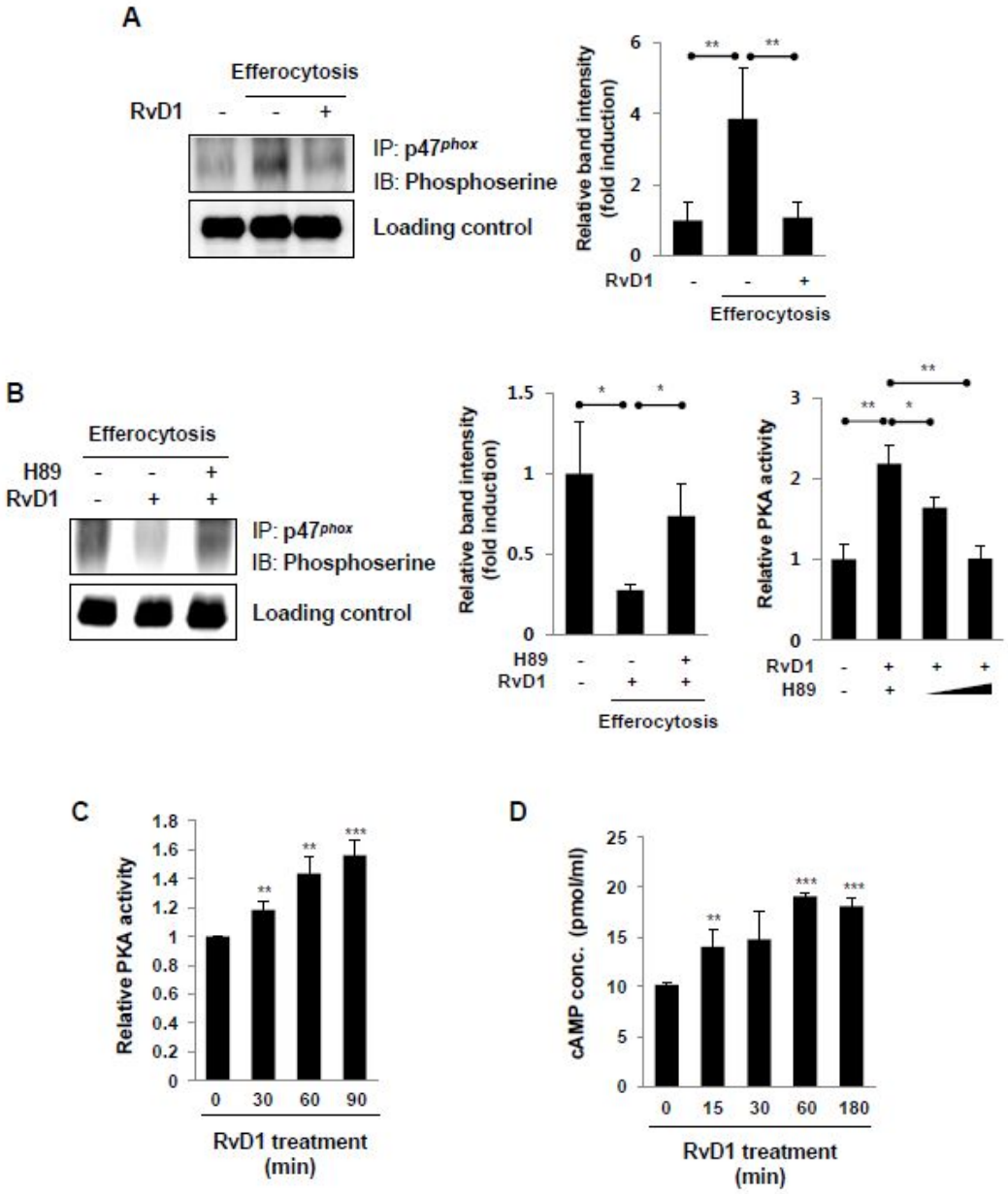
A
Efferocytosis
RvD1 - - +
IP: p47phox
IB: Phosphoserine
Loading control
Relative band intensity (fold induction)
RvD1 - - +
Efferocytosis
B
Efferocytosis
H89 - - +
RvD1 - + +
IP: p47phox
IB: Phosphoserine
Loading control
Relative band intensity (fold induction)
H89 - - +
RvD1 - + +
Efferocytosis
Relative PKA activity
RvD1 - + + +
H89 - + ▲
C
Relative PKA activity
RvD1 treatment (min)
D
cAMP conc. (pmol/ml)
RvD1 treatment (min)

Fig. 3-5. RvD1 inhibits the phosphorylation of p47^{phox} through activation of cAMP/PKA signaling. (A) RAW264.7 cells were co-incubated with apoptotic Jurkat T cells for 1 h, extensively washed and incubated with or without RvD1 for additional 1 h. p47^{phox} was immunoprecipitated from cell lysates, followed by Western blot analysis for detecting phosphoserine. (B) After efferocytosis for 1 h, RAW264.7 cells were exposed to RvD1 or H89 (20 μM) for additional 1 h. p47^{phox} was immunoprecipitated from cell lysates, followed by Western blot analysis for phosphoserine. In the presence of RvD1, RAW264.7 cells were stimulated with H89 (5 or 20 μM) for 1 h. PKA activity was determined by ELISA. (C, D) RAW264.7 cells were treated with RvD1 for indicated time periods. The activity of PKA and the intracellular level of cAMP were measured by ELISA. Means ± S.D. (n=3), $^{*}p<0.05$, $^{**}p<0.01$, $^{***}p<0.001$

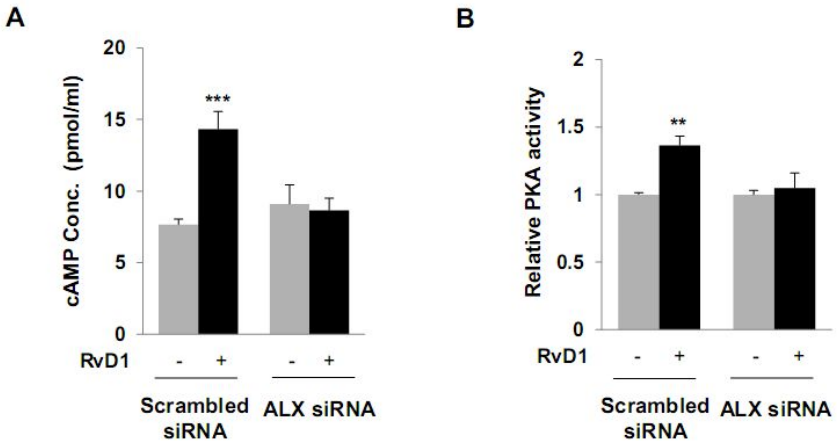

Fig. 3-6. RvD1 stimulates cAMP/PKA signaling in an ALX/FPR2-dependent manner. RAW264.7 cells were transfected with scrambled or ALX siRNA for 16 h, and then exposed to RvD1 for additional 1 h. The activity of PKA (A) and the intracelluar level of cAMP (B) were measured by ELISA. Means ± S.D. (n=3), $^{**}p<0.01$, $^{***}p<0.001$

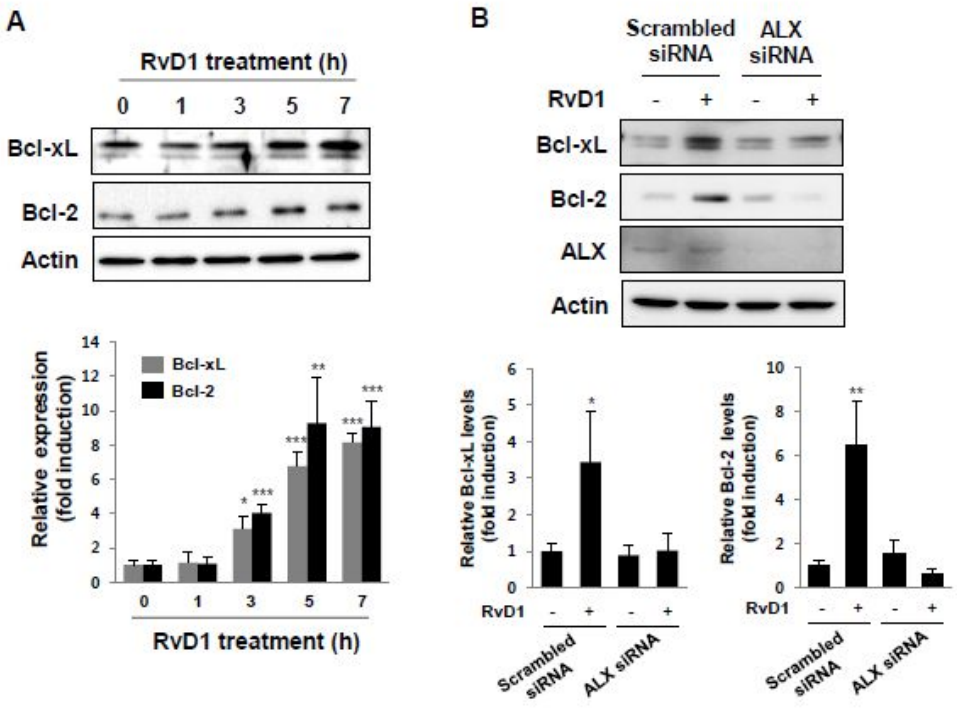
A
RvD1 treatment (h)
0 1 3 5 7
Bcl-xL
Bcl-2
Actin
Relative expression (fold induction)
Bcl-xL
Bcl-2
RvD1 treatment (h)
B
Scrambled siRNA
ALX siRNA
RvD1
Bcl-xL
Bcl-2
ALX
Actin
Relative Bcl-xL levels (fold induction)
Relative Bcl-2 levels (fold induction)
Scrambled siRNA
ALX siRNA
C
H2O2
RvD1
Bad
Actin
Relative Bad levels (fold induction)
D
Efferocytosis
RvD1
Bad
Actin
Relative Bad levels (fold induction)

Fig. 3-7. RvD1 upregulates the expression of anti-apoptotic Bcl-2 proteins while down-regulating oxidative stress-induced expression of pro-apoptotic Bad protein. (A) RAW264.7 cells were treated with RvD1 for the indicated time. (B) Cells were transfected with scrambled or ALX siRNA for 16 h, and then exposed to RvD1 for additional 7 h. The protein levels of Bcl-xL, Bcl-2, ALX and actin were determined by Western blot analysis. (C, D) RAW264.7 cells were treated with H_2O_2 (800 μM) and RvD1 (50 nM) for 1 h (left), or co-incubated with apoptotic Jurkat T cells for 1 h, extensively washed and incubated with RvD1 for 3 h (right). The protein levels of Bad and actin were determined by Western blot analysis. Histograms represent the relative band intensity. Means ± S.D. (n=3), $^{*}p<0.05$, $^{**}p<0.01$, $^{***}p<0.001$

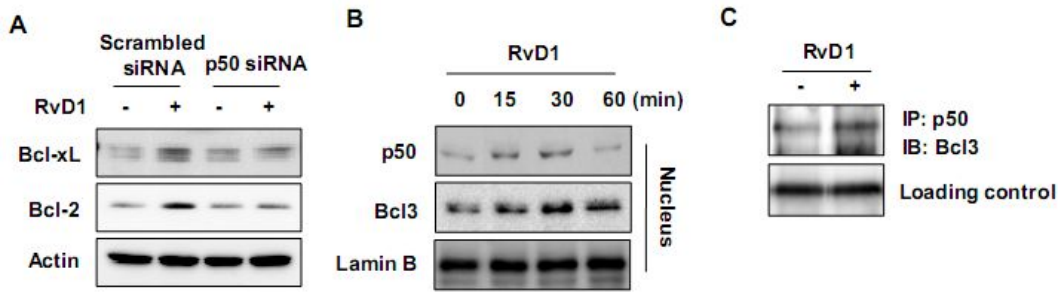

Fig. 3-8. RvD1 upregulates the expression of anti-apoptotic Bcl-2 proteins by inducing formation of p50 homodimer/Bcl3 complex. (A) RAW264.7 cells were transfected with scrambled or p50 siRNA for 16 h, and then exposed to RvD1 (50 nM) for additional 30 min. The protein levels of Bcl-xL, Bcl-2 and actin were determined by Western blot analysis. (B) RAW264.7 cells were treated with RvD1 for indicated time periods, and nuclear extracts were prepared. Levels of p50 and Bcl3 in nucleus were assayed by Western blot analysis. (C) Cells were incubated with RvD1 or DMSO for 30 min. p50 was immunoprecipitated from cell lysates, followed by Western blot analysis for detecting Bcl3.

5. Discussion

During the resolution of inflammation, macrophages play a central role in clearance of apoptotic neutrophils to prevent secondary necrosis of apoptotic cells, finally allowing the termination of inflammatory responses (Serhan et al, 2007). In this regard, macrophage death during resolution of inflammation causes failure in resolution of inflammation, which may lead to chronic inflammatory disorders such as atherosclerosis (Seimon & Tabas, 2009). Recently, Yvan-Charvet *et al*. reported that efferocytosis which is fundamental to the resolution of inflammation evokes excessive oxidative burst with subsequent induction of apoptosis in macrophages. Their study revealed that macrophage apoptosis induced by co-incubation with apoptotic cells was not caused by molecules released from cells undergoing apoptosis, but rather through engulfment of apoptotic cells (Yvan-Charvet et al, 2010). In agreement with this report, our present study shows that uptake of apoptotic cells induces the accumulation of intracellular ROS, followed by macrophage apoptosis. Even though macrophages engulfing apoptotic cells suffer from oxidative stress, they normally overcome this and leave the inflamed site via lymphatics in physiological conditions. However, the mechanism underlying macrophage survival after efferocytosis has not been elucidated. In this study, we have uncovered the novel role of anti-inflammatory and pro-resolving lipid mediator RvD1 in preserving the viability of macrophages involved in efferocytosis. To the best of our knowledge, this is the first report demonstrating that

RvD1 prevents efferocytosis-induced ROS generation and suppresses oxidative stress-induced apoptosis of macrophages, thereby successfully completing its pro-resolving functions. Interestingly, it has been suggested that RvE1, one of E-series resolvins possessing the same properties with RvD1, promotes phagocytosis-induced neutrophil apoptosis via ROS generation (El Kebir et al, 2012). Unlike macrophages whose death retards the termination of inflammation, neutrophils infiltrated into the inflamed site must undergo apoptosis after completion of its mission, and it is the critical control point in resolution of inflammation. Thus, resolvins seem to act differently depending on the cell type, in promoting the resolution of inflammation.

A recent study has demonstrated that efferocytosis-induced ROS generation is associated with the activation of NOX2, the major NADPH oxidase complex present in macrophages (Yvan-Charvet et al, 2010). We found that engulfment of apoptotic cells activated NOX2 in macrophages by inducing the association between the membrane-bound factor gp91^{phox} and cytosolic factor p47^{phox} on phagosomal membranes. Here, we describe for the first time that RvD1 can attenuate the activation of NOX2 in macrophages with engulfed apoptotic cells, thereby blocking efferocytosis-induced ROS generation.

Even though phosphorylation of p47^{phox} is considered as the key event required for NOX2 activation, the regulatory mechanism involved in inhibition of p47^{phox} phosphorylation is poorly understood. It has been reported that PKA inhibits p47^{phox}

phosphorylation as well as oxidative burst (Bengis-Garber & Gruener, 1996). Accumulating data indicate that PKA activates protein phosphatase 2A (PP2A), which is responsible for dephosphorylation of serine and threonine residues (Ahn et al, 2007; Feschenko et al, 2002). Therefore, PKA-mediated activation of PP2A may account for suppression of efferocytosis-induced $p47^{phox}$ phosphorylation. As RvD1 is known as a ligand of G-protein coupled receptor which is related to PKA signaling, we speculate that RvD1 might inhibit $p47^{phox}$ phosphorylation via PKA activation. In support of this supposition, RvD1 suppressed efferocytosis-induced phosphorylation of $p47^{phox}$ by activating cAMP/PKA signaling. Furthermore, in ALX/FPR2 knockdown cells, RvD1 failed to increase the level of cAMP as well as the activity of PKA, indicating that RvD1 is a novel activator of cAMP-PKA by acting as an endogenous ligand of for ALX/FPR2. Interestingly, it has been suggested that the macrophage phenotype, which is classified into pro-inflammatory M1 and anti-inflammatory M2, is controlled by cAMP. When cAMP concentrations in M1 macrophages were increased, the macrophage phenotype became prone to resolution of inflammation (Bystrom et al, 2008), implying that cAMP is a key factor which triggers transition from inflammation to resolution. Moreover, recent studies have demonstrated that RvD1 enhances macrophage polarization toward the M2 phenotype via G protein-coupled receptor-triggered signaling, which induces cAMP formation (Hsiao et al, 2013; Titos et al, 2011). In this regard, our findings support the important role of cAMP in RvD1-

mediated resolution of inflammation.

Besides suppression of NOX2-mediated ROS generation, RvD1 protected macrophages against efferocytosis-induced apoptosis by modulating the expression of apoptosis-related proteins. It has been suggested that ROS increases the expression of pro-apoptotic proteins and decreases the expression of anti-apoptotic proteins by modulating their phosphorylation and ubiquitination (Li et al, 2004). Moreover, Li et al. reported that apocynin-mediated inhibition of NOX activity resulted in upregulation of Bcl-2 expression as well as downregulation of pro-apoptotic protein Bax expression (Li et al, 2012). Similar to apocynin, RvD1 attenuates ROS generation by suppressing NOX2 activation. Therefore, RvD1 seems to regulate the expression of apoptosis-related genes by suppressing ROS generation.

Taken together, our findings suggest that the pro-resolving lipid mediator RvD1, generated during resolution of inflammation, plays an important role in macrophage survival after efferocytosis. RvD1 suppressed efferocytosis-induced ROS generation and subsequent apoptosis through inhibition of assembly of the NOX2 complex. This cytoprotective activity of RvD1 is attributable, at least in part, to cAMP production and consequent PKA activation which appears to be mediated by ALX/FPR2. RvD1 also potently attenuated efferocytosis-triggered pro-apoptotic signaling, while it stimulated the anti-apoptotic pathway, thereby helping macrophages overcome efferocytosis-induced apoptosis (**Fig. 3-9**). The results from our present study suggest a novel

mechanism underlying efferocytosis-induced apoptosis, which will be valuable in better understanding the pathogenesis of chronic inflammatory disorders associated with macrophage death. In this context, RvD1 and its synthetic derivatives are expected to be utilized as the potent therapeutic agents in the management of inflammatory diseases.

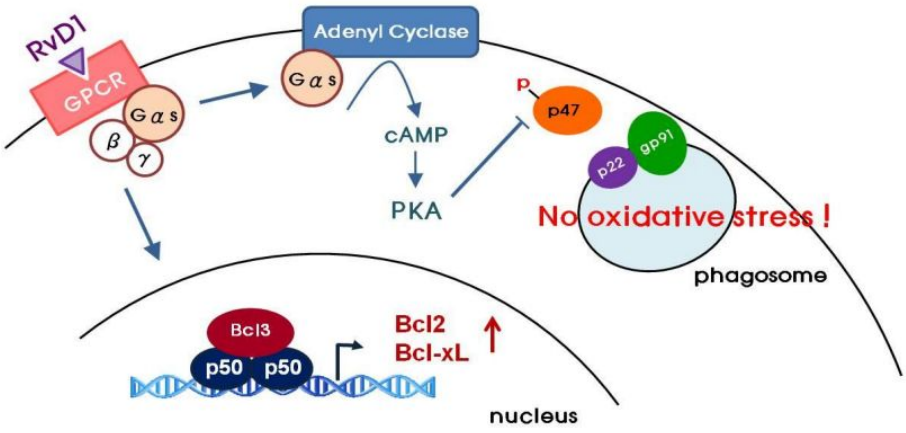

Fig. 3-9. The molecular mechanisms underlying RvD1-mediated protection of macrophages against efferocytosis-induced apoptosis. During efferocytosis, macrophages are suffered from oxidative stress. Pro-resolving lipid mediator RvD1 prevents efferocytosis-induced ROS generation and subsequent apoptosis through inhibition of assembly of the NOX2 complex. This cytoprotective activity of RvD1 is dependent on cAMP production and PKA activation which appears to be mediated by ALX/FPR2. RvD1 also potently attenuated efferocytosis-triggered pro-apoptotic signaling, thereby helping macrophages overcome efferocytosis-induced apoptosis.

6. References

Adams JM, Cory S (1998) The Bcl-2 protein family: arbiters of cell survival. *Science* **281:** 1322-1326

Ahn JH, McAvoy T, Rakhilin SV, Nishi A, Greengard P, Nairn AC (2007) Protein kinase A activates protein phosphatase 2A by phosphorylation of the B56delta subunit. *Proceedings of the National Academy of Sciences of the United States of America* **104:** 2979-2984

Bedard K, Krause KH (2007) The NOX family of ROS-generating NADPH oxidases: physiology and pathophysiology. *Physiological reviews* **87:** 245-313

Belambri SA, Hurtado-Nedelec M, Senator A, Makni-Maalej K, Fay M, Gougerot-Pocidalo MA, Marie JC, Dang PM, El-Benna J (2012) Phosphorylation of p47phox is required for receptor-mediated NADPH oxidase/NOX2 activation in Epstein-Barr virus-transformed human B lymphocytes. *American journal of blood research* **2:** 187-193

Bengis-Garber C, Gruener N (1996) Protein kinase A downregulates the phosphorylation of p47 phox in human neutrophils: a possible pathway for inhibition of the respiratory burst. *Cellular signalling* **8:** 291-296

Brennan AM, Suh SW, Won SJ, Narasimhan P, Kauppinen TM, Lee H, Edling Y, Chan PH, Swanson RA (2009) NADPH oxidase is the primary source of superoxide induced by NMDA receptor activation. *Nature neuroscience* **12:** 857-863

Bystrom J, Evans I, Newson J, Stables M, Toor I, van Rooijen N, Crawford M, Colville-Nash P, Farrow S, Gilroy DW (2008) Resolution-phase macrophages possess a unique inflammatory phenotype that is controlled by cAMP. *Blood* **112:** 4117-4127

El Kebir D, Gjorstrup P, Filep JG (2012) Resolvin E1 promotes phagocytosis-induced neutrophil apoptosis and accelerates resolution of pulmonary inflammation. *Proceedings of the National Academy of Sciences of the United States of America* **109:** 14983-14988

Feschenko MS, Stevenson E, Nairn AC, Sweadner KJ (2002) A novel cAMP-stimulated pathway in protein phosphatase 2A activation. *The Journal of pharmacology and experimental therapeutics* **302:** 111-118

Fredman G, Serhan CN (2011) Specialized proresolving mediator targets for RvE1 and RvD1 in peripheral blood and mechanisms of resolution. *The Biochemical journal* **437:** 185-197

Groemping Y, Rittinger K (2005) Activation and assembly of the NADPH oxidase: a structural perspective. *The Biochemical journal* **386:** 401-416

Hsiao HM, Sapinoro RE, Thatcher TH, Croasdell A, Levy EP, Fulton RA, Olsen KC, Pollock SJ, Serhan CN, Phipps RP, Sime PJ (2013) A novel anti-inflammatory and pro-resolving role for resolvin D1 in acute cigarette smoke-induced lung inflammation. *PloS one* **8:** e58258

Krishnamoorthy S, Recchiuti A, Chiang N, Yacoubian S, Lee CH, Yang R, Petasis NA, Serhan CN (2010) Resolvin D1 binds human phagocytes with evidence for

proresolving receptors. *Proceedings of the National Academy of Sciences of the United States of America* **107:** 1660-1665

Kurland JF, Kodym R, Story MD, Spurgers KB, McDonnell TJ, Meyn RE (2001) NF-kappaB1 (p50) homodimers contribute to transcription of the bcl-2 oncogene. *The Journal of biological chemistry* **276:** 45380-45386

Li D, Ueta E, Kimura T, Yamamoto T, Osaki T (2004) Reactive oxygen species (ROS) control the expression of Bcl-2 family proteins by regulating their phosphorylation and ubiquitination. *Cancer science* **95:** 644-650

Li M, Liu Z, Zhuan L, Wang T, Guo S, Wang S, Liu J, Ye Z (2012) Effects of apocynin on oxidative stress and expression of apoptosis-related genes in testes of diabetic rats. *Molecular medicine reports*

Miller RL, James-Kracke M, Sun GY, Sun AY (2009) Oxidative and inflammatory pathways in Parkinson's disease. *Neurochemical research* **34:** 55-65

Mukherjee PK, Marcheselli VL, Serhan CN, Bazan NG (2004) Neuroprotectin D1: a docosahexaenoic acid-derived docosatriene protects human retinal pigment epithelial cells from oxidative stress. *Proceedings of the National Academy of Sciences of the United States of America* **101:** 8491-8496

Murillo MM, Carmona-Cuenca I, Del Castillo G, Ortiz C, Roncero C, Sanchez A, Fernandez M, Fabregat I (2007) Activation of NADPH oxidase by transforming growth factor-beta in hepatocytes mediates up-regulation of epidermal growth factor receptor ligands through a nuclear factor-kappaB-dependent mechanism. *The Biochemical journal* **405:** 251-259

Randolph GJ (2008) Emigration of monocyte-derived cells to lymph nodes during resolution of inflammation and its failure in atherosclerosis. *Current opinion in lipidology* **19:** 462-468

Rotrosen D, Yeung CL, Leto TL, Malech HL, Kwong CH (1992) Cytochrome b558: the flavin-binding component of the phagocyte NADPH oxidase. *Science* **256:** 1459-1462

Russell DG (2007) New ways to arrest phagosome maturation. *Nature cell biology* **9:** 357-359

Seimon T, Tabas I (2009) Mechanisms and consequences of macrophage apoptosis in atherosclerosis. *Journal of lipid research* **50 Suppl:** S382-387

Serhan CN, Brain SD, Buckley CD, Gilroy DW, Haslett C, O'Neill LA, Perretti M, Rossi AG, Wallace JL (2007) Resolution of inflammation: state of the art, definitions and terms. *FASEB journal : official publication of the Federation of American Societies for Experimental Biology* **21:** 325-332

Serhan CN, Chiang N (2008) Endogenous pro-resolving and anti-inflammatory lipid mediators: a new pharmacologic genus. *British journal of pharmacology* **153 Suppl 1:** S200-215

Serhan CN, Savill J (2005) Resolution of inflammation: the beginning programs the end. *Nature immunology* **6:** 1191-1197

Shimohama S, Tanino H, Kawakami N, Okamura N, Kodama H, Yamaguchi T, Hayakawa T, Nunomura A, Chiba S, Perry G, Smith MA, Fujimoto S (2000) Activation of NADPH oxidase in Alzheimer's disease brains. *Biochemical and*

biophysical research communications **273:** 5-9

Tabas I (2010) Macrophage death and defective inflammation resolution in atherosclerosis. *Nature reviews Immunology* **10:** 36-46

Titos E, Rius B, Gonzalez-Periz A, Lopez-Vicario C, Moran-Salvador E, Martinez-Clemente M, Arroyo V, Claria J (2011) Resolvin D1 and its precursor docosahexaenoic acid promote resolution of adipose tissue inflammation by eliciting macrophage polarization toward an M2-like phenotype. *J Immunol* **187:** 5408-5418

Yvan-Charvet L, Pagler TA, Seimon TA, Thorp E, Welch CL, Witztum JL, Tabas I, Tall AR (2010) ABCA1 and ABCG1 protect against oxidative stress-induced macrophage apoptosis during efferocytosis. *Circulation research* **106:** 1861-1869

Chapter IV

Resolvin D1 suppresses inflammation-induced colon tumorigenesis in mice by inhibiting cyclin D1-induced mitotic spindle abnormality

1. Abstract

Inflammation is considered to increase the risk of colorectal cancer, possibly by inducing chromosomal instability. However, the precise pathologic mechanisms underlying inflammation-induced chromosomal instability and subsequent tumorigenesis are not well understood. Resolvin D1 (RvD1), an endogenous lipid mediator generated from docosahexaenoic acid, is known to suppress excessive inflammatory responses and promote resolution of inflammation, and is hence speculated to prevent chronic inflammation-induced cancer. Using the azoxymethane (AOM)-initiated and dextran sodium sulfate (DSS) colitis-promoted colorectal cancer model, we revealed that RvD1 attenuates inflammation-induced tumorigenesis. Moreover, it reduced AOM/DSS-induced production of pro-inflammatory cytokine interleukin-6 (IL-6), which is implicated in chronic inflammation and cancer. IL-6 triggered malignant transformation and abnormalities of mitotic spindle and nucleus in intestinal epithelial CCD841CoN cells, and these oncogenic events were abolished by RvD1 treatment. The inhibitory effect of RvD1 on chromosomal instability was associated with downregulation of IL-6-induced cyclin D1 expression, which appears to be mediated by blocking the Janus kinase 2-signal transducer and activator of transcription 3 axis. Knockdown of cyclin D1 abolished IL-6-induced mitotic spindle abnormality, whereas cyclin D1 overexpression increased the number of cells containing multipolar spindles. In AOM plus DSS-treated mice, cyclin D1 expression

was upregulated in colon, and this was abrogated by RvD1 treatment. The elevated level of cyclin D1 was also observed in human colon tumor tissues. Taken together, these findings suggest that RvD1-mediated downregulation of cyclin D1 expression may contribute to its maintenance/restoration of chromosomal stability and suppression of inflammation-associated colon tumorigenesis.

Key words

Inflammation-associated colorectal cancer, IL-6, RvD1, Cyclin D1, Mitotic spindle abnormality

2. Introduction

Chronic inflammation is a well-known risk factor for colorectal cancer. Epidemiological studies suggest that inflammation-associated colorectal cancer develops in patients with inflammatory bowel diseases including Crohn's disease and ulcerative colitis. It has been estimated that the risk of colorectal cancer increases by 0.5 to 1% per year after 8 to 10 year of inflammatory bowel diseases (Askling et al., 2001). Whereas the contribution of chronic inflammation to tumorigenesis has been focused on its ability to cause genetic mutations via oxidative DNA damage, growing body of data propose a direct effect of inflammation on tumor growth (Waldner et al., 2012). Prolonged and excessive production of pro-inflammatory cytokines, such as interleukin 6 (IL-6) and tumor necrosis factor-α (TNF-α), is considered to contribute to intestinal tumorigenesis (Popivanova et al., 2008; Grivennikov et al., 2009). IL-6 is involved in survival, proliferation, and invasiveness of colorectal cancer cells (Kishimoto, 2005). The oncogenic effect of IL-6 is mainly mediated by activation of Janus kinase (JAK) and its downstream effector signal transducer and activator of transcription 3 (STAT3) via the IL-6 receptor (IL-6R)/gp130 complex. IL-6-induced STAT3 activation leads to its translocation to the nucleus, thereby promoting transcription of a variety of target genes, most of which are oncogenes (Bromberg et al., 1999).

Cyclin D1, transcriptionally regulated by STAT3 signaling, is known as a G1 phase

regulatory protein. Cyclin D1 overexpression is a common feature of several human malilgnancies including colorectal cancer (Nelsen et al., 2005). Under physiological conditions, cyclin D1 is transiently upregulated and promotes cell proliferation by mitogens and other extracellular stimuli (Malumbres and Barbacid, 2001). However, constitutive overexpression of cyclin D1 can trigger malignant transformation by reducing the dependence on extracellular signals that normally control cell proliferation. Beside regulation of cell cycle, cyclin D1 has recently been suggested to induce chromosomal instability (Casimiro et al., 2012), which is a hallmark of cancer.

Chromosomal instability, defined as alteration in the structure or the number of chromosomes, is highly correlated with tumorigenesis (Saunders, 2005). One of the major causes of chromosomal instability is an increased rate of chromosome segregation errors during the mitotic division of cells. For accurate chromosome segregation, the formation of a bipolar mitotic spindle is critical, which is influenced by the number of centrosomes serving as the major microtubule organizing center (Nelsen et al., 2005). In cancer cells, it is often observed that mitotic spindles have more than two poles, resulting in asymmetric chromosome segregation and subsequent generation of the daughter cells with an abnormal number of chromosomes (Saunders, 2005). Changes in chromosome composition can lead to gain of oncogenic functions or loss of tumor suppressor functions that further promote malignant transformation (Nelsen et al., 2005). Several studies have demonstrated a relatively high frequency of

chromosomal instability in colitis-associated colorectal cancer (Araujo et al., 2007; Gerling et al., 2010). However, the precise pathologic mechanisms underlying chronic inflammation-induced chromosomal instability and subsequent tumorigenesis are poorly understood.

Chronic inflammation is a result of failure in resolution of inflammation. Accumulating evidence suggests that resolution of inflammation is a coordinated process which is actively regulated by several anti-inflammatory and pro-resolving lipid mediators such as resolvins (resolution-phase interaction products) (Serhan, 2007). Resolvin D1 (RvD1) is one of the endogenous pro-resolving lipid mediators formed from docosahexaenoic acid (DHA; C22:6) during resolution of inflammation (Hong et al., 2003). RvD1 exerts the anti-inflammatory and pro-resolving effects by regulating inflammatory cell trafficking and downregulating pro-inflammatory signaling (Serhan and Chiang, 2008). It has been reported that RvE1, aspirin-triggered RvD1 and RvD2 have the preventive effect on dextran sulfate sodium (DSS)-induced colitis in mice (Ishida et al., 2010; Bento et al., 2011). However, the effect of resolvins on protection against inflammation-induced cancer has not been investigated at all. Here, we firstly report that RvD1 has the preventive effect on azoxymethane (AOM) plus DSS-induced mouse colon carcinogenesis and suggest inhibition of cyclin D1-dependent mitotic spindle abnormality under pro-inflammatory conditions as a potential underlying molecular mechanism.

3. Materials and Methods

Materials

RvD1 was purchased from Cayman Chemical Co. (Ann Arbor, MI, USA). Interleukin-6 (IL-6) was obtained from Sigma-Aldrich (St Louis, MO, USA). Minimum Essential Medium (MEM) and fetal bovine serum (FBS) were purchased from Gibco BRL (Grand Island, NY, USA). Primary antibodies against STAT3, gp130, lamin B, CDK4, E2F1, Rb, α-tubulin and actin were purchased from Santa Cruz Biotechnology (Santa Cruz, CA, USA), and pJAK2, JAK2, pSTAT3, cyclin D1, pRb and PLK4 antibodies were obtained from Cell Signaling (Beverly, MA, USA). The anti-rabbit and anti-mouse horseradish peroxidase-conjugated secondary antibodies were purchased from Zymed Laboratories (San Francisco, CA, USA).

AOM/DSS-induced colon cancer model

Male Institute of Cancer Research (ICR) mice (5 weeks of age) were purchased from Orient Bio Inc. (Republic of Korea). All animals were kept in climate-controlled quarters (24 °C at 50% humidity) with 12 h light/12 h dark cycle. Mice were weighed and given an intraperitoneally injection of AOM (10 mg/kg) or vehicle (PBS) on experimental day 0. One week later, animals received either 2.5 % DSS or normal drinking water for 1 week. Either RvD1 or PBS was intraperitoneally given before and during DSS administration once three days. At the time of harvest, colons were

resected, flushed with PBS, opened longitudinally, and measured. Macroscopic polyps were counted. Colon sections were fixed in formalin (for immunohistochemistry staining) or snap frozen (for western blotting). Paraffin-embedded colon sections (4 μm) were stained with hematoxylin-eosin and examined by light microscopy to histology. Immunohistochemical staining was performed on paraffin-embedded colon sections using anti-cyclin D1 or pSTAT3 antibodies according to the procedure described previously (Cui et al., 2010). Also, plasma was prepared from mouse blood taken from the heart and stored at -70 °C.

Measurement of IL-6

The concentrations of IL-6 in mouse colon tissues were determined by using Mouse IL-6 ELISA kit (KOMA BIOTECH Inc., Seoul, Korea) according to the manufacturer's instructions.

Measurement of RvD1

Lipids were extracted using C_{18} reverse phase extraction columns as previously described (Moore et al., 2000). The concentrations of RvD1 in tissues and blood plasma were determined by using Resolvin D1 EIA kit (Enzo life sciences, Farmingdale, NY) according to the manufacturer's instructions.

Cell culture

Intestinal epithelial CCD841CoN cells were purchased from American Type Culture Collection (ATCC, Manassas, VA, USA). Cells were cultured in MEM with 10% FBS, 100 μg/ml streptomycin and 100 U/ml penicillin in humidified 5% CO_2 at 37 °C.

Protein extraction and Western blot analysis

Cell extracts were prepared by suspending the cells directly in the RIPA lysis buffer [20 mM Tris-HCl (pH 7.5), 150 mM NaCl, 1 mM Na_2EDTA, 1 mM ethylene glycol tetraacetic acid (EGTA), 1% Triton X-100, 2.5 mM sodium pyrophosphate, 1 mM β-glycerophosphate, 1 mM Na_3VO_4, 1 μg/ml leuptin, 1 mM PMSF, 0.1% sodium dodecyl sulfate (SDS)] for 1 h on ice and this was followed by centrifugation for 15 min at 12000 x *g*. Collected colon tissues were homogenized in RIPA lysis buffer and lysed for 1 h on ice, followed by by centrifugation for 15 min at 12000 x *g*. Nuclear extracts from cells and mouse colon were prepared as described previously (Chun et al., 2003; Park et al., 2009). Protein lysates (15 μg) were electrophoresed by SDS-polyacrylamide gel electrophoresis (PAGE) and the separated proteins were transferred to polyvinyl difluoride (PVDF) membrane (0.22 μm thickness; Gelman Laboratory, Ann Arbor, MI, USA). The blots were prepared and visualized according to the procedure described previously (Chen et al., 2005).

Immunocytochemistry

CCD841CoN were seeded at 3 x 10^4 cells per well in an 8 chamber plate. The cells were pretreated with RvD1 (100 nM) or DMSO for 30 min and then stimulated with IL-6 (50 ng/mL) for 3 days and then fixed with 10% buffered formalin solution (20 min). The cells were then washed in PBS (twice for 5 min each), permeabilized with 0.1% triton X-100 (5 min), washed in PBS (twice for 5 min each), and blocked with 5% BSA in PBS (30 min). Polyclonal mouse anti-α-tubulin, diluted 1:100 in 1% bovine serum albumin (BSA) in PBS, was applied overnight at 4 °C. This was followed by washing cells in PBS (twice for 5 min each) and then incubation for 1 h at room temperature with PE-conjugated anti-mouse IgG secondary antibodies diluted at 1:1000 in 1% BSA-PBS. After washing (twice for 5 min each), cells were treated with 4',6-diamidino-2-phenylindole. The signals were detected using a microscope (Nikon, Tokyo, Japan).

Electrophoretic mobility-gel shift assay (EMSA)

Customized double-stranded oligonucleotide containing the STAT binding domains was obtained from Promega, and 100 ng of the oligonucleotide was labeled with [γ-^{32}P]ATP by employing T4 polynucleotide kinase and was purified on a Nick column (Amersham Pharmacia Biotech, Buckinghamshire, UK). The nuclear protein (10 μg) was mixed with 2 μl of concentrated incubation buffer [10 mM Tris-HCl (pH7.5), 100

mM NaCl, 1 mM DTT, 1 mM EDTA, 4% glycerol and 0.1 mg/ml sonicated salmon sperm DNA] and the hypertonic buffer was added to make up the final volume 20 μl. After preincubation at room temperature for 15 min, the labeled oligonucleotide (400,000 cpm) was added to the nuclear fraction and incubation was continued for additional 50 min at room temperature. To ensure the specific binding of the labeled oligonucleotide to nuclear protein, a competition assay was carried out with the excess amounts of unlabeled oligonucleotide. After the incubation, 0.1% bromophenol blue (2 μl) was added, and STAT-DNA complexes were separated from the unbound free probe by electrophoresis on 6% nondenaturing polyacrylamide gel in 1X TBE buffer [90 mM Tris base, 90 mM boric acid and 0.5 mM EDTA (pH 8.0)] at 140 V for 3 h. Gels were dried and exposed to X-ray film.

Immunoprecipitation

Cells were washed with ice-cold PBS and lysed in RIPA buffer for 1 hr on ice, followed by centrifugation for 15 min at 12000 x *g*. 300 μg of pre-cleared lystates were incubated with 10 μl of anti-IL-6R or anti-E2F1 antibodies for overnight. 20 μl of protein G-agarose beads (Santa Cruz Biotech) was then added to the mixture and rotated for 4 h at 4 °C. The beads were washed with ice-cold PBS prior to western blot analysis.

Transfection

siRNA oligonucleotides targeting for *STAT3* and *cyclin D1* were purchased from Genolution Pharmaceuticals (Seoul, Korea). CCD841CoN cells (3 x 10^5/60-mm dish) were transfected with 25 nM of specific or scrambled siRNA oligonucleotides using Lipofectamine RNAiMAX according to manufacturer's instruction (Invitrogen, Carlsbad, CA, USA).

Chromatin immunoprecipitation (ChIP) assay

ChIP material was prepared in accordance with the EZ-ChIP (Millipore) manufacturer's instructions. Immunoprecipitation was performed using 10 μg of anti-STAT3 antibody. Washes and eluted DNA were used for PCR analysis using specific primers for *CCND1*. The primers employed are as follows (forward and reverse, respectively): 5'-GGA ACC TTC GGT GGT CTT GTC-3' and 5'-GAA TGG AAA GCT GAG AAA CAG TGA-3'. PCR products were visualized by agarose gel electrophoresis.

Anchorage-independent assay

To prepare the hard agar layer, 3.3% agarose dissolved in PBS were autoclaved and added immediatedly to 60-mm dishes. To prepare the soft agar layer containing cells, CCD841CoN cells (0.8 x 10^4) were suspended in the 0.33% agarose solution, and 2.5

mL of this mixture were added to the top of the hard agar layer. Three hour later, 2.5 mL of the fresh medium were added to the top of the soft agar layer. On the next day, cells were exposed either to IL-6 or RvD1, separately or in combination, once in 3 days for 3 weeks. After 3 weeks of incubation, anchorage-independent growth was scored using a light microscope and the total number of foci in a dish was counted.

4. Results

RvD1 suppresses AOM plus DSS-induced mouse colon carcinogenesis

To determine the chemopreventive effect of RvD1 on inflammation-associated carcinogenesis, we used an AOM plus DSS-induced mouse colorectal cancer model, with or without RvD1 (0.1 or 1 μg/mouse). Mice were intraperitoneally injected with the carcinogen AOM followed by DSS administration in the drinking water in 7 days cycles. RvD1 was intraperitoneally administered before (day 4) and during (day 7, 10 and 13) DSS administration. As a result, mice injected with RvD1 were protected from AOM plus DSS-induced colonic dysplasia (**Fig. 4-1F**). Decreases in the body weight and increases in intestinal bleeding and diarrhea were observed during DSS treatment, but these were relatively suppressed by RvD1 treatment (**Fig. 4-1A-C**). The length of colon was measured as one of indicators for inflammation severity. Compared with the control group, colon length decreased in the AOM plus DSS-treated group, but this was attenuated in the RvD1 (1 μg)-treated group (**Fig. 4-1D**). Macroscopic analysis of the colons at day 28 after AOM administration indicated the preventive effect of RvD1 on AOM and DSS-induced colonic polyp formation (**Fig. 4-1E**). Furthermore, using H&E staining, AOM plus DSS-induced infiltration of inflammatory cells and disruption in the architecture of colonic mucosa was observed. However, mice given RvD1 exhibited a preserved colonic structure and less infiltration of inflammatory cells (**Fig. 4-1F**). These results support the protective effect of RvD1 on inflammation-induced

colon carcinogenesis. Moreover, in AOM and DSS-treated mice, the level of pro-inflammatory cytokine IL-6 was highly increased, but RvD1 prevented the IL-6 overproduction (**Fig. 4-1G**).

RvD1 inhibits IL-6-induced neoplastic transformation and mitotic spindle abnormality

Malignant transformation is the major process by which cells acquire the oncogenic characteristics, and it is often accompanied by chromosomal instability (Putz et al., 2010). IL-6, a prototypic pro-inflammatory cytokine capable of triggering chronic inflammation and subsequently cancer, has been reported to induce neoplastic transformation (Sansone et al., 2007). To clarify the potential role of IL-6 in colon carcinogenesis and the preventive effect of RvD1 on inflammation-induced carcinogenesis, we checked anchorage-independent growth of normal intestinal epithelial CCD841CoN cells stimulated with IL-6 in the presence of or absence of RvD1. The long term exposure to IL-6 caused malignant transformation of these cells, as evidenced by increased anchorage-independent growth. Both the size and the number of foci were markedly increased in IL-6-treated cells compared with the vehicle-treated cells. However, with RvD1 treatment, IL-6-induced formation of transformed foci was significantly suppressed (**Fig. 4-2A**). To determine whether the inhibition of neoplastic transformation by RvD1 is mediated by preventing

chromosomal instability, the morphology of mitotic spindle was examined. In vehicle-treated cells, the proportion of cells with multipolar spindles was 6.5%, whereas in IL-6-treated cells, this percentage increased up to 34.3%. IL-6-induced spindle abnormality was attenuated by 16.7% in the presence of RvD1 (**Fig. 4-2B**). Multipolar spindles induce aberrant chromosomal segregation during mitosis, thereby leading to the formation of multinuclei and micronuclei. As shown in **Fig. 4-2C**, the number of cells with multinuclei or micronuclei was significantly increased in IL-6-treated cells compared with that in control cells. Again, RvD1 treatment abrogated IL-6-induced chromosomal instability.

Cyclin D1 is critical for IL-6-induced mitotic spindle abnormality.

In IL-6-treated cells, the levels of cyclin D1 as well as its downstream target retinoblastoma protein (RB) phosphorylation were increased, while there was no apparent change in the level of CDK4. IL-6-induced cyclin D1 expression was completely blocked by RvD1 pretreatment. Likewise, RvD1 dampened IL-6-induced phosphorylation of RB (**Fig. 4-3A**). Next, we attempted to explore the correlation between cyclin D1 and chromosomal instability in IL-6-treated cells. To clarify the potential role for cyclin D1 in spindle multipolarity and formation of abnormal nuclei, siRNA against cyclin D1 was transfected into CCD841CoN cells, followed by IL-6 treatment for 3 days. In cyclin D1 knockdown cells, there was a remarkable reduction

in IL-6-induced formation of multipolar spindles compared to IL-6-treated cells expressing the high level of cyclin D1 (**Fig. 4-3B**). Consistent with this observation, IL-6 failed to enhance in the number of cells with multinuclei or micronuclei in the absence of cyclin D1 (**Fig. 4-3C**), indicating that cyclin D1 is responsible for IL-6-induced chromosomal instability. To further confirm the involvement of cyclin D1 in mitotic spindle abnormality, CCD841CoN cells were transfected with the vector expressing HA-conjugated cyclin D1. Overexpression of cyclin D1 led to phosphorylation of RB (**Fig. 4-3D**). Similar to the effect of IL-6, overexpression of cyclin D1 increased the number of cells with irregular multipolar spindles (**Fig. 4-3E**) and aberrant nuclei (**Fig. 4-3F**). Based on these findings, it is evident that IL-6 causes chromosomal instability through upregulation of cyclin D1 expression, and that the preventive effect of RvD1 on IL-6-induced carcinogenesis is mediated by downregulation of cyclin D1 expression.

The inhibitory effect of RvD1 on IL-6-induced cyclin D1 expression is mediated through suppression of STAT3 signaling

Within the human *CCND1* promoter region, there are four putative STAT binding sites, known as the gamma-activated sites (GAS; TTN_5AA). It has been reported that activated STAT3 binds to the GAS site at -984 with the highest affinity (Leslie et al., 2006). In order to determine whether RvD1 downregulates IL-6-induced cyclin D1

expression by disrupting the binding of STAT3 to the *CCND1* promoter, the ChIP assay was carried out using primers specific for the GAS site at -984. In the presence of RvD1, IL-6-induced association of STAT3 with the *CCND1* promoter was completely downregulated (**Fig. 4-4A**). To further verify that IL-6-induced overexpression of cyclin D1 was mediated by STAT3 signaling, CCD841CoN cells were transfected with siRNA against STAT3. As shown in **Fig. 4-4B**, IL-6 failed to upregulate cyclin D1 expression in STAT3 knockdown cells, indicative that STAT3 as a principal transcription factor responsible for cyclin D1 upregulation.

RvD1 attenuates the IL-6-induced JAK2/STAT3 signaling pathway by inhibiting the interaction between IL-6R and gp130

Next, we examined the inhibitory effect of RvD1 on STAT3 signaling. When CCD841CoN cells were stimulated with IL-6, STAT3 and its upstream kinase JAK2 were transiently phosphorylated, and this was significantly inhibited by RvD1 treatment (**Fig. 4-4C**). Phosphorylation of STAT3 at Y705 plays an important role in activity and nuclear translocation of this transcription factor (Corvinus et al., 2005). Consistent with this notion, the inhibition of STAT3 phosphorylation by RvD1 resulted in the blockade of IL-6-induced nuclear translocation of STAT3 (**Fig. 4-4D**). RvD1 also abrogated IL-6-induced DNA binding of STAT3 (**Fig. 4-4E**). To elucidate the mechanism underlying RvD1-mediated suppression of JAK2/STAT3 signaling, the

interaction between IL-6R and gp130 was checked. While stimulation with IL-6 triggered the interaction of IL-6R with gp130, their interaction was blocked by RvD1, suggesting that RvD1 interferes IL-6-induced recruitment of IL-6R and gp130 (**Fig. 4-4F**).

RvD1 inhibits cyclin D1 expression in inflammation-associated colon carcinogenesis

In another experiment, we measured the levels of cyclin D1 and phosphorylated STAT3 in AOM/DSS-induced colon cancer. AOM plus DSS-treated mice showed the increase in cyclin D1 expression, and RvD1 attenuated AOM plus DSS-induced cyclin D1 expression (**Fig. 4-5A,C**). Furthermore, the level of phosphorylated STAT3 was significantly elevated in AOM and DSS-treated mice, which was abolished by RvD1 administration (**Fig. 4-5B,C**). Taken together, these results indicate that RvD1 prevents colitis-induced colon carcinogenesis through blockade of STAT3 signaling and its downstream target. We then assessed the levels of cyclin D1 and its associated proteins in colon tissues from colorectal cancer patients. The expression of cyclin D1 was highly upregulated in human colon tumor specimens compared with the normal counterparts. However, there were no significant differences in the level of cyclin D1-associated proteins including CDK4, E2F1 and pRB between normal and tumor tissues (**Fig. 4-6**).

The plasma RvD1 concentrations are reduced during colon carcinogenesis

As exogenous administration of RvD1 showed the preventive effect on inflammation-induced colorectal carcinogenesis, it is worthwhile determining whether endogenously produced RvD1 during inflammation also has a potential in preventing the development of colorectal cancer. To better examine the correlation between failure in resolution of inflammation and colon carcinogenesis, we evaluated the severity of inflammation as well as polyp formation at the different time intervals in AOM and DSS-treated mice (**Fig. 4-7A**). The length of colon was decreased in maximum at the completion of DSS treatment, but its restoration was observed from the week 4, indicating that DSS-induced colitis may have physiologically resolved after termination of DSS administration (**Fig. 4-7B**). Even though colitis is resolved, the formation of colonic polyps was observed from the week 4. The number of polyps was gradually increased with the course of time (**Fig. 4-7C**). Moreover, increased incidence of malignant colorectal cancers was detected in a time-dependent manner from the week 4 to 10 (**Fig. 4-7D**). Next, we examined the expression of enzymes involved in lipid mediator class switching from pro-inflammatory to anti-inflammatory/pro-resolving mediators. As shown in **Fig. 4-7E**, the levels of COX-2, PGES and 15-LOX were significantly increased during DSS treatment, compared with control group. After termination of DSS administration, the expression of COX-2 and 15-LOX was downregulated, but PGES was still upregulated. However, there was no significant

change in 5-LOX levels. Notably, all these four enzymes were overexpressed at the week 10 (**Fig. 4-7E**). Although the expression of 15-LOX, the enzyme involved in RvD1 biosynthesis, was highly upregulated at the week 10, the concentrations of RvD1 in blood and colon tissues were not correspond with the level of 15-LOX. Both in blood and colon tissues, abundant amounts of endogenous RvD1 were produced during DSS administration, but its production declined after termination of DSS administration. As tumorigenesis progressed, the plasma RvD1 levels were constantly reduced, whereas RvD1 concentrations in colon tissues were remained at a control level in tissues (**Fig. 4-7F,G**). Similar results were obtained from biospecimens of colorectal cancer patients. RvD1 levels in blood from patients with stage I or II colorectal cancer were higher (average: 905.1 pg/mL) than from patients with more advanced colorectal cancer (average: 278.5 pg/mL) (**Fig. 4-7H**). However, there was no significant difference between colon tumors and normal counterparts (**Fig. 4-7I**).

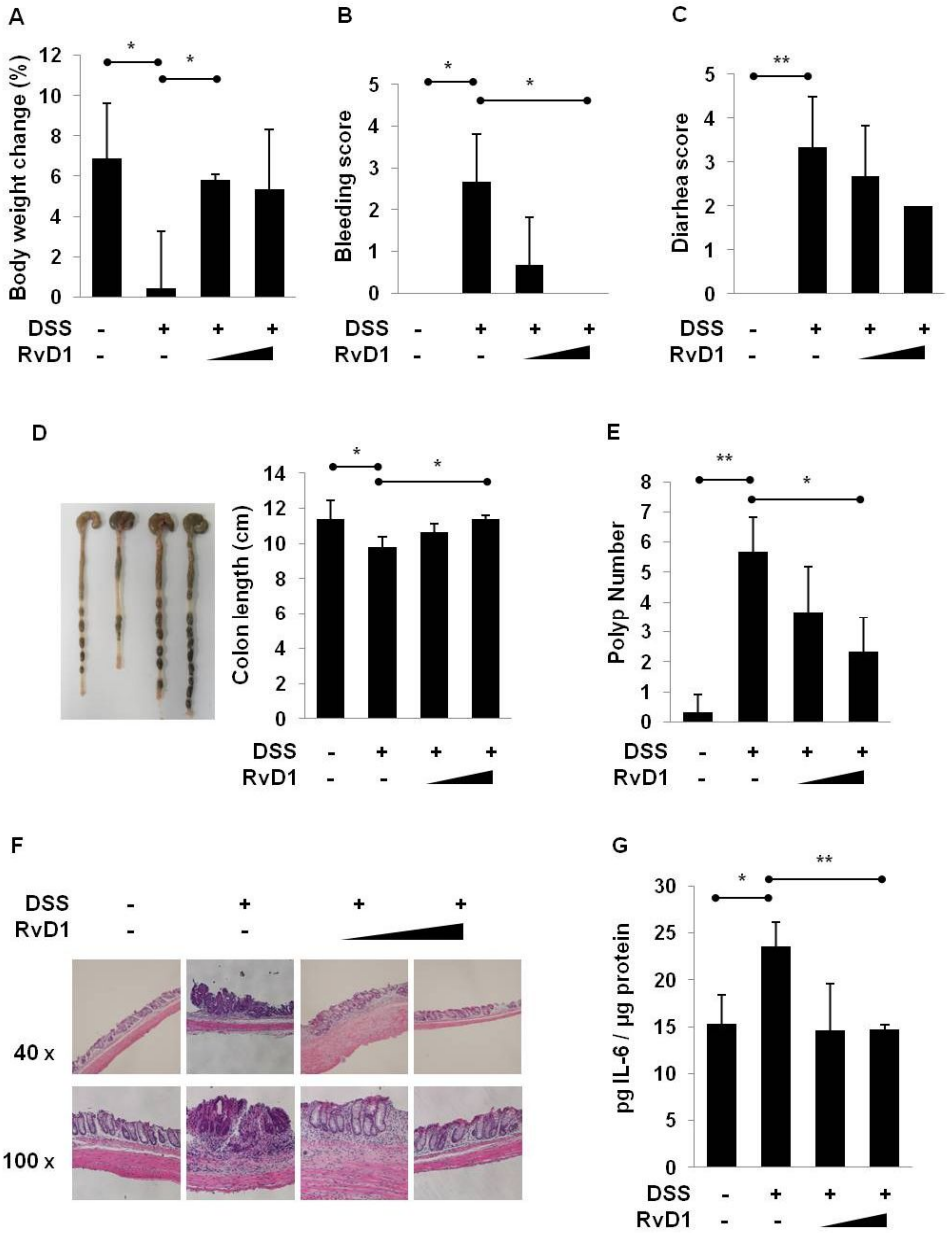
A
Body weight change (%)
12
10
8
6
4
2
0
*
*
DSS - + + +
RvD1 - - ▲
B
Bleeding score
5
4
3
2
1
0
*
*
DSS - + + +
RvD1 - - ▲
C
Diarhea score
5
4
3
2
1
0
**
DSS - + + +
RvD1 - - ▲
D
Colon length (cm)
14
12
10
8
6
4
2
0
*
*
DSS - + + +
RvD1 - - ▲
E
Polyp Number
8
7
6
5
4
3
2
1
0
**
*
DSS - + + +
RvD1 - - ▲
F
DSS - + + +
RvD1 - - ▲
40 x
100 x
G
pg IL-6 / µg protein
30
25
20
15
10
5
0
*
**
DSS - + + +
RvD1 - - ▲

Fig. 4-1. RvD1 inhibits AOM plus DSS-induced mouse colon carcinogenesis. Mice were injected intraperitoneally with AOM on the day 0, followed by DSS administration from the day 7 for 1 week. RvD1 was given before and during DSS administration once three days. (A) During DSS administration, the changes in body weight of mice were checked. (B,C) At the completion of DSS treatment, mice were monitored for bleeding (B) and diarrhea (C). On the day 28 after AOM injection, all mice were sacrificed. The length of colon were measured (D) and macroscopic polyps were counted (E). (F) Paraffin-embedded colon tissue block were stained with hematoxylin-eosin. Photomicrographs of representative sections are shown at 40x and 100x. (G) Tissue lysates were subjected to ELISA for measuring IL-6 concentrations (G). Data are expressed as means ± S.D. (n = 3, each group), $^{*}p<0.05$, $^{**}p<0.01$.

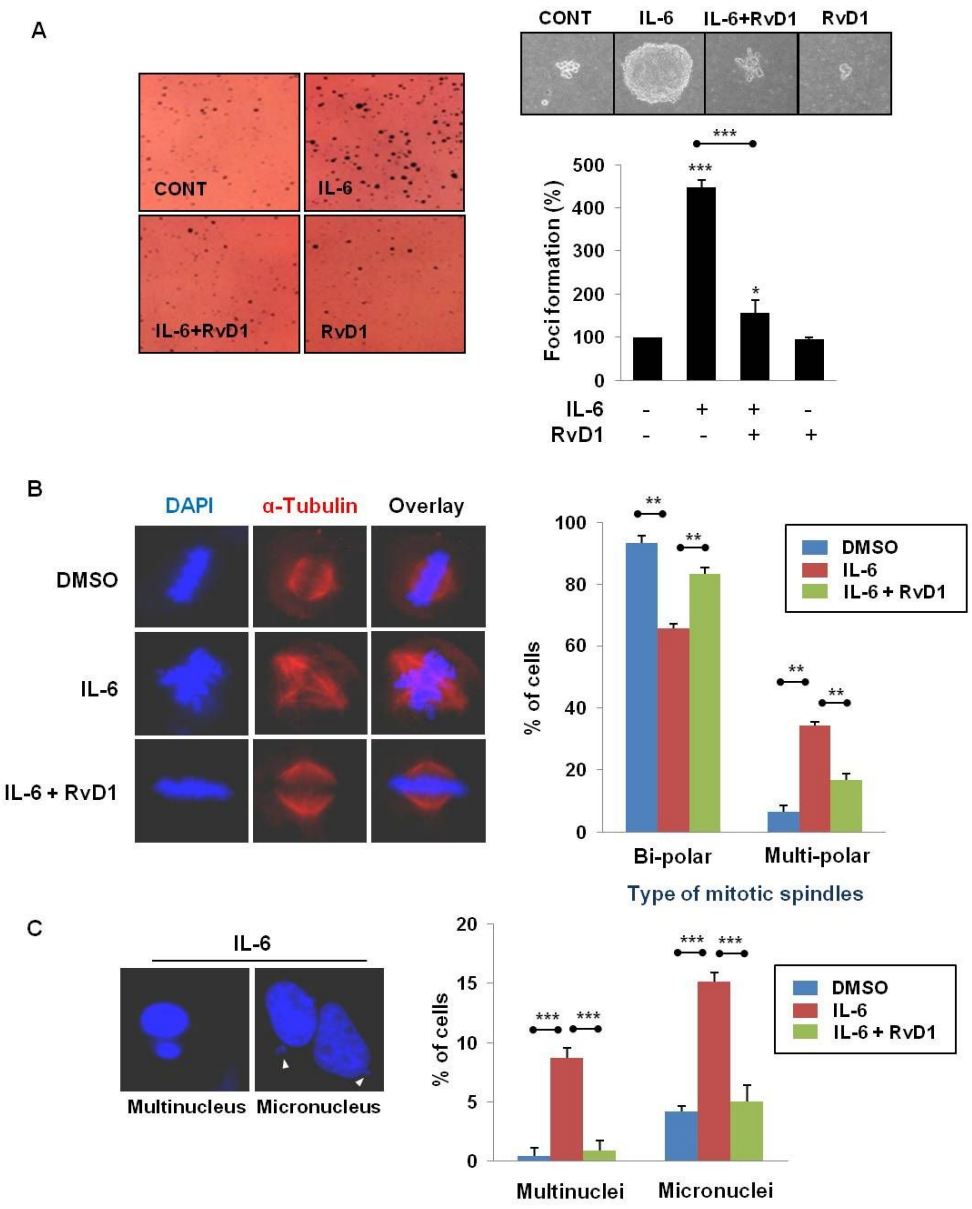
A
CONT
IL-6
IL-6+RvD1
RvD1
Foci formation (%)
IL-6
RvD1
B
DAPI
α-Tubulin
Overlay
DMSO
IL-6
IL-6 + RvD1
% of cells
Bi-polar
Multi-polar
Type of mitotic spindles
C
IL-6
Multinucleus
Micronucleus
% of cells
Multinuclei
Micronuclei

Fig. 4-2. IL-6-induced neoplastic cell transformation and chromosomal instability was reduced by RvD1 treatment. (A) CCD841CoN cells were subjected to an anchorage-independent cell growth assay (soft agar assay). *Treatment* of IL-6 or RvD1 was repeated *every 3 days* during a period of 2 weeks. (B,C) Cells were treated with IL-6 (50 ng) or RvD1 (100 nM) for 3 days. Polar spindles and chromosomes were visualized by immunostaining with anti-α-tubulin antibody (red) and DAPI (blue). The numbers of bi- and multi-polar spindles were counted (B). Cells were stained with DAPI to observe the nuclei. The numbers of multinucleated cells and cells with micronuclei were counted (C). Data are means S.D. (n=3), $^{*}p<0.05$, $^{**}p<0.01$, $^{***}p<0.001$.

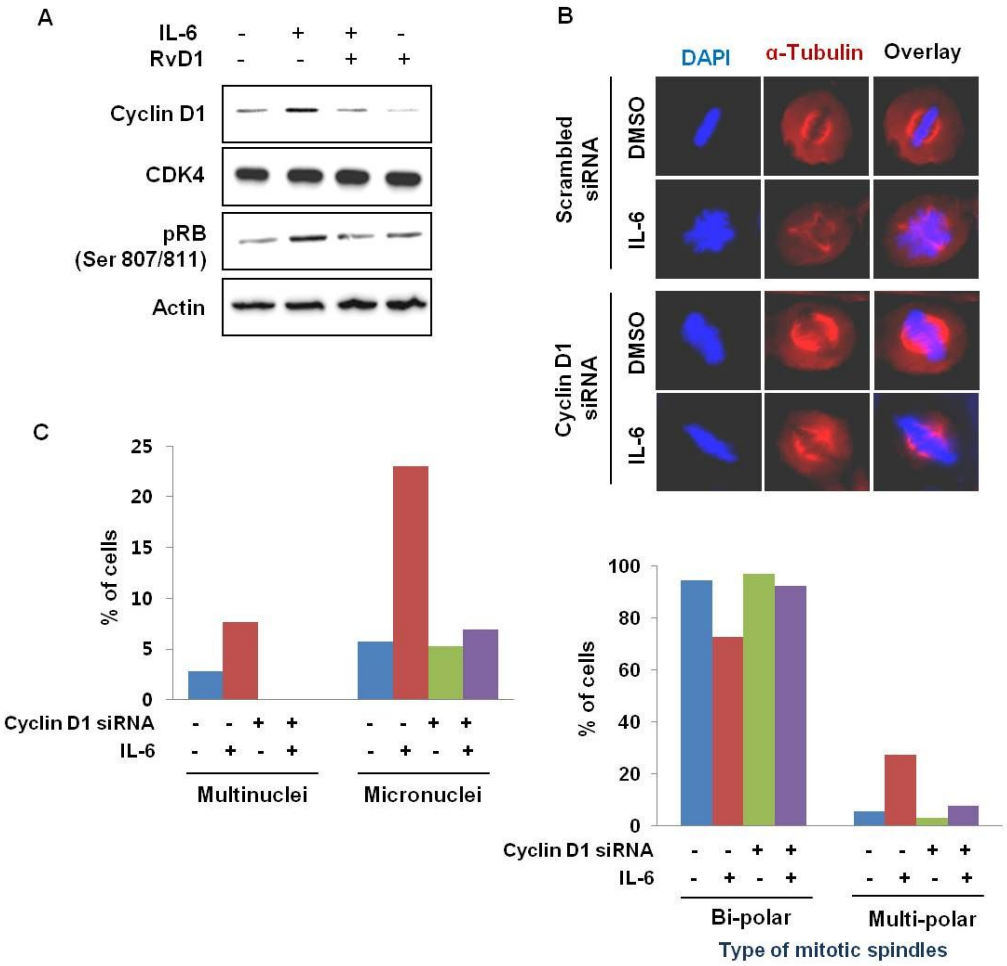
A
IL-6 - + + -
RvD1 - - + +
Cyclin D1
CDK4
pRB
(Ser 807/811)
Actin
B
DAPI
α-Tubulin
Overlay
Scrambled siRNA
DMSO
IL-6
Cyclin D1 siRNA
DMSO
IL-6
C
% of cells
25
20
15
10
5
0
Cyclin D1 siRNA - - + + - - + +
IL-6 - + - + - + - +
Multinuclei
Micronuclei
% of cells
100
80
60
40
20
0
Cyclin D1 siRNA - - + + - - + +
IL-6 - + - + - + - +
Bi-polar
Multi-polar
Type of mitotic spindles

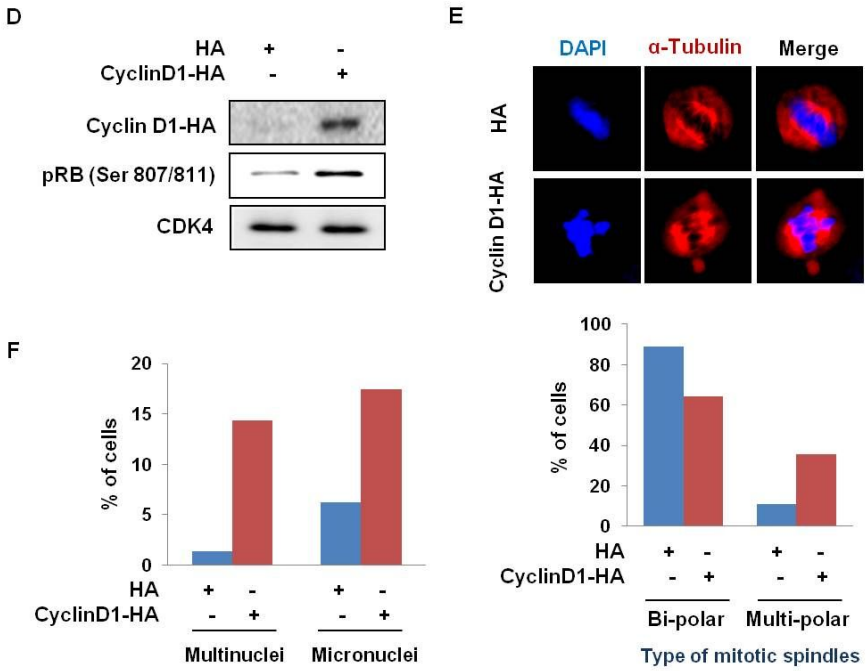

Fig. 4-3. Overexpression of cyclin D1 is critical for chromosomal instability. (A) CCD841CoN cells were pretreated with RvD1 (100 nM) or DMSO for 30 min and then stimulated with IL-6 (50 ng/mL) for 12 h. Cell lysates were subjected to immunoblot analysis for measuring the levels of cyclin D1, CDK4 and RB. Actin was used as an equal loading control for normalization. (B,C) CCD841CoN cells were transfected with scrambled or cyclin D1 siRNA for 16 h, and then incubated with or without IL-6 for 3 days. Cells were immunostained with anti-α-tubulin antibody (red) and DAPI (blue) (B). To check the number of multinucleated cells and cells with

micronuclei, cells were stained with DAPI (C). (D-F) CCD841CoN cells were transfected with empty vector or the plasmid containing cyclin D1. Cell lysates were subjected to immunoblot analysis for measuring the levels of cyclin D1, CDK4, pRB and actin (D). Cyclin D1-overexpressing cells were immunostained with anti-α-tubulin antibody (red) and DAPI (blue) (E). To check the number of multinucleated cells and cells with micronuclei, cells were stained with DAPI (F).

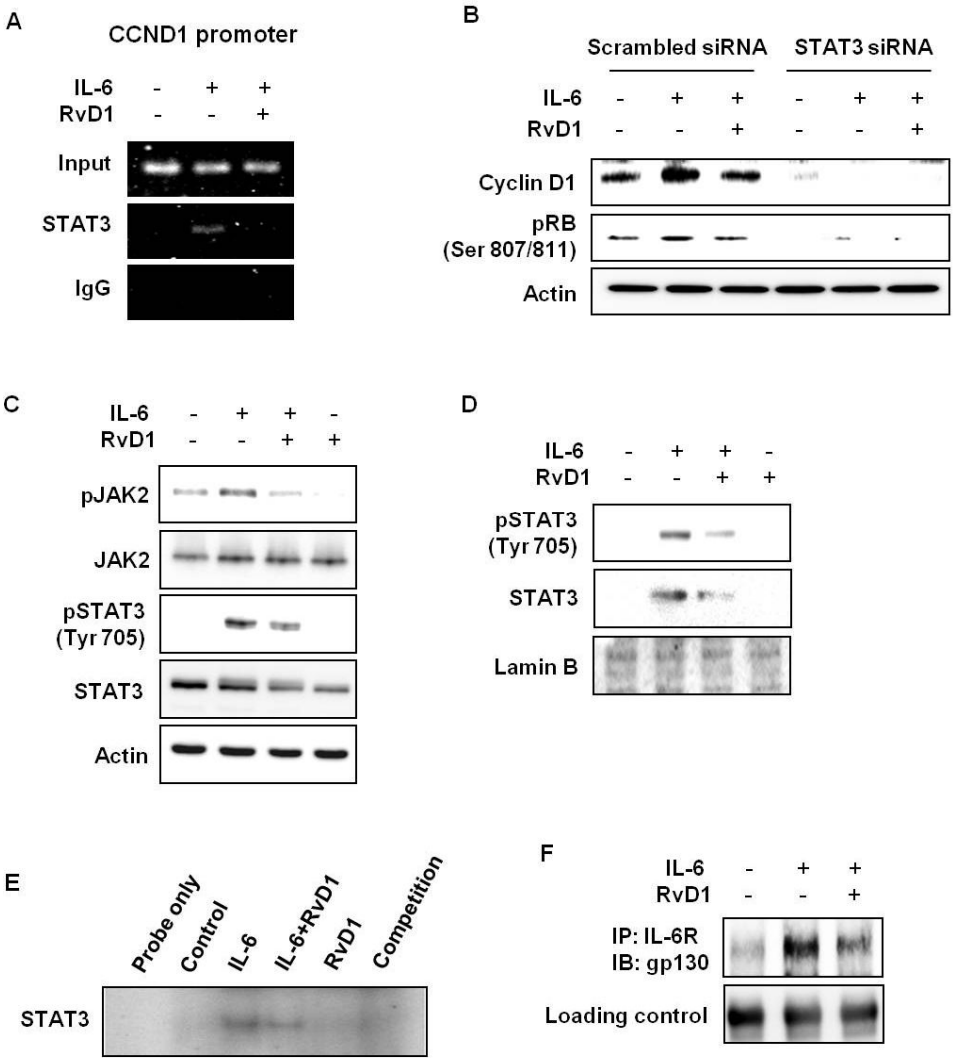

Fig. 4-4. RvD1-mediated suppression of STAT3 signaling is linked to inhibition of IL-6-induced cyclin D1 expression. (A) CCD841CoN cells, pretreated with RvD1 (100 nM) for 30 min and further stimulated with IL-6 (50 ng/mL) for 12 h, were

subjected to the ChIP analysis using an antibody against STAT3. ChIP-enriched DNA was amplified by PCR with specific primers for cyclin D1 promoter. (B) Cells were transfected with scrambled or *STAT3* siRNA for 16 h, and then IL-6 was treated in the absence or presence of RvD1 for additional 12 h. The protein levels of cyclin D1, CDK4, E2F1, pRB and actin were determined by Western blot analysis. (C) CCD841CoN cells were pretreated with RvD1 or DMSO for 30 min and then stimulated with IL-6 for 15 min. Cell lysates were subjected to immunoblot analysis for measuring the levels of pJAK2, total JAK2, pSTAT3 and total STAT3. Actin was used as an equal loading control for normalization. (D,E) CCD841CoN cells were pretreated with RvD1 or DMSO for 30 min and then stimulated with IL-6 for 30 min. Nuclear proteins were isolated, and levels of phosphorylated and total STAT3 in the nucleus were determined by Western blot analysis. Lamin B was measured to ensure equal amounts of nuclear fractions (D). Nuclear proteins were incubated with the [γ-^{32}P]-labeled oligonucleotides containing the STAT3 consensus motif. Protein-DNA complexes were separated from free probe by electrophoresis (E). To check the interaction between IL-6R and gp130, IL-6R was immunoprecipitated from total cell lysates, followed by Western blot analysis for gp130 (F).

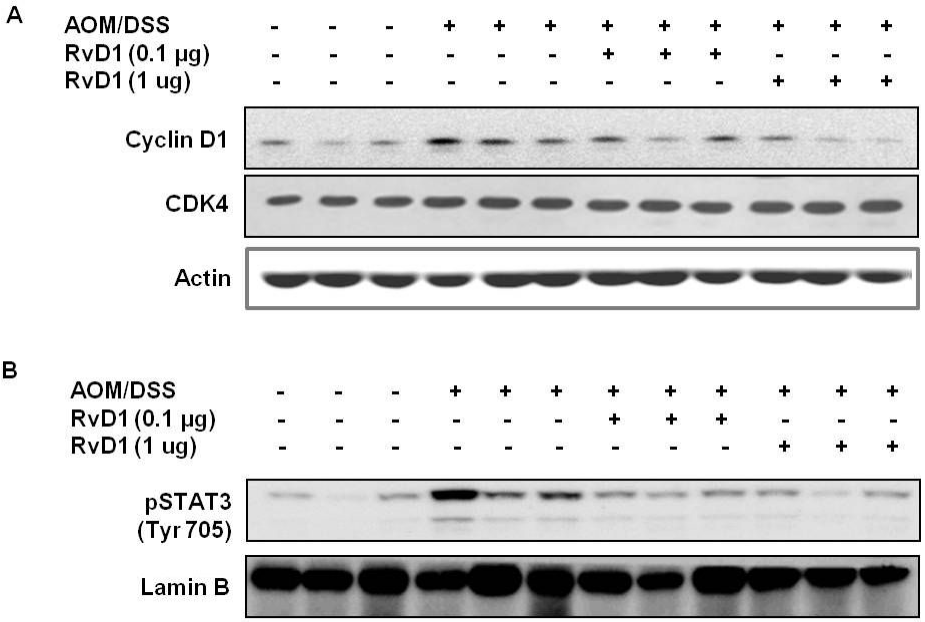
A
AOM/DSS
RvD1 (0.1 μg)
RvD1 (1 ug)
Cyclin D1
CDK4
Actin
B
AOM/DSS
RvD1 (0.1 μg)
RvD1 (1 ug)
pSTAT3
(Tyr 705)
Lamin B

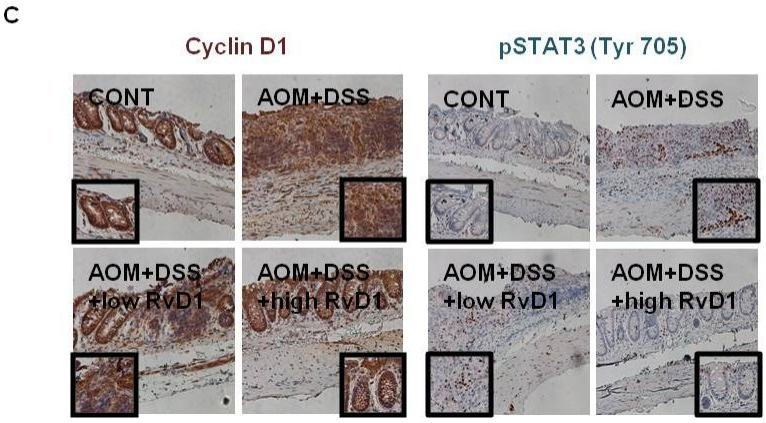
C
Cyclin D1
pSTAT3 (Tyr 705)
CONT
AOM+DSS
CONT
AOM+DSS
AOM+DSS
+low RvD1
AOM+DSS
+high RvD1
AOM+DSS
+low RvD1
AOM+DSS
+high RvD1

Fig. 4-5. RvD1 inhibits cyclin D1 overexpression and STAT3 phosphorylation in AOM plus DSS-induced mouse colon carcinogenesis. Mice were injected intraperitoneally with AOM on the day 0, followed by DSS administration from the day 7 for 1 week. RvD1 was given before and during DSS administration once three days. On the day 28 after AOM injection, all mice were sacrificed. (A) Tissue lysates were subjected to immunoblot analysis for determining the levels of cyclin D1, CDK4 and actin. (B) Nuclear proteins were isolated from colon tissues, and levels of pSTAT3 in the nucleus were determined by Western blot analysis. (C) Tissue sections were analyzed by immunohistochemistry for cyclin D1 and pSTAT3 expression. Photomicrographs of representative sections are shown at 40x and 100x. Data are expressed as means ± S.D. (n = 3, each group).

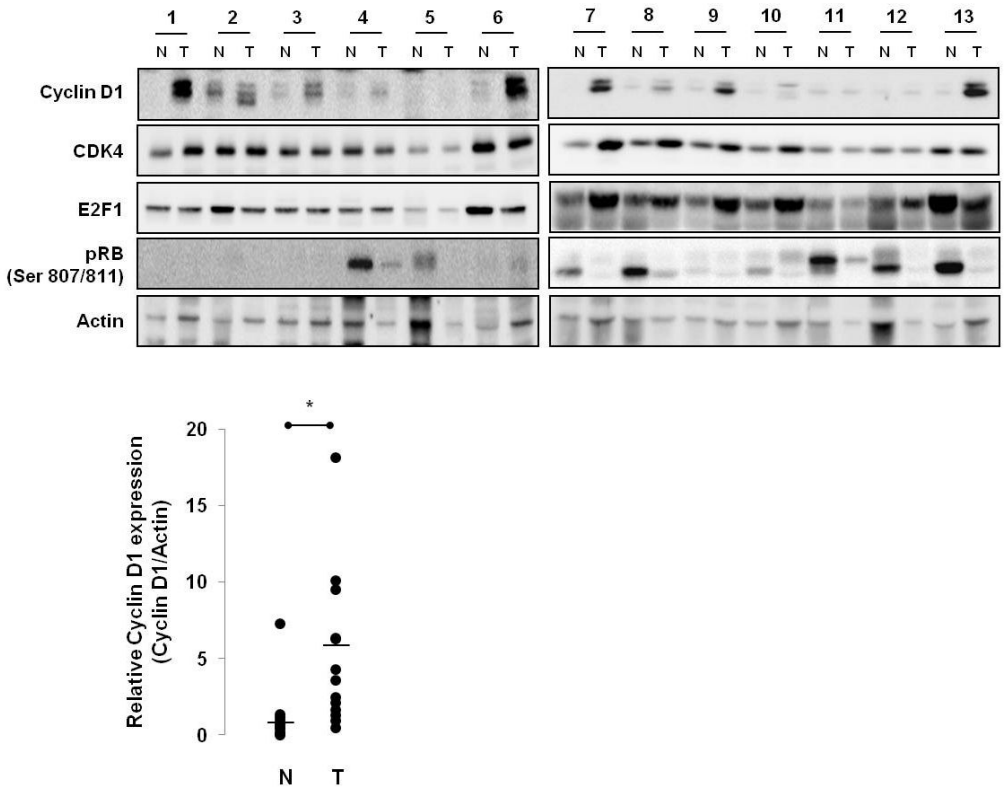

Fig. 4-6. The elevated level of cyclin D1 is observed in the human colon tumor specimens. The expression level of cyclin D1, CDK4, E2F1, pRB and actin was measured in total 13 pairs of colon tumor and adjacent normal tissues. The band intensities were quantified by densitometry.

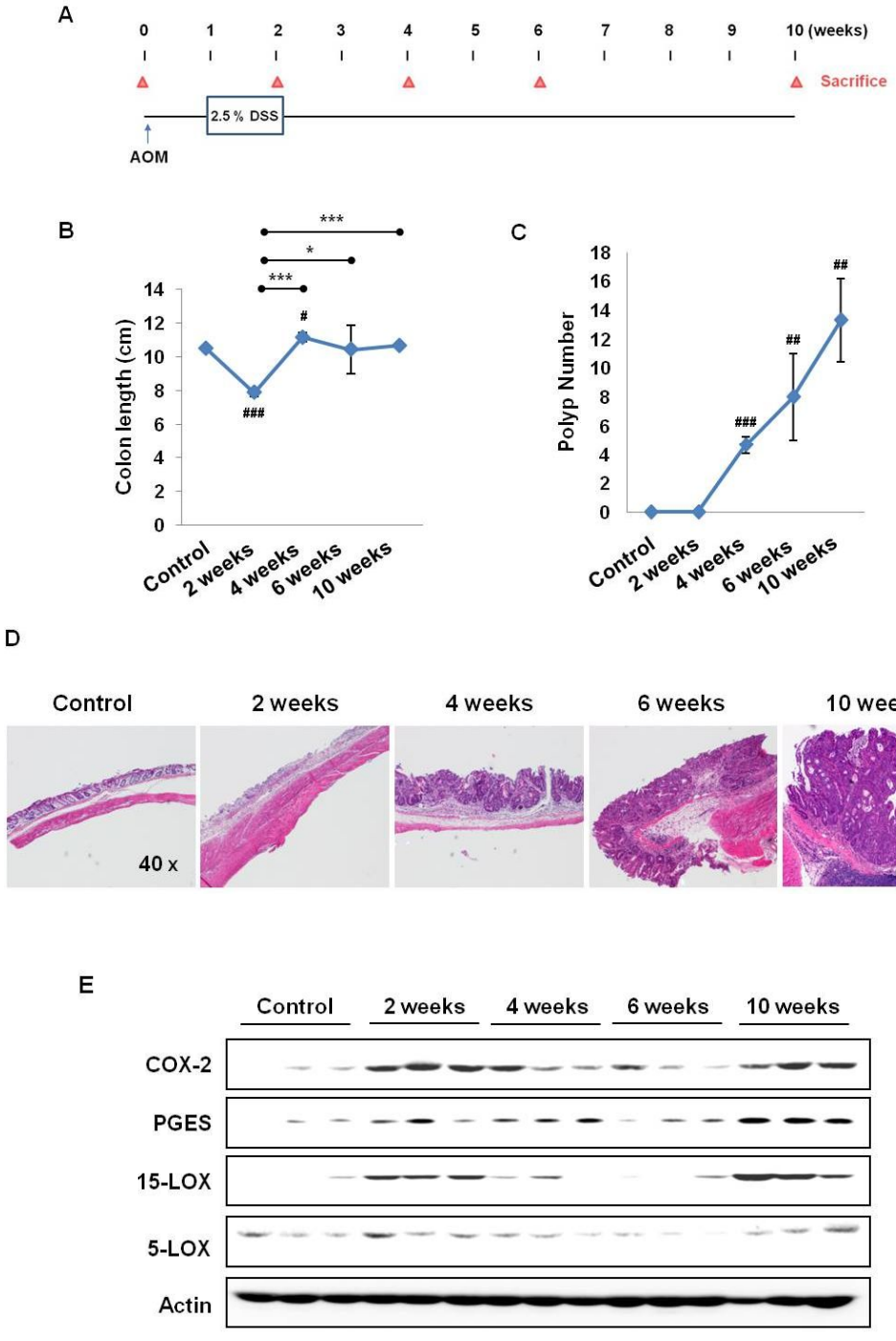
A
0
1
2
3
4
5
6
7
8
9
10 (weeks)
Sacrifice
2.5 % DSS
AOM
B
Colon length (cm)
Control
2 weeks
4 weeks
6 weeks
10 weeks
C
Polyp Number
Control
2 weeks
4 weeks
6 weeks
10 weeks
D
Control
2 weeks
4 weeks
6 weeks
10 weeks
40 x
E
Control
2 weeks
4 weeks
6 weeks
10 weeks
COX-2
PGES
15-LOX
5-LOX
Actin

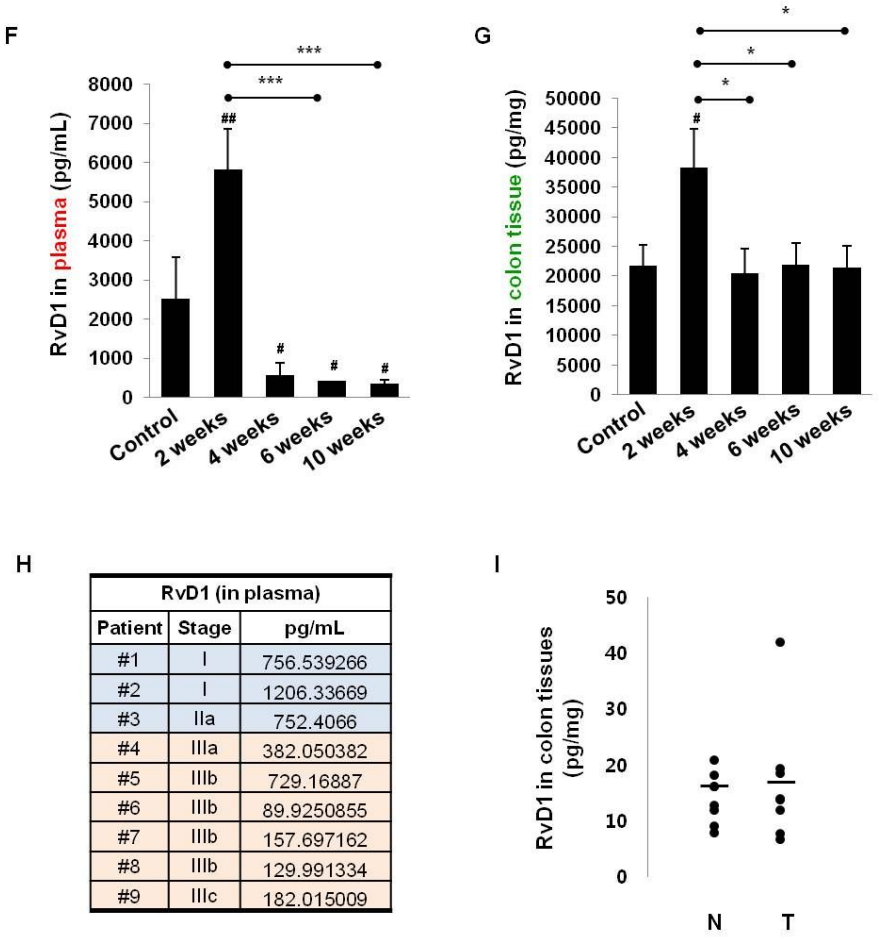

RvD1 (in plasma)		
Patient	Stage	pg/mL
#1	I	756.539266
#2	I	1206.33669
#3	IIa	752.4066
#4	IIIa	382.050382
#5	IIIb	729.16887
#6	IIIb	89.9250855
#7	IIIb	157.697162
#8	IIIb	129.991334
#9	IIIc	182.015009

Fig. 4-7. Dysfunction of pro-resolving signaling is potentially linked to carcinogenesis. Mice were injected intraperitoneally with AOM on the day 0, followed by DSS administration from the day 7 for 1 week. Mice were sacrificed at the indicated time. (A) A scheme for time-course study of AOM plus DSS-induced colorectal carcinogenesis. The length of colon were measured (B) and macroscopic polyps were counted (C). (D) Paraffin-embedded colon tissue block were stained with hematoxylin-

eosin. (E) Tissue lysates were subjected to immunoblot analysis for determining the levels of COX-2, PGES, 15-LOX, 5-LOX and actin. The band intensities were quantified by densitometry. (F-I) Total lipid was extracted from plasma (F) and colon tissues in mice (G) or plasma (H) and colon tumor and adjacent normal tissues from 9 colorectal cancer patients (I). The concentration of RvD1 was determined by ELISA. Data are expressed as means ± S.D. (n = 3, each group of mice), $^{*}p<0.05$, $^{**}p<0.01$, $^{***}p<0.001$; $^{\#}p<0.05$, $^{\#\#}p<0.01$, $^{\#\#\#}p<0.001$ as compared with control group.

5. Discussion

Multipolar spindles and multi/micronuclei reflecting chrosomomal instability are observed in colitis-associated colorectal cancer with higher frequency as compared to the sporadic counterpart (Gerling et al., 2010), indicating that inflammation is a key risk factor for chromosomal instability. As reported by other investigators, it is plausible that pro-inflammatory cytokine IL-6, whose level is elevated both in inflammatory bowel diseases and colorectal cancer, may play a essential role in developing chronic inflammation-associated cancer (Grivennikov et al., 2009). However, the correlation between chronic overproduction of IL-6 and chromosomal instability has not been elucidated. In this study, we revealed that IL-6 promotes malignant transformation of normal colon epithelial cells by inducing mitotic spindle abnormality. Multipolar spindles leads to aneuploidy, multinuclei formation and chromosome lagging. These lagging chromosomes are excluded from daughter nuclei, and instead form a micronucleus in one of daughter cells (Holland and Cleveland, 2012). Consistent with this, it was observed that IL-6 increased not only mitotic spindle abnormality, but also formation of multinuclei and micronuclei formation. Casimiro et al. also demonstrated that cyclin D1 induces chromosomal instability, including aneuploidy, supernumerary centrosomes and spindle defects, by upregulating the expression of genes involved in mitosis (Casimiro et al., 2012). We also observed that IL-6-induced formation of multipolar spindles and abnormal nuclei is mediated by

overexpression of cyclin D1. In *CCND1* knockdown cells, the oncogenic effect of IL-6 was abolished, suggesting that cyclin D1 is required for IL-6-induced spindle abnormality and subsequent malignant transformation.

In inflammatory microenvironment, chronic overproduction of IL-6 is considered as a result of failure in resolution of inflammation. It is clearly defined that defects in resolution of inflammation lead to chronic diseases including inflammatory bowel disease, rheumatoid arthritis, pulmonary disease and cardiovascular disease (Medzhitov, 2008). However, there is no evidence supporting the correlation between failure in resolution of inflammation and cancer. In this study, we notably found that the decreased level of pro-resolving RvD1 in blood is correlated with severity of colorectal cancer. Especially, the blood levels of RvD1 in mice having invasive colorectal carcinoma were lower than those in normal mice. However, significant differences in RvD1 levels between normal and tumor tissues were not detected. From these findings, we indirectly support that decreased levels of plasma pro-resolving lipid mediators correlate with colon tumorigenesis, and suggesting plasma RvD1 as a potential biomarker for monitoring colorectal cancer.

Interestingly, the levels of RvD1 in blood and tissues were extremely increased during DSS-induced inflammation, and the expression of 15-LOX, one of important enzymes involved in RvD1 biosynthesis, was also significantly upregulated in colon tissues with severe inflammation. After termination of DSS administration, 15-LOX

expression was subsequently downregulated in colon tissues with dysplasia (the week 4 and 6), but reversely increased at the week 10, when the invasive adenocarcinoma manifests. However, the discordance between the expression of a RvD1 synthesizing enzyme and RvD1 levels was observed. RvD1 levels in colon tissues suddenly decreased after inflammation and then remained steady as tumorigenesis progressed. This may be explained by exhaustion of RvD1 precursors (e.g., DHA) during inflammation, therefore changes in 15-LOX expression do not appear to influence RvD1 production at the later stage.

RvD1 counteracts excessive inflammatory responses and stimulates pro-resolving mechanisms through suppression of pro-inflammatory signaling, regulating the trafficking of leukocytes and stimulating non-inflammatory phagocytosis of apoptotic neutrophils by macrophages (Lee and Surh, 2012). Accumulating data have shown that these anti-inflammatory and pro-resolving effects of resolvins are mostly dependent on downregulation of NF-κB signaling. In our previous study, we also demonstrated that RvD1 suppresses classical NF-κB signaling, thereby stimulating efferocytosis. Not only NF-κB, but STAT3 also plays a key role in both inflammation and cancer. Here, we firstly report that RvD1 has an inhibitory effect on STAT3 signaling. RvD1 suppressed IL-6-induced activation of JAK2/STAT3 signaling by inhibiting the interaction between IL-6 receptor and gp130, indicating that RvD1 can act as an IL-6 antagonist. In addition, RvD1-mediated abrogation of IL-6 effects resulted in

suppression of cyclin D1 expression and cyclin D1-induced chromosomal instability, thereby preventing malignant transformation. Although RvD1 has a therapeutic potential for treatment of multiple inflammatory diseases including dry eyes, retinal diseases, asthma, inflammatory bowel disease, rheumatoid arthritis and cardiovascular diseases (Lee and Surh, 2012), therapeutic potential of RvD1 and other resolvins in prevention and treatment of cancer remains to be clarified.

Taken together, our findings suggest that RvD1 inhibits inflammation-induced tumorigenesis in the colon by suppressing the production of IL-6 and its oncogenic. RvD1 inhibited IL-6-induced chromosomal instability mediated by cyclin D1 overexpression, thereby preventing malignant transformation of colon epithelial cells. In addition, RvD1 attenuates IL-6-induced upregulation of cyclin D1 expression via suppression of JAK2/STAT3 signaling. As RvD1 prevents inflammation-induced malignant transformation in colon, this molecule and its analogues are anticipated as desirable therapeutics in the management of inflammatory disorders and possibly for the prevention of cancer.

6. References

Araujo, S. E., Bernardo, W. M., Habr-Gama, A., Kiss, D. R. and Cecconello, I. (2007). DNA ploidy status and prognosis in colorectal cancer: a meta-analysis of published data. *Diseases of the colon and rectum* 50, 1800-1810.

Askling, J., Dickman, P. W., Karlen, P., Brostrom, O., Lapidus, A., Lofberg, R. and Ekbom, A. (2001). Family history as a risk factor for colorectal cancer in inflammatory bowel disease. *Gastroenterology* 120, 1356-1362.

Bento, A. F., Claudino, R. F., Dutra, R. C., Marcon, R. and Calixto, J. B. (2011). Omega-3 fatty acid-derived mediators 17(R)-hydroxy docosahexaenoic acid, aspirin-triggered resolvin D1 and resolvin D2 prevent experimental colitis in mice. *J Immunol* 187, 1957-1969.

Bromberg, J. F., Wrzeszczynska, M. H., Devgan, G., Zhao, Y., Pestell, R. G., Albanese, C. and Darnell, J. E., Jr. (1999). Stat3 as an oncogene. *Cell* 98, 295-303.

Casimiro, M. C., Crosariol, M., Loro, E., Ertel, A., Yu, Z., Dampier, W., Saria, E. A., Papanikolaou, A., Stanek, T. J., Li, Z. et al. (2012). ChIP sequencing of cyclin D1 reveals a transcriptional role in chromosomal instability in mice. *The Journal of clinical investigation* 122, 833-843.

Chen, Z. H., Na, H. K., Hurh, Y. J. and Surh, Y. J. (2005). 4-Hydroxyestradiol induces oxidative stress and apoptosis in human mammary epithelial cells: possible protection by NF-kappaB and ERK/MAPK. *Toxicology and applied pharmacology* 208, 46-56.

Chun, K. S., Keum, Y. S., Han, S. S., Song, Y. S., Kim, S. H. and Surh, Y. J. (2003). Curcumin inhibits phorbol ester-induced expression of cyclooxygenase-2 in mouse skin through suppression of extracellular signal-regulated kinase activity and NF-kappaB activation. *Carcinogenesis* 24, 1515-1524.

Corvinus, F. M., Orth, C., Moriggl, R., Tsareva, S. A., Wagner, S., Pfitzner, E. B., Baus, D., Kaufmann, R., Huber, L. A., Zatloukal, K. et al. (2005). Persistent STAT3 activation in colon cancer is associated with enhanced cell proliferation and tumor growth. *Neoplasia* 7, 545-555.

Cui, X., Jin, Y., Hofseth, A. B., Pena, E., Habiger, J., Chumanevich, A., Poudyal, D., Nagarkatti, M., Nagarkatti, P. S., Singh, U. P. et al. (2010). Resveratrol suppresses colitis and colon cancer associated with colitis. *Cancer Prev Res (Phila)* 3, 549-559.

Gerling, M., Meyer, K. F., Fuchs, K., Igl, B. W., Fritzsche, B., Ziegler, A., Bader, F., Kujath, P., Schimmelpenning, H., Bruch, H. P. et al. (2010). High Frequency of Aneuploidy Defines Ulcerative Colitis-Associated Carcinomas: A Comparative Prognostic Study to Sporadic Colorectal Carcinomas. *Annals of surgery*.

Grivennikov, S., Karin, E., Terzic, J., Mucida, D., Yu, G. Y., Vallabhapurapu, S., Scheller, J., Rose-John, S., Cheroutre, H., Eckmann, L. et al. (2009). IL-6 and Stat3 are required for survival of intestinal epithelial cells and development of colitis-associated cancer. *Cancer cell* 15, 103-113.

Holland, A. J. and Cleveland, D. W. (2012). Chromoanagenesis and cancer:

mechanisms and consequences of localized, complex chromosomal rearrangements. *Nature medicine* 18, 1630-1638.

Hong, S., Gronert, K., Devchand, P. R., Moussignac, R. L. and Serhan, C. N. (2003). Novel docosatrienes and 17S-resolvins generated from docosahexaenoic acid in murine brain, human blood, and glial cells. Autacoids in anti-inflammation. *The Journal of biological chemistry* 278, 14677-14687.

Ishida, T., Yoshida, M., Arita, M., Nishitani, Y., Nishiumi, S., Masuda, A., Mizuno, S., Takagawa, T., Morita, Y., Kutsumi, H. et al. (2010). Resolvin E1, an endogenous lipid mediator derived from eicosapentaenoic acid, prevents dextran sulfate sodium-induced colitis. *Inflammatory bowel diseases* 16, 87-95.

Kishimoto, T. (2005). Interleukin-6: from basic science to medicine--40 years in immunology. *Annual review of immunology* 23, 1-21.

Lee, H. N. and Surh, Y. J. (2012). Therapeutic potential of resolvins in the prevention and treatment of inflammatory disorders. *Biochemical pharmacology* 84, 1340-1350.

Leslie, K., Lang, C., Devgan, G., Azare, J., Berishaj, M., Gerald, W., Kim, Y. B., Paz, K., Darnell, J. E., Albanese, C. et al. (2006). Cyclin D1 is transcriptionally regulated by and required for transformation by activated signal transducer and activator of transcription 3. *Cancer research* 66, 2544-2552.

Malumbres, M. and Barbacid, M. (2001). To cycle or not to cycle: a critical decision in cancer. *Nature reviews. Cancer* 1, 222-231.

Medzhitov, R. (2008). Origin and physiological roles of inflammation. *Nature* 454, 428-435.

Moore, B. B., Coffey, M. J., Christensen, P., Sitterding, S., Ngan, R., Wilke, C. A., McDonald, R., Phare, S. M., Peters-Golden, M., Paine, R., 3rd et al. (2000). GM-CSF regulates bleomycin-induced pulmonary fibrosis via a prostaglandin-dependent mechanism. *J Immunol* 165, 4032-4039.

Nelsen, C. J., Kuriyama, R., Hirsch, B., Negron, V. C., Lingle, W. L., Goggin, M. M., Stanley, M. W. and Albrecht, J. H. (2005). Short term cyclin D1 overexpression induces centrosome amplification, mitotic spindle abnormalities, and aneuploidy. *The Journal of biological chemistry* 280, 768-776.

Park, S. A., Na, H. K., Kim, E. H., Cha, Y. N. and Surh, Y. J. (2009). 4-hydroxyestradiol induces anchorage-independent growth of human mammary epithelial cells via activation of IkappaB kinase: potential role of reactive oxygen species. *Cancer research* 69, 2416-2424.

Popivanova, B. K., Kitamura, K., Wu, Y., Kondo, T., Kagaya, T., Kaneko, S., Oshima, M., Fujii, C. and Mukaida, N. (2008). Blocking TNF-alpha in mice reduces colorectal carcinogenesis associated with chronic colitis. *The Journal of clinical investigation* 118, 560-570.

Putz, S. M., Vogiatzi, F., Stiewe, T. and Sickmann, A. (2010). Malignant transformation in a defined genetic background: proteome changes displayed by 2D-PAGE. *Molecular cancer* 9, 254.

Sansone, P., Storci, G., Tavolari, S., Guarnieri, T., Giovannini, C., Taffurelli, M., Ceccarelli, C., Santini, D., Paterini, P., Marcu, K. B. et al. (2007). IL-6 triggers

malignant features in mammospheres from human ductal breast carcinoma and normal mammary gland. *The Journal of clinical investigation* 117, 3988-4002.
Saunders, W. (2005). Centrosomal amplification and spindle multipolarity in cancer cells. *Seminars in cancer biology* 15, 25-32.
Serhan, C. N. (2007). Resolution phase of inflammation: novel endogenous anti-inflammatory and proresolving lipid mediators and pathways. *Annual review of immunology* 25, 101-137.
Waldner, M. J., Foersch, S. and Neurath, M. F. (2012). Interleukin-6--a key regulator of colorectal cancer development. *International journal of biological sciences* 8, 1248-1253.

CONCLUSION

Acute inflammation is a protective mechanism, but excessive uncontrolled inflammatory responses lead to chronic inflammatory diseases as well as cancer. To prevent chronic inflammation, complete resolution of inflammation is important. The lipid mediator class switching, from pro-inflammatory (derived from omega-6 PUFAs) to anti-inflammatory and pro-resolving mediators (mostly derived from omega-3 PUFAs), is a key event for driving resolution of inflammation. RvD1, one of endogenous anti-inflammatory and pro-resolving lipid mediators, promotes resolution of inflammation through facilitating apoptosis of PMNs, efferocytosis and exfiltration of inflammatory cells from the inflamed site. Our present study shows RvD1-mediated suppression of TNF-α expression is responsible for enhancing the efferocytic ability of macrophages. Since sustained production of TNF-α is implicated in the pathogenesis of a variety of human diseases, RvD1-mediated blockade of TNF-α overproduction should be essential for resolution of inflammation and prevention of chronic inflammatory diseases. Moreover, RvD1 shows the preventive effect on efferocytosis-induced ROS generation and subsequent apoptosis by inhibiting assembly of the NOX2 complex. The results from our present study suggest a novel mechanism underlying efferocytosis-induced apoptosis, which will be valuable in efficient management of chronic inflammatory disorders associated with macrophage death.

Multiple lines of evidence from population-based clinical studies as well as animal experiments support a strong association between inflammation and development of cancer. Our findings also suggest that RvD1 suppresses inflammation-induced tumorigenesis in the colon by suppressing the production as well as the oncogenic effect of IL-6, which induces chromosomal instability.

Interestingly, RvD1 exerted its anti-inflammatory and pro-resolving actions by interacting with receptors, ALX/FPR2 (as an agonist) and IL-6 receptor (possibly as an antagonist). Via receptors, RvD1 stimulated ERK1/2 activation, but suppressed pro-inflammatory stimuli-induced activation of IKK and JAK2 in 15 min. Along with these actions, RvD1 modulated nuclear translocation of transcription factors such as p50 homodimer, p65/p50 heterodimer and STAT3 in 30 min. These results indicate that RvD1-mediated actions are rapidly progressed, thereby inducing timely resolution of inflammation and blocking inflammation immediately. Collectively, as RvD1 promotes resolution of inflammation, and prevents inflammation-induced malignant transformation in colon, this molecule is anticipated as desirable therapeutics for the management of inflammatory diseases and the prevention of cancer.

국 문 초 록

염증이란 생체조직이 외부로부터 자극을 받을 때, 유해인자를 제거하고 손상부위를 정상으로 회복시킴으로써 그 영향을 국소화 하려는 생체 방어기전 중 하나이다. 그러나 염증의 해소가 제대로 이루어지지 못하면, 급성 염증은 만성 염증으로 발전하여 암을 비롯한 인체 대부분의 질환의 원인이 된다. 따라서 만성 염증성 질환 및 암 치료제 개발에 있어 염증의 해소에 대한 이해는 필수적이다. 염증 반응은 개시부터 해소에 이르는 일련의 과정동안 다양한 매개체에 의해 조절한다. 이전까지만 해도 친염증성 매개체(pro-inflammatory mediator)가 분해되어 염증반응이 멈추는 것으로 알려져 있었지만, 최근에는 염증의 해소 과정을 레졸빈과 같은 내인성 pro-resolving 매개체에 의해 조절되는 능동적 과정으로 인식되고 있다. 레졸빈은 염증부위로의 호중구 유입을 막고, 염증부위에 유입된 백혈구의 세포사멸을 유도하고, 사멸된 세포를 대식세포가 제거한 후 림프관을 통해 빠져나가게 하고, 혈관 확장 및 투과를 복원시키며, 친염증성 신호전달을 종결시킴으로써 염증이 유발된 조직을 회복시키는 작용을 한다.

염증반응 후기에 내생적으로 생성되어 염증의 해소를 촉진시킨다고 보고된 레졸빈은 ‘resolution phase interaction products’ 에서 기인하였으며, EPA에서 기인한 레졸빈은 레졸빈 E (RvE), DHA가 대사되어 합성된 레졸빈은 레졸빈 D (RvD)라 일컫는다. 레졸빈 D 중 하나인 RvD1은 염증 해소에 있어 가장 중요한 단계인 사멸된 백혈구를 제거하는 과정, 즉 efferocytosis 과정을 효과적으로 촉진시킨다고 보

고되어 있다. Chronic inflammatory lung disease, chronic granulomatous disease 등 만성염증 관련 질환에서 대식세포의 efferocytosis 능력 손상이 발견되고 있기에, RvD1이 만성염증 관련 질환의 치료제로 기대되고 있지만 아직 그 분자적 기전에 대한 이해는 부족한 편이다. 따라서 본 연구에서는 RvD1이 어떠한 분자적 기전을 통하여 염증해소와 efferocytosis를 촉진시키는지 알아보았다.

우선 zymosan A를 이용하여 마우스에 복막염을 유도시킨 후, 염증이 최대치에 도달한 순간 RvD1을 처리하여 RvD1의 pro-resolving 효과를 살펴보았다. RvD1 처리한 그룹에서는 복강 내 유입된 염증세포의 수가 현저히 감소되었지만, 염증 해소에 있어 중요한 단핵구의 비율은 상대적으로 증가함을 보였다. 또한 RvD1 처리 시, efferocytosis를 한 대식세포의 비율이 높아졌다. 이러한 RvD1의 pro-resolving 효과는 TNF-α 생성 저해를 통해 나타났다. RvD1이 TNF-α 발현을 억제하는 데 있어 classical NF-κB pathway의 차단이 중요한 것으로 보여진다. 뿐만 아니라 RvD1은 p65/p50의 경쟁자로 작용하여 classical NF-κB signaling을 저해하는 역할을 하는 p50/p50 homodimer의 형성을 촉진하여 보다 효과적으로 TNF-α 의 생성을 저해하였다. 이상의 결과를 요약하면, 염증 유발물질은 만성염증의 원인 중 하나인 TNF-α의 과다 생성을 유도하여 대식세포의 efferocytosis를 억제함으로써 염증의 resolution을 방해하는 것으로 보여진다. 하지만 생체 내에서 resolution동안 합성되는 RvD1이 classical NF-κB pathway 를 저해할 뿐만 아니라 p50/p50 homodimer의 형성을 촉진하여 TNF-α 의 생성을 효과적으로 억제하고, 이를 통하여 대식세포의 efferocytosis 능력을 회복시켜 염증의 종결을 촉진하

는 것으로 사료된다

일반적으로 포식세포는 식세포작용 시 발생되는 활성산소종(reactive oxygen species, ROS)에 의하여 산화적 스트레스를 받는다. 하지만 대식세포가 efferocytosis 후 세포사멸을 일으켜 염증부위에 남게 되면 동맥경화증과 같은 만성염증을 일으킬 수 있다. 하지만 정상적 생리 환경에서 어떠한 메커니즘으로 대식세포가 efferocytosis에 의한 산화적 스트레스를 극복하고 생존할 수 있는지에 대한 연구는 전무한 상태이다. 본 연구에서는 염증의 resolution을 매개하는 물질 중 하나인 RvD1이 efferocytosis에 의한 산화적 스트레스로부터 대식세포를 보호하는 역할을 할 수 있는지 확인해 보고자 하였다.

RAW264.7 마우스 대식세포를 apoptotic Jurkat T 세포와 공배양하여 efferocytosis를 유도한 결과, RAW264.7 세포의 세포사멸을 관찰할 수 있었다. 이를 통하여 대식세포가 efferocytosis 후 사멸이 되지 않는 원인이 대식세포의 자체적 방어기전에 의함이 아니라는 결론을 도출할 수 있다. Efferocytosis에 의한 세포사멸은 RvD1 처리한 대식세포에서는 현저히 감소되었고, 이는 RvD1이 efferocytosis에 의한 ROS 발생을 저해하여 나타난 결과임을 확인하였다. 대개 포식작용 후 증가되는 활성산소종은 포식세포 내 존재하는 NADPH oxidase (NOX)를 통해 생성이 된다. Efferocytosis에 의하여 증가된 ROS가 NOX2 활성화에 의해 비롯되었는지 확인하고자, NOX2 억제제인 apocynin을 처리한 후 세포사멸과 ROS 생성을 측정하였다. 그 결과, apocynin 처리한 대식세포에서는 efferocytosis에 의해 유도된 세포사멸과 ROS 발생이 저해되었다. 또한 RvD1 처리시, $p47^{phox}$의 인산

화가 억제되어 NOX2 활성화를 억제함으로써 O_2^-의 발생을 저해하여 산화적 스트레스의 감소를 유도함을 관찰하였다. Protein kinase A (PKA)가 $p47^{phox}$ 인산화 저해를 유도한다는 보고를 바탕으로 RvD1에 의한 NOX2 활성 억제에 있어 PKA의 관여 가능성을 살펴보았다. RvD1 처리 시 시간에 따라 PKA 활성이 증가됨을 관찰하였고, PKA 저해제인 H89를 처리한 세포에서는 RvD1에 의한 $p47^{phox}$ 인산화 감소효과가 나타나지 않음을 확인할 수 있었다. 이러한 결과를 통하여 RvD1에 의한 PKA 활성화가 efferocytosis에 의한 NOX2 활성 억제를 유도하여, 산화적 스트레스의 발생을 저해한다는 사실을 규명하였다.

이러한 RvD1의 염증 해소 촉진 작용은 염증에 의한 암 발생을 억제하는데 기여할 것으로 예상된다. 이를 규명하기 위하여 염증에 의한 암화 과정을 설명할 수 있는 azoxymethane/dextran sulfate sodium (AOM/DSS) 유발 대장암 동물모델을 구축한 후, RvD1을 주입하여 그 효과를 살펴보았다. 그 결과, AOM/DSS에 의하여 증가된 용종의 수 및 이형증성 대장병변이 고농도의 RvD1을 처리한 경우 현저히 감소됨을 확인할 수 있었다. RvD1의 암화 억제기전을 보다 자세히 살펴보기 위해 정상 대장상피세포주인CCD841CoN에 염증에 의한 대장암 유발에 관여한다고 보고된 IL-6를 처리해 보았다. IL-6에 의한 세포의 악성변이 및 다극성 방추사 형성이 RvD1을 함께 처리한 세포에서 현저히 감소됨을 확인하였다. 이 때, IL-6에 의한 세포의 악성변이 및 다극성 방추사 형성이 cyclin D1의 과발현을 통하여 일어남을 확인할 수 있었고, RvD1이 IL-6에 의한 cyclin D1 발현을 저해하여 암화 억제 효과를 나타낸다는 사실을 규명하였다.

본 연구를 통해 제시된 RvD1에 의한 염증 해소 및 염증관련 대장암 예방 효과를 기반으로 RvD1가 다양한 염증성 질환 및 암 예방 치료제로 개발 가능할 것이라 사료된다.

주요어

레졸빈 D1 (RvD1), 염증 해소, 식세포작용(Efferocytosis), NF-κB, 산화적 스트레스, 세포사멸, NADPH oxidase 2, 염증으로 유도된 대장암, 다극성 방추사, Cyclin D1

학 번: 2008-31002